

Novel light-activated antibacterial
surfaces


by

James Michael Rudman

A thesis submitted in partial fulfilment for the degree of
Doctor of Philosophy in the
Department of Chemistry
University College London

Declaration

I, James Michael Rudman, confirm that the work presented in this thesis is my own. Where information has been derived from other sources, I confirm that this has been indicated in the thesis.

Signed:  _____

Date: 13/02/2017 _____

Abstract

The aim of this project was to covalently link chemically modified organic dyes, such as methylene blue, toluidine blue O, or crystal violet, to the surface of a polymer, *via* a 1,3-dipolar cycloaddition reaction.

The synthesis of variants of methylene blue and toluidine blue O was attempted; unfortunately, we were unable to synthesise any analogues from phenothiazine or from the dyes themselves.

The synthesis of a crystal violet analogue *via* a double Grignard reaction was investigated. We were unable to isolate the desired product in the final step. Instead, two leucocrystal violet analogues were prepared by reacting appropriately functionalised tertiary anilines with Michler's hydrol. Another leucocrystal violet analogue was prepared by reacting 4-(prop-2-yn-1-yloxy)benzaldehyde with two equivalents of *N,N*-dimethylaniline. The leucocrystal violet analogues were oxidised to give the corresponding crystal violet analogues, which were incorporated into polyurethane by a dip-coating process. The antibacterial activities of the resultant polymer films were assessed: each displayed differing antibacterial properties when illuminated (no activity was observed in the dark).

We were unable to covalently attach any crystal violet analogues to the surface of pre-functionalised silicone, polyurethane, or poly(vinyl chloride) (PVC).

Considering the differences that were observed between the antibacterial activities of the crystal violet analogues, the antibacterial activity of silicone incorporated with commercially available ethyl violet was compared with that of the same material containing crystal violet. The superiority of crystal violet over ethyl violet as a photobactericidal agent was demonstrated.

Several porphyrins and metalloporphyrins were synthesised and incorporated into silicone. The resultant films were characterised by measuring their UV-Vis, IR, and fluorescence spectra. Unfortunately, due to time constraints, the antibacterial properties of these polymers were not assessed.

Finally, we were unable to synthesise polyurethane with covalently attached crystal violet moieties *via* a polymerisation reaction.

Table of Contents

1 Introduction	9
1.1 Bacterial biofilms: a brief overview.....	10
1.2 Antibiotics	10
1.2.1 Antibiotic lock therapy.....	11
1.2.2 The impregnation or coating of polymeric medical devices with antibiotics	12
1.2.3 Surface-bound antibiotics	14
1.2.4 The future of antibiotics	18
1.3 Non-metallic disinfectants.....	19
1.3.1 <i>N</i> -Halamines.....	19
1.3.2 Quaternary ammonium compounds (QACs)	21
1.3.3 Quaternary phosphonium compounds (QPCs).....	24
1.3.4 Antimicrobial peptides (AMPs)	25
1.3.5 Nitric oxide (NO)	26
1.3.6 Crystal violet.....	27
1.3.7 Triclosan.....	29
1.3.8 Other non-metallic biocides	30
1.3.9 The future of non-metallic disinfectants	31
1.4 Metallic disinfectants.....	31
1.4.1 Silver	31
1.4.2 Copper.....	35
1.5 Light-activated antibacterial surfaces.....	36
1.5.1 Photocatalytic surfaces.....	37
1.5.2 Surfaces incorporated with photosensitiser molecules	39
2 Results and discussion	49
2.1 Preparation of alkyne-functionalised dyes, and their antibacterial activities.....	50
2.1.1 Methylene blue analogues.....	50
2.1.2 Toluidine blue O analogues.....	54
2.1.3 Crystal violet analogues <i>via</i> a Grignard reaction	55
2.1.4 Leucocrystal violet analogues from Michler's hydrol.....	59
2.1.5 Leucocrystal violet analogues from aryl aldehydes	67

2.1.6 Oxidation of leucocrystal violet analogues.....	71
2.1.7 Physical and biological characterisation of crystal violet- polyurethane samples	73
2.2 Attempted grafting of alkyne-functionalised dyes to a variety of polymer surfaces	76
2.2.1 Synthesis of a mono-amine, mono-azide-terminated PEG linker .	77
2.2.2 Attempted 1,3-dipolar cycloaddition reaction between a PEG linker and an alkyne-functionalised dye	78
2.2.3 Attempted modification of silicone	80
2.2.4 Attempted modification of polyurethane	83
2.2.5 Attempted covalent attachment of a PEG linker to PVC	84
2.2.6 Modification of PVC with sodium azide.....	85
2.2.7 Attempted grafting of an alkyne to an azide-functionalised PVC film <i>via</i> a 1,3-dipolar cycloaddition	91
2.3 Ethyl violet as an alternative to crystal violet?	94
2.3.1 Preparation and characterisation of dye-incorporated polymer samples	95
2.3.2 Antibacterial activity of dye-incorporated polymer samples	97
2.4 Assessment of the antibacterial activity and physical properties of silicone incorporated with different porphyrins	98
2.4.1 Synthesis of related analogues of meso-tetraphenylporphyrin (TPP).....	98
2.4.2 Preparation and characterisation of porphyrin-incorporated polymer films.....	104
2.5 Attempted formation of polyurethane with a covalently attached crystal violet analogue <i>via</i> a polymerisation reaction	110
2.5.1 Attempted preparation of an amine-functionalised crystal violet analogue.....	110
2.5.2 Preparation of a modified polyurethane film	112
3 Conclusions and future work.....	114
4 Experimental	117
4.1 Techniques, materials, and instrumentation	117
4.2 Procedures for the synthesis of organic compounds and associated data.....	118

4.3 Procedures for surface modifications, incorporations, leaching experiments, and other miscellaneous experiments	142
4.3.1 Incorporation of crystal violet analogues into polyurethane	142
4.3.2 Preparation of a PVC film	142
4.3.3 Modification of PVC with sodium azide.....	142
4.3.4 Incorporation of crystal/ethyl violet into medical grade silicone ..	143
4.3.5 The extent of dye leaching from medical grade silicone incorporated with crystal/ethyl violet	143
4.3.6 Incorporation of porphyrins into medical grade silicone.....	143
5 References.....	144

Acknowledgements

Firstly, I would like to thank Mike and Ivan for their support throughout. Their respective doors were always open for frequent chats regarding the direction of my project, which threw its fair share of challenges in my path. I am sure that without their guidance, I would not have reached this stage.

I would also like to pay tribute to many fellow PhD students at UCL, past and present. There are surely too many people to list here, but I'll highlight a few people. Helen and Tom, who were there from start to finish. Chris, Emily, Farzaneh, Oli, and Steve: I enjoyed many fascinating discussions about chemistry as well as other unrelated topics with you all. Kealan, Dave, Natasha, and Alex for being fantastic neighbours in the lab. Will, who helped me with a number of experiments throughout my time at UCL. There are many others who I won't mention here. It goes without saying that I am sure I'll stay in contact with you all for a very long time.

Without a number of great friends outside UCL, I wouldn't be the whole and rounded person I am today. I would like to mention Liam and Marv, two of my closest friends and people I can always rely upon when the going gets tough.

Finally, without the love and support of my family and Deborah, who I met almost 2 years ago (at the time of writing), I would surely have not got through this. I love you all very dearly and hope you will always remember that, no matter what happens.

Abbreviations

AMP	antimicrobial peptide
CFU	colony forming units
DCM	dichloromethane
DMF	<i>N,N</i> -dimethylformamide
DMSO	dimethyl sulfoxide
EDC	1-ethyl-3-(3-dimethylaminopropyl)carbodiimide hydrochloride
ePTFE	expanded polytetrafluoroethylene
F ₁₂ TPP	<i>meso</i> -tetra(2,4,6-trifluorophenyl)porphyrin
F ₂₀ TPP	<i>meso</i> -tetra(pentafluorophenyl)porphyrin
F ₄ TPP	<i>meso</i> -tetra(4-fluorophenyl)porphyrin
ISC	intersystem crossing
MDI	4,4'-methylenebis(phenylisocyanate)
NBS	<i>N</i> -bromosuccinimide
PBS	phosphate buffered saline
PEG	poly(ethylene glycol)
PVC	poly(vinyl chloride)
QAC	quaternary ammonium compound
QPC	quaternary phosphonium compound
ROS	reactive oxygen species
TEM	transmission electron microscopy
THF	tetrahydrofuran
TPP	<i>meso</i> -tetraphenylporphyrin
XPS	X-ray photoelectron spectroscopy

1 Introduction

The development of bacterial biofilms on polymeric surfaces is a serious cause for concern, particularly in places such as hospitals, where the chance of immunocompromised patients contracting infections is greatly heightened. Despite the implementation of rigorous cleaning protocols, hospital surfaces are continuously subjected to further bacterial contamination. Moreover, and perhaps more alarmingly, medical implant devices such as catheters are frequently colonised by bacteria, regardless of whether medical staff adhere strictly to proper insertion techniques. This results in the proliferation of malignant infections within the hospital environment, which can lead to the death of patients in some instances. The development of robust antibacterial polymeric surfaces that prevent the attachment of bacteria and subsequent biofilm formation, would therefore appear to be an excellent strategy to combat this problem.

In recent years, numerous antibacterial polymeric surfaces have been developed. Broadly speaking, antibacterial surfaces can be divided into three categories: those that kill bacteria, those that resist the adhesion of bacteria, and those that release attached bacteria.¹ The main focus of this project was the development of light-activated antibacterial surfaces that kill bacteria; therefore, those that resist bacterial adhesion, or release attached bacteria, will not be discussed here. For more information about surfaces with these properties, the reader is directed towards a number of publications and reviews that discuss a range of topics including quorum sensing inhibition,^{2,3} the use of biosurfactants to disperse bacterial biofilms,⁴ surface micropatterning,⁵ the utility of zwitterionic coatings,^{6,7} and the development of either super-hydrophobic or highly hydrophilic surfaces.⁸⁻¹¹ In addition, there are a number of broader reviews that discuss these topics, and many others, in excellent detail.¹²⁻¹⁶

In the following sections, the antibacterial properties of a variety of different antibacterial surfaces, prepared in a number of different ways, will be discussed. The utility of light-activated antibacterial surfaces is considered in

significant detail, as the production of such materials was the main focus of this project.

1.1 Bacterial biofilms: a brief overview

A bacterial biofilm is a sessile bacterial community encased within a hydrated polymeric matrix, which consists of proteins, polysaccharides, teichoic acids, and extracellular DNA. The first stage of biofilm formation involves the attachment of planktonic bacteria to a surface by various means, such as with pili, which are proteinaceous outer membrane structures. Once attached to the surface, some bacteria are capable of secreting “slimes” that engulf the bacteria present, and effectively bind them irreversibly to the surface. The bacterial colonies that form within this biofilm matrix are extremely difficult to eradicate: they are up to 1000 times more resistant to biocides than planktonic bacteria. The intermittent release of planktonic bacteria from a mature biofilm means that new biofilms can form elsewhere, or it can result in a persistent infection where indwelling devices, such as catheters, are concerned (Figure 1).¹⁷⁻²⁰

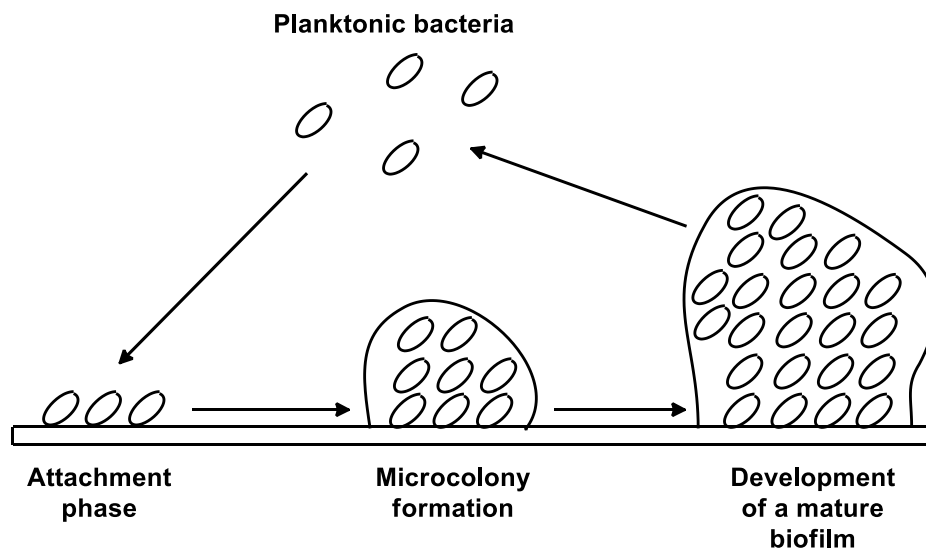


Figure 1. A simplified schematic detailing each phase of biofilm development.

1.2 Antibiotics

The most common way of preventing, or combatting, medical device related infections involves the use of antibiotics such as penicillin, rifampicin, minocycline, vancomycin, and cefoxitin. An antibiotic is a compound that is

either a bactericide, which means that it works by killing bacteria directly; or a bacteriostatic, which means that it works by preventing bacteria from reproducing, and hence proliferating. The term “antibiotic” is often used loosely, and incorrectly, to refer to any compounds that eliminate microbes of any type, such as viruses. Such compounds should be labelled as “disinfectants” or “antimicrobials”, and will be discussed in section 1.3.

There are a number of different ways in which antibiotics can be employed to prevent the bacterial colonisation of polymeric surfaces. The most common strategy involves impregnating, or coating, the polymer with such compounds. Alternatively, antibiotics can be covalently attached to the surface of a polymer, to biodegradable thin-film coatings, or to surface adsorbed vesicles. In the case of catheter associated infections, the catheter can be flushed with antibiotics to eliminate bacterial colonies that have already developed – this process is known as “antibiotic lock therapy”. In the next few sections these differing strategies, including their pros and cons, will be discussed.

1.2.1 Antibiotic lock therapy

In 1988, Messing *et al.*²¹ developed a new strategy to eliminate catheter-related infections. In a clinical trial, a highly concentrated antibiotic solution in isotonic saline was injected into the lumen of the contaminated catheter of each participant, who was suffering from a catheter-related infection, every twelve hours for two weeks. The group found that catheter removal wasn't required to cure the eleven patients who participated in this clinical trial, and concluded that this method could be utilised in the future to successfully combat catheter-related infections.

Up until 1998, a number of clinical trials had indicated that antibiotic lock therapy was effective at curing catheter-related infections that were caused by a variety of different bacteria; however, limited *in vitro* laboratory experiments had been performed.²²⁻²⁸ Andris *et al.*²⁹ investigated the efficacy of a number of different antibiotic systems for the elimination of a range of microbial colonies. They found that different antibiotics exhibited varying levels of effectiveness against different strains of bacteria. For example, nafcillin, ceftriaxone, and vancomycin caused a significant decrease in colonisation of

the intraluminal membrane by various staphylococcal species. On the other hand, aztreonam, ceftriaxone, and gentamicin were all highly efficacious against Gram-negative bacteria. Moreover, it was shown that amphotericin and fluconazole were effective against two different yeast species: *C. albicans* and *C. tropicalis*.

The use of antibiotic lock therapy is well documented; it has been shown on numerous occasions that it is an effective tool when it comes to eradicating catheter-related infections.³⁰ There are, however, three discrete disadvantages associated with this approach. Firstly, there is a chance that a blockage might occur in the interior of the catheter lumen, caused by precipitation of the active agent. Secondly, exposure to high concentrations of antibiotics is often associated with localised toxicity and/or undesired side-effects. Finally, and most importantly, the patient is already suffering from a catheter-related infection, as a result of prior catheter contamination.³⁰ In addition, although not a disadvantage of the technique itself, the use of this method is limited exclusively to catheters.

Clearly, a preventative approach would be better than a reactive one, as patients would not have to endure the trauma of becoming infected in the first place. In the next two sections, the ability of antibiotics to prevent the bacterial colonisation of polymeric surfaces will be explored.

1.2.2 The impregnation or coating of polymeric medical devices with antibiotics

There is a vast amount of literature describing the impregnation, or coating, of different polymeric materials with a range of antibiotics. Throughout the 1990s, many groups incorporated a multitude of different antibiotics into a range of different medical devices. The effectiveness of such devices in preventing bacterial colonisation has been demonstrated in *in vitro* and *in vivo* experiments.³¹

A variety of different methods were developed to facilitate the physical adsorption of different antibiotics to the surfaces of various medical devices. One approach involved the pre-treatment of a polymeric device with a cationic surfactant, tridodecylmethylammonium chloride, in ethanol. This allowed for

the non-covalent binding of a negatively charged antibiotic, such as cefoxitin or vancomycin, to the surface.^{32,33}

Many groups utilised the ability of polymers such as silicone and polyurethane to swell in certain solvent systems. They dissolved the antibiotic(s) in a solution that also caused the polymer to swell. After a certain amount of time the solvent was removed and the polymer returned to its original size, with the antibiotics encapsulated within the polymer matrix.³⁴⁻³⁷

A few highly original techniques were also developed. For example, DiTizio *et al.*³⁸ produced a hydrogel-coated catheter that contained embedded liposomes, which were loaded with the antibiotic ciprofloxacin. Presumably, it was expected that the liposomes would be able to store more of the active compound than the polymeric matrix, thus giving rise to a more efficacious antibacterial surface with an extended shelf-life. The modified catheter resisted colonisation by *P. aeruginosa* for one week in an *in vitro* experiment. In a similar vein, Marconi *et al.*³⁹ generated a sulfated polyurethane, which was able to sequester large amounts of the antibiotics cefamandole and vancomycin. The resultant polymer was effective at eliminating *S. epidermidis* in an *in vitro* study. Although both of these methods of generating antibacterial surfaces are clearly very interesting, it's impossible to compare the effectiveness of these polymers with ones that were less technically demanding to generate.

Commonly, a combination of two or more antibiotics with different modes of action are incorporated: this reduces the risk of resistant bacterial strains developing, as bacteria are very unlikely to undergo two simultaneous mutations that make them resistant to both antibiotics at once.⁴⁰ Moreover, combinations of antibiotics have frequently been shown to act in synergy.^{33,41} This is often because the mode of action of one antibiotic causes the bacterium in question to become less resistant to the other.

There are a number of commercially available medical devices incorporated with antibiotics that have been shown, in numerous clinical trials, to significantly reduce the onset of catheter-related infections.⁴²⁻⁴⁴ For example, in 1999 Darouiche *et al.*⁴⁵ conducted a large clinical trial, where they

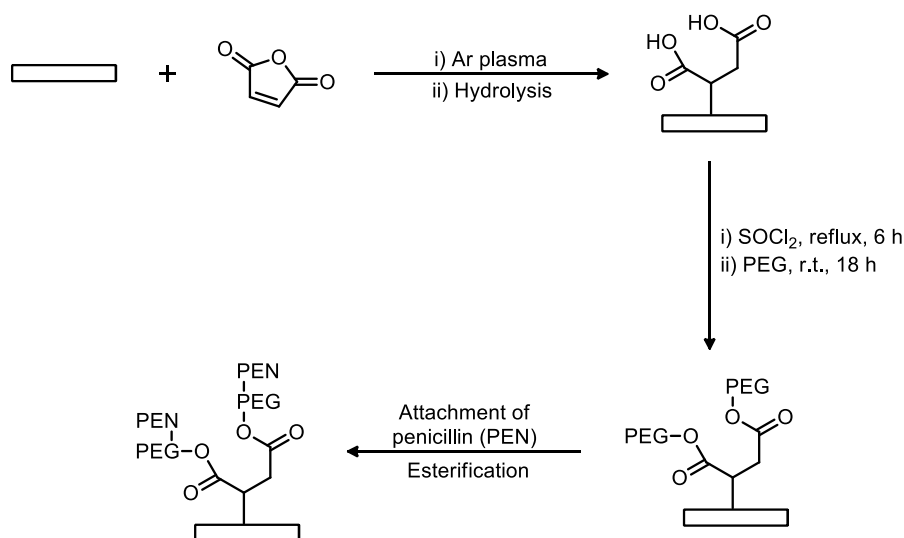
established that the use of catheters incorporated with a combination of minocycline and rifampicin resulted in a statistically significant reduction in the amount of patients acquiring catheter-related infections. Interestingly, in 2014, Jamal *et al.*⁴⁶ coated a minocycline-rifampicin catheter with the disinfectant, chlorhexidine, and demonstrated that it was significantly more effective than the unmodified variant. This indicates that there may be good reason to combine antibiotics with disinfectants, as this seems to improve the antibacterial properties of the resultant polymer. More recently, Fisher *et al.*⁴⁷ produced a urinary catheter impregnated with a mixture of rifampicin, sparfloxacin, and the disinfectant triclosan, and found that it too was highly effective at inhibiting microbial contamination.

The coating, or incorporation, of polymers with antibiotics is a proven strategy for preventing the occurrence of device related infections. The major issue associated with this method is a consequence of the way that antibiotic incorporated medical devices prevent bacterial contamination. Over time, antibiotics diffuse into the surrounding medium. The rate at which this occurs depends upon the antibiotic(s) used, the composition of the surrounding medium, and the composition of the polymer. The rate of diffusion from the device is correlated with how effective it is, as well as its shelf-life. After a certain period of time, the concentration of antibiotic that diffuses from the polymeric matrix into the surrounding medium will be sub-inhibitory. Not only does this mean that no further antibacterial activity is observed, but also that the chance of resistant strains of bacteria developing is greatly increased.

1.2.3 Surface-bound antibiotics

In the previous section, surfaces that release physically adsorbed antibiotics passively into their surroundings were discussed. In this section, examples of the covalent linkage of antibiotics to various surfaces, or surface coatings, will be discussed. This approach offers a far greater degree of control, as the antibiotic in question could either be permanently bound to the surface, or released in the presence of bacteria if cellular uptake is required for it to be active. In both cases, the antibiotics would only be depleted as and when they are needed.

In 2007, the Urban group developed a method for covalently attaching penicillin to the surface of expanded polytetrafluoroethylene (ePTFE).^{48,49} Initially, an argon plasma discharge was generated in a microwave in the presence of ePTFE and maleic anhydride. This resulted in the formation of a reactive surface containing carboxylic acid functional groups. The modified surface was then reacted with a poly(ethylene glycol) (PEG) linker, and this was followed by subsequent attachment of the antibiotic penicillin (Scheme 1).



Scheme 1. Attachment of penicillin (PEN) to the surface of functionalised ePTFE.

The penicillin-functionalised polymer surface was shown to retard the growth of *S. aureus* (a Gram-positive bacterium), but was ineffective against *P. aeruginosa* (a Gram-negative bacterium).^{48,49} Penicillin is a β -lactam antibiotic that inhibits the action of DD-transpeptidase, an enzyme that catalyses the formation of cross-links between peptidoglycan units in the cell wall of Gram-positive bacteria. This creates an imbalance, as enzymes that hydrolyse these links remain active: the result is degradation of the cell wall and subsequent cell death. Conversely, Gram-negative bacteria have an outer membrane that consists of lipopolysaccharides and phospholipids. The inability of penicillin to penetrate this layer renders it inactive against Gram-negative bacteria.

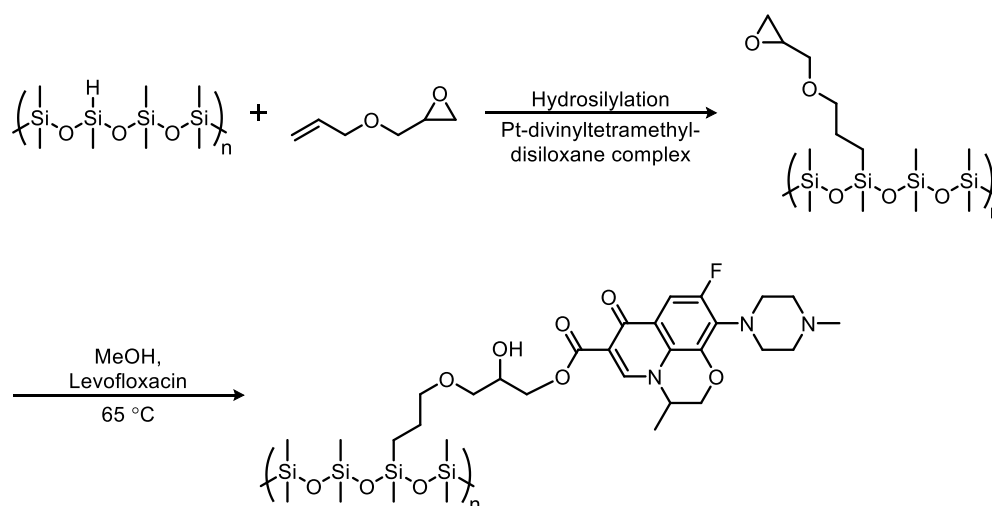
The Urban group demonstrated that penicillin is active when bound to the surface of ePTFE, and speculated that the mixed molecular weight PEG linkers probably facilitated this. They noted that, after one day in phosphate buffered saline (PBS) solution, 32% of the originally bound penicillin had been released from the surface due to hydrolysis of the ester linkage between the

PEG linker and penicillin; however, even after this loss of active compound, the resultant polymer was still able to resist bacterial contamination effectively.^{48,49} The uncontrollable release of penicillin from the surface due to some hydrolysis is not ideal, but this approach is clearly a major improvement on previously designed surfaces where the antibiotic is only physically adsorbed.

In more recent work conducted by the same group, Aumsuwan *et al.*⁵⁰ attached ampicillin to the surface of ePTFE by a similar method to that which is described above. Although ampicillin is a β -lactam, and has a similar mode of action to penicillin, it has a broader spectrum of activity and is active against some Gram-negative bacteria. The Urban group showed that this new surface was effective against a variety of Gram-positive and Gram-negative bacteria, including *S. aureus*, *B. thuringiensis*, *E. faecalis*, *E. coli*, *P. putida*, and *S. enterica*. They also showed that approximately 90% of the originally bound ampicillin was present after exposure to different bacterial solutions for one day.

In 2009, Aumsuwan *et al.*⁵¹ used the same synthetic strategy, as detailed in scheme 1, to attach both penicillin and gentamicin (active against Gram-negative bacteria) to the surface of polypropylene. They demonstrated that this surface was effective against the Gram-positive bacterium *S. aureus*, and the Gram-negative bacterium *P. putida*.

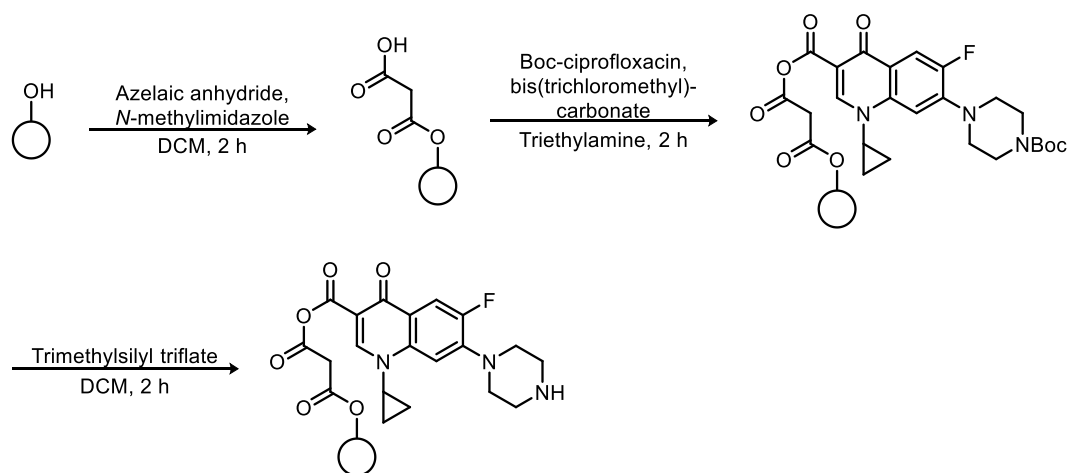
In the following year, another group devised a method for covalently attaching levofloxacin to a functionalised poly(methylhydro-co-dimethyl)siloxane coating (Scheme 2).⁵²



Scheme 2. Covalent attachment of levofloxacin to a modified siloxane surface.

In this instance, slow hydrolysis is desirable and gives rise to “free” levofloxacin, which is responsible for the observed antimicrobial activity. The modified polymer had a more uniform distribution of covalently bound levofloxacin, and showed a higher initial kill, as well as sustained antimicrobial activity, relative to a polysiloxane coating that had simply been blended with levofloxacin.

In 2012, Komnatny *et al.*⁵³ covalently attached ciprofloxacin to the surface of (4-hydroxymethylbenzoic acid)-linked ChemMatrix polymer beads *via* a lipase-sensitive anhydride linkage (Scheme 3). They found that, in the presence of a strain of *P. aeruginosa* that produces lipases, ciprofloxacin was released from the beads and this resulted in complete eradication of the bacterial population within four hours. On the other hand, when lipase-defective mutants were used an insignificant decrease in the bacterial population was observed. To show that release of the antibiotic was vital, they attached ciprofloxacin to the polymer beads by an amide linkage, which is not susceptible to the action of lipases. In the presence of these beads, the population of lipase-producing *P. aeruginosa* was unaffected.



Scheme 3. Covalent attachment of ciprofloxacin to the surface of (4-hydroxymethylbenzoic acid)-linked ChemMatrix polymer beads by an anhydride linkage.

Despite ongoing improvements in this area, producing polymeric surfaces with covalently bound antibiotics is still technically challenging. On the other hand, the generation of surfaces with physically adsorbed antibiotics is often relatively simple. There is one major problem with all the aforementioned antibiotic-loaded polymers: the antibacterial activity is not permanent. Once the antibiotics have served their function and/or have been released from the polymer surface, they are not replaced.

1.2.4 The future of antibiotics

Throughout this section, the ability of antibiotics to prevent the colonisation of various polymeric surfaces has been discussed. Despite all the research that has been carried out in this area, the use of antibiotics has a major disadvantage in that they commonly have a very specific mode of action. This means that the effectiveness of antibiotics is in rapid decline due to growing resistance as a result of their overuse in various applications.^{54,55} Moreover, the low discovery rate of new antibiotic drug classes compounds this problem: over thirty years passed between the approval of nalidixic acid in 1967 and linezolid in the year 2000.⁴⁰

One way of combatting the development of antibiotic resistant bacterial strains might involve the use of carefully selected combinations of antibiotics, perhaps even along with adjuvants that enhance their activity. The premise behind this strategy is that, as previously mentioned, bacteria are less likely to undergo more than one mutation at the same time. As a result, every bacterium within

a colony will be susceptible to the mode of action of at least one of the antibiotics; therefore, the chance of resistant strains developing is greatly reduced.⁴⁰

In recent times the isolation and development of new antibiotics appears to be heading towards a new golden era, but who knows how long this will last?^{56,57} Considering the slow supply of new antibiotics, the rapid development of antibiotic-resistant strains of bacteria, and the fact that the antibacterial activity of antibiotic-incorporated surfaces can only ever be finite, new and improved methods for preventing the bacterial colonisation of polymeric surfaces need to be developed.

1.3 Non-metallic disinfectants

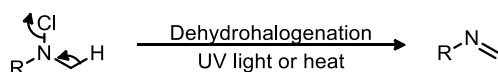
In addition to antibiotics, a huge variety of disinfectants and other organic natural products have been incorporated into, or covalently bound to the surface of, various polymers. Unlike antibiotics, these compounds are often extremely harmful towards humans, which means that their potential to be used in indwelling medical devices, such as catheters, is somewhat limited; however, the covalent attachment of disinfectants, such as quaternary ammonium salts, to the surface of an indwelling device, may prevent them from being toxic towards the human host. In any case, their use in external surfaces, where cytotoxicity is not an issue, should not cause any problems. In the ensuing sections, the utility of numerous disinfectants in preventing the adhesion of bacteria to a range of different surfaces is considered.

1.3.1 N-Halamines

An *N*-halamine is a compound that contains at least one nitrogen-halogen (N-X) bond. They are formed by the halogenation of an N-H bond of an imide, amine, or amide. The N-H bond can be halogenated by a variety of different reagents, including X_2 , HOX, and OX^- , where X symbolises a halogen atom. The resultant *N*-halamines are potent biocides because the halogen atom is in the +1 oxidation state. In essence, they are a source of X^+ , which can be released into cells upon contact and induce cell death. Alternatively, dissociation of the N-X bond can give rise to free X^+ in the surrounding

environment, which results in a zone of inhibition around the polymer in question. The evidence appears to suggest that both processes occur to some extent. The inactivation of bacteria by X^+ is accompanied by reformation of the corresponding *N*-halamine precursor, and a subsequent loss of antibacterial activity over time. To overcome this, the precursor can be recharged by halogenation, as described above.⁵⁸

The stability of *N*-halamines is reduced by the presence of an α -hydrogen atom, as dehydrohalogenation can take place (Scheme 4). In fact, very few *N*-halamines actually contain an α -hydrogen because of this decomposition pathway.⁵⁸



Scheme 4. The mechanism of dehydrohalogenation.

The stability of the N-X bond towards hydrolysis increases as the nitrogen atom becomes more electron rich. This means that, in general, the rate of dissociation of N-X bonds decreases in the following order: imides > amides > amines. Unsurprisingly, an inverse trend is observed when the biocidal activities of the *N*-halamines are compared, as dissociation of the N-X bond is required for these compounds to effect bacterial kill. It is important to consider both the stability and the associated antimicrobial activity of the resultant *N*-halamine incorporated polymer when attempting to design an antimicrobial surface. If one wishes to produce a polymer surface that exhibits long-term activity, without the need for frequent “recharging”, then it would be wise to utilise amine *N*-halamine compounds. On the other hand, if a high level of activity is required in short, intermittent bursts, imide *N*-halamine compounds should be used.⁵⁸

There are numerous strategies for producing antimicrobial *N*-halamine-functionalised polymers. One method used involves the grafting of an *N*-halamine precursor onto a commercially available, occasionally pre-functionalised, polymer surface.⁵⁸⁻⁶⁹ Alternatively, a polymer containing reactive groups can be spin-coated onto the surface of a chemically inert polymer, either prior to the covalent attachment of an *N*-halamine precursor, or with an *N*-halamine precursor already bound.⁷⁰⁻⁷³ The N-H bond can then

be “activated” by treatment with an appropriate halogenating agent. Another strategy that has been invoked involves polymerisation of an *N*-halamine monomer with, or without, other monomeric units to give a homo-, or copolymer respectively.^{58,74-76}

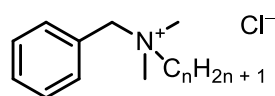
The fact that *N*-halamine-functionalised polymers are rechargeable (by treatment with a halogenating agent, as discussed above) is a disadvantage: the surface must undergo frequent maintenance to ensure that it continues to exhibit antimicrobial activity. Clearly, this might not be very practical for medical implant devices such as catheters, or in other applications where access to the surface in question is restricted; however, for their use in most fields this shouldn't pose too much of a problem. In most cases, the *N*-halamine moiety is either part of, or covalently attached to, the polymer; therefore, toxicity is not considered to be an issue, as there is little to no chance of it being released into the surrounding environment. Surfaces that are modified with *N*-halamines have been shown to be extremely effective at significantly reducing bacterial contamination in numerous areas, such as in water disinfection, due to their potent bactericidal properties.⁵⁸

1.3.2 Quaternary ammonium compounds (QACs)

For a number of years, it has been known that QACs, like *N*-halamines, are potent, broad spectrum bactericides which act against both Gram-positive and Gram-negative bacteria. The exact mechanism of antimicrobial action is still debated, though it is generally accepted that QACs kill bacteria, as well as other microorganisms, on contact. It is believed that the positively charged QAC disrupts the charge distribution of the bacterial cell membrane, which results in loss of low molecular weight components from the cell and subsequent necrosis.^{77,78}

In 1935, Domagk first demonstrated that benzalkonium chloride is a highly effective disinfectant; since then, QACs have been used extensively in this role (Figure 2).⁷⁹ Throughout the 1990s, a number of groups investigated the efficacy of a range of different catheters coated with benzalkonium chloride to prevent bacterial adhesion by a killing mechanism.⁸⁰⁻⁸⁴ The results were varied, with some groups reporting that the resultant catheters demonstrated

excellent long-term activity, whilst others found them to be ineffective. The fact that different types of catheter were impregnated with benzalkonium chloride does not make a comparative account easy, though. In 2010, a woman reportedly suffered anaphylactic shock following insertion of a catheter that was coated with benzalkonium chloride; however, once again it is impossible to say whether or not this was actually caused by benzalkonium chloride.⁸⁵ Clearly, more research is required to ascertain the effectiveness of benzalkonium chloride, and whether it is even safe to use.



$$n = 8, 10, 12, 14, 16, 18$$

Figure 2. Benzalkonium chloride is a mixture of alkylbenzyltrimethylammonium chlorides.

Many research groups have investigated whether chitosan, a linear polysaccharide containing amine moieties, could be exploited in a number of different applications where materials with antibacterial properties are desired (Figure 3). It is produced by the de-acetylation of naturally occurring chitin under basic conditions. The conjugate acid of the amino substituents of chitosan have a pK_a of ~ 6.5 , so are protonated to some extent under mildly acidic conditions. Its use as a food packaging material is of particular interest, due to the fact that it is both biodegradable and non-toxic.⁸⁶ It can also be covalently bound, or physically adsorbed, to the surface of various polymeric surfaces, thus rendering them antibacterial.^{87,88}

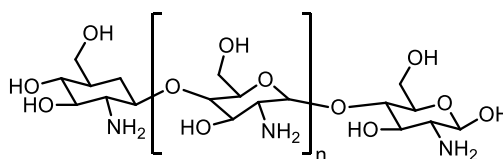


Figure 3. Chitosan, produced by the de-acetylation of chitin.

Many research groups have synthesised a wide variety of polymeric materials with covalently bound QACs. In 1977, Rembaum *et al.*⁸⁹ demonstrated that a series of ionenes, which are polymers that have ionic groups as part of the main chain, were biocidal. In this case, the main chain was composed of a sequence of quaternary ammonium centres. The preparation of ionenes containing QACs, or of polymers with a pendant QAC moiety can be achieved

by the polymerisation of an appropriately functionalised QAC monomer, or by the copolymerisation of a QAC monomer with other compounds.^{78,90-99} If the QAC is unstable to the polymerisation conditions, a precursor, i.e. a tertiary amine, or an alkyl halide, can be used. Then once the desired polymer has been produced, the quaternary centres can be generated. These types of polymer have exhibited excellent antibacterial properties, regardless of whether the quaternary ammonium centre is located in the main chain, or is part of a pendant moiety.^{78,100}

Instead of conducting polymerisation reactions, many other groups have used various surface grafting methods, plasma polymerisation, or layer-by-layer deposition, to attach QACs, or their precursors, to the surface of a polymer.^{78,100,101} In many of these instances, inert polymers were used; therefore, surface modification (e.g. ozonolysis, argon plasma discharge) was necessary for the subsequent covalent attachment of a QAC.¹⁰²⁻¹⁰⁴ Alternatively, preparation of a closely related polymer that incorporated reactive groups (e.g. a silicone polymer containing Si-H bonds), also proved to be an effective tactic.¹⁰⁵⁻¹⁰⁷

Ongoing research in this area has led to some interesting observations regarding the characteristics of different QACs. In 2010, Sharma *et al.*¹⁰⁸ investigated the effect of changing the counter-ion of poly(4-vinyl 2-hydroxyethyl pyridinium) chloride on the antimicrobial activity. They found that the polymer with hydroxide as the counter-ion was the most efficacious at killing both bacteria (*B. coagulans*) and fungi (*A. niger* and *M. circenelliods*). In another study, Garg *et al.*¹⁰⁹ showed that, for poly[1-vinyl-3-(2-sulfoethyl imidazolium betaine)], varying the anion had a profound effect on the biocidal activity against different types of bacteria. For example, the polymer with the hydroxide counter-ion was the most effective against a Gram-positive bacterium; whereas against a Gram-negative bacterium, it was found that fluoride, sulphide, and nitrate were the best anions to have. The effect of changing the counter-ion on the antibacterial activity of the polymer appears to depend quite heavily on the type of bacterium used in the study, as well as on the structure of the QAC and the rest of the polymer.

It has been shown by many research groups that changing the length of the substituted alkyl chain of a QAC can have a drastic effect on its effectiveness as a bactericide. It is thought that the hydrophobic alkyl chain facilitates binding to the bacterial cell membrane; thus QACs with a longer alkyl chain are often found to be more biologically active.^{90,101,102} If the chain length is too long, however, then one would expect aggregation of the hydrophobic chains and a subsequent loss of activity: this has also been demonstrated by a number of research groups.^{91,101} This clearly demonstrates that a balance between hydrophobicity and hydrophilicity is required, as both the positive charge and the length of the alkyl chain are important with regards to the antibacterial activity of QACs.^{100,101}

Though they demonstrate excellent antimicrobial properties, there are concerns regarding the cytotoxicity of polymers containing QACs; however, this shouldn't be an issue if they are covalently bound to a surface. These concerns do not extend to the semi-synthetic polymer chitosan, though. In addition to concerns about toxicity, there is also evidence of bacteria becoming less susceptible to the mode of action of QACs, which appears to be associated with increased efflux pump activity.⁷⁷ That said, there is certainly potential for the use of surfaces with covalently bound QACs in almost any conceivable application, including for the development of medical implant devices.

1.3.3 Quaternary phosphonium compounds (QPCs)

In almost every respect, from the way they are prepared through to their mode of action against bacteria, QPCs are identical to QACs.¹⁰⁰ A number of research groups have compared the antibacterial activities of structurally related polymers containing QPCs and QACs; in almost every case it was found that QPCs are more effective biocides than their QAC counterparts.¹¹⁰⁻¹¹⁶ The larger atomic radius of phosphorus means that the association between the anion and the cation of a QPC is weaker than would be observed for an analogous QAC. It is believed that this results in improved binding of QPSs to bacterial cell membranes.¹⁰⁰

The use of QPCs to prevent the bacterial colonisation of polymeric surfaces appears to have many advantages, even over the formidable QACs; however, due to the susceptibility of their phosphine precursors towards reduction, QPCs are somewhat more difficult to produce.¹⁰⁰ This would appear to explain why the development of surfaces containing QPCs is relatively much less advanced than for those with incorporated QACs.

1.3.4 Antimicrobial peptides (AMPs)

In recent years, a number of research groups have physically adsorbed or covalently attached a variety of naturally occurring AMPs to different polymeric surfaces. They are broad-spectrum antimicrobial agents that constitute an important part of the immune system of many different types of organisms, including humans.⁷⁸ As they contain cationic amino acid residues, it is perhaps no surprise that their mode of action is thought to be very similar to that of the previously described QACs: it has been proposed that they kill bacteria by disrupting the charge distribution of the cell membrane, resulting in cell permeabilisation and subsequent necrosis.¹¹⁷

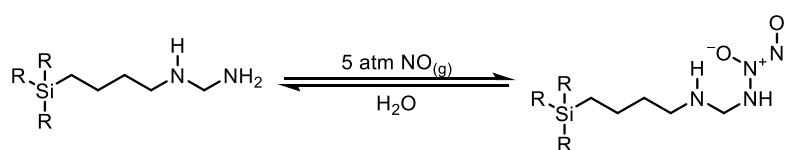
The methods used to produce surfaces containing AMPs are, somewhat unsurprisingly, very similar to those used for the generation of surfaces that contain QACs/QPCs. The use of layer-by-layer assembly is very popular, and a number of other research groups have utilised the fact that AMPs tend to be highly functionalised by covalently linking them to commercially available, or pre-functionalised, polymeric surfaces.¹¹⁷

Since they exist in living organisms, there is unlikely to be an issue with regards to cytotoxicity, which has been highlighted as a potential drawback of synthetically produced QACs and QPCs. On the other hand, due to their structural complexity, AMPs are notoriously difficult to synthesise; therefore, for their use to become widespread, more practical and cost-effective synthetic routes need to be elucidated. Alternatively, biological production methods could be improved.

1.3.5 Nitric oxide (NO)

Even though NO is not biocidal in its own right, the fact that its mode of action induces the killing of bacteria, albeit indirectly, is the reason it will be discussed herein. It has been known since the 1980s that NO is an important signalling molecule, which is involved in various physiological processes, including cardiovascular homeostasis, immune response, bone metabolism, and neurotransmission. Several research groups have tried to develop biomaterials that release NO, as it is felt that they could be used to prevent various complications (e.g. thrombus formation, neointimal hyperplasia, cerebral vasospasms, or blood perfusion) which arise because of the implantation of medical devices such as cardiovascular grafts. As well as their use in other applications, including the treatment of female sexual dysfunction and in wound healing, it has also been proposed that polymers which can release NO might be effective at preventing unwanted microbial contamination. This is because it is believed that an additional supply of NO should enhance the immune system's response to the presence of foreign microorganisms, which would lead to their subsequent eradication.¹¹⁸

In the last fifteen years, Schoenfisch and co-workers have developed an NO-releasing sol-gel coating, which has been shown to prevent bacterial adhesion in a range of different *in vitro* and *in vivo* experiments.¹¹⁹⁻¹²⁴ The coating contains nitrogen-based diazeniumdiolates, which can be hydrolysed under physiological conditions to generate NO (Scheme 5).



Scheme 5. Synthesis of a generic nitrogen-based diazeniumdiolate, as described by Schoenfisch and co-workers.¹¹⁹

Unfortunately, the oxidative decomposition of nitrogen-based diazeniumdiolates can also result in the generation of carcinogenic nitrosamines; therefore, Engelsman *et al.*¹²⁵ devised a novel carbon-based NO-releasing coating (Scheme 6). They applied this coating to surgical meshes, and found that it was effective at preventing the adhesion of *S. aureus*, *E. coli*, and *P. aeruginosa* in *in vitro* experiments; however, they found

the modified meshes were not effective when subcutaneously tested in mice. It was observed that the rate of NO release from the carbon-based coating was six times less than that of the nitrogen-based coating; therefore, the amount of NO that was released might have been too low to prevent microbial colonisation *in vivo*.

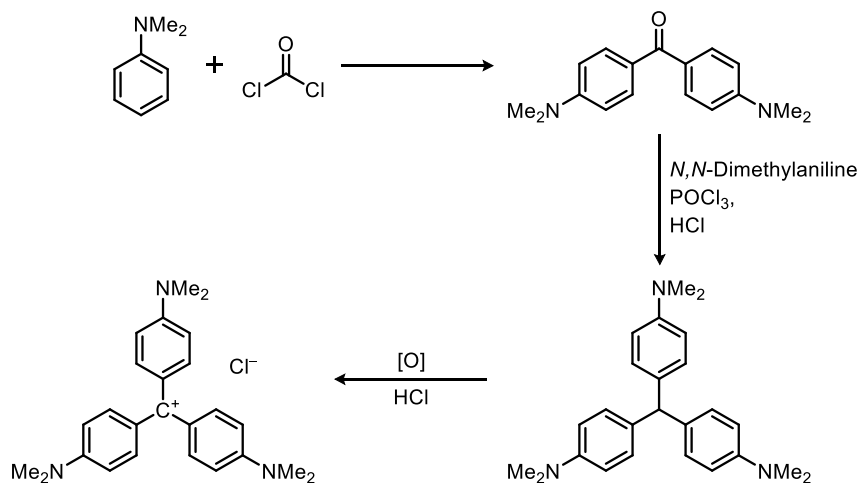


Scheme 6. Synthesis of a functionalised poly(ethylene-vinylacetate) coating containing carbon-based diazeniumdiolate moieties.¹²⁵

Though NO-releasing materials have demonstrated efficacy in *in vitro* and in *in vivo* studies, there is scope to improve their storage efficiency, as well as their antibacterial lifetimes. Moreover, particularly with regards to coatings that contain nitrogen-based diazeniumdiolates, the release of potentially cytotoxic compounds, including nitrosamines, and their subsequent effect, needs to be taken into consideration. The way by which NO is released from the surface coatings that have been discussed also implies that their use is probably restricted to indwelling medical devices.

1.3.6 Crystal violet

In 1883, Kern and Caro described the first synthesis of crystal violet. Firstly, *N,N*-dimethylaniline was reacted with phosgene to give 4,4'-bis(dimethylamino)benzophenone (otherwise known as Michler's ketone). This was then reacted with *N,N*-dimethylaniline and phosphorus oxychloride under acidic conditions. Finally, the colourless, reduced form of crystal violet (known as leucocrystal violet) was oxidised in the presence of hydrochloric acid (Scheme 7).¹²⁶ Since 1883, a number of different syntheses of crystal violet have been described, though they will not be discussed here.¹²⁷



Scheme 7. The first described synthesis of crystal violet.

In 1912, Churchman *et al.*¹²⁸ found crystal violet to be an effective antibacterial agent against Gram-positive bacteria in both *in vitro* and *in vivo* experiments. It was, however, found that crystal violet was somewhat less effective against Gram-negative bacteria: this is thought to be related to its mode of action. It is known that the cell wall of a typical Gram-positive bacterium contains more acidic components than that of a Gram-negative bacterium; therefore, the cell wall of a Gram-positive bacterium tends to have a lower isoelectric point and thus binds to crystal violet more readily.¹²⁹ In any case, crystal violet was used widely for the treatment of various ailments, including trench mouth, thrush, impetigo, burns, pinworm, and cutaneous and systemic fungal infections; however, the discovery of penicillin in 1928, and the subsequent mass production of antibiotics in the 1940s, resulted in a decline in its popularity.¹³⁰

In 1992, Bakker *et al.*¹³¹ were on the hunt for an antimicrobial drug that was inexpensive, simple to prepare, chemically stable, and active in low concentrations. This led to crystal violet being revisited as a potential antimicrobial. The group found that it was a highly effective biocide against several different species' Gram-positive bacteria, as well as against *C. albicans*, in an *in vitro* experiment.

In more recent times, a number of research groups have demonstrated that polymeric surfaces that have been coated with gendine, which is a combination of crystal violet and chlorhexidine, are highly effective at preventing bacterial adhesion and the subsequent development of biofilms, in both *in vitro* and *in vivo* studies.¹³²⁻¹³⁴ It is not clear whether this combination

of antiseptics acts in synergy, as appropriate control experiments were not conducted.

Despite its extensive use in various clinical applications, there are concerns regarding the toxicity of crystal violet. In particular, it is known to be carcinogenic due to its ability to interact with intracellular DNA.¹³⁵ That said, large amounts of crystal violet were used in studies which have shown this; therefore, one might argue that if this substance was to be used sparingly, then it should not pose a significant risk to human health.¹³⁰

1.3.7 Triclosan

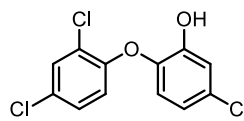


Figure 4. Triclosan.

Since the 1960s, triclosan has been utilised in numerous applications, owing to it being a potent broad-spectrum antimicrobial agent.¹³⁶ Its incorporation into various polymeric materials has often resulted in the generation of surfaces that are resistant to the adhesion of bacteria and subsequent biofilm formation.^{137,138} There have, however, been instances where the modified polymers have not functioned as hoped, with little to no antimicrobial activity observed.^{139,140}

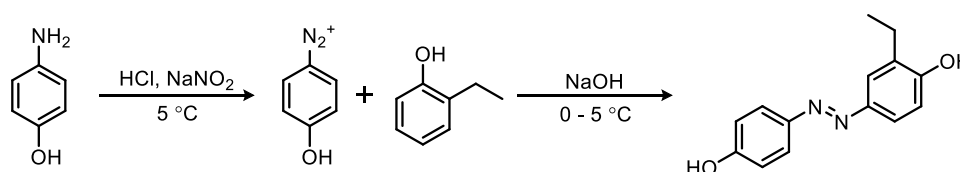
Until 1998, it was presumed that triclosan killed bacteria by interacting with multiple cellular sites; however, it has since been shown that it targets a specific fatty acid biosynthetic enzyme, enoyl-[acyl-carrier protein] reductase. There are thus serious concerns regarding its widespread use, as resistant strains of bacteria can evolve in much the same way as they do when antibiotics are over-used. Moreover, a number of laboratory based studies have shown that bacterial strains which are resistant to triclosan are also not affected by some antibiotics: in essence, cross-resistance has been observed.¹³⁶ That said, the use of triclosan in the clinical environment over the last few decades has not given rise to a single reported incidence of bacterial resistance.¹³⁸

1.3.8 Other non-metallic biocides

In addition to the previously discussed non-metallic biocidal agents, many other disinfectants have been incorporated into, or covalently bound to the surface of, various polymers. Three recent examples are given to highlight the seemingly limitless range of possibilities with regards to producing effective antibacterial surfaces.

In 2010, Luo *et al.*¹⁴¹ prepared polyurethane films that were incorporated with iodine, a well-known disinfectant. The resultant films demonstrated excellent antibacterial, antifungal, and antiviral properties. In the past, other groups have developed iodine containing polymers and obtained similar results.³¹ Luo *et al.*¹⁴¹ showed that iodine containing polyurethane is toxic towards mammalian cells when the iodine content is greater than, or equal to, 3.46%. Conversely, when the polymer had an iodine content of less than, or equal to, 0.96%, no toxicity was observed. Further *in vivo* studies are required to assess the suitability of iodine containing polymers for use as antibacterial surfaces, or as medical devices.

In 2013, Piotta *et al.*¹⁴² synthesised a novel azobenzene compound (Scheme 8), which they incorporated into polypropylene and low-density polyethylene. They discovered that the resultant polymeric films had excellent antibacterial and antifungal properties. They found that this was true even when the concentration of the azobenzene dye was below 0.01%.



Scheme 8. Synthesis of a novel azobenzene compound.

In the same year, Tran *et al.*¹⁴³ coated poly(vinyl chloride) (PVC), polyurethane, and silicone with selenium nanoparticles. They demonstrated that the growth of *S. aureus* was significantly reduced on the surfaces of these polymers, when compared with the unmodified control samples.

1.3.9 The future of non-metallic disinfectants

The use of broad-spectrum antimicrobial disinfectants, whether they are commercially available or newly synthesised, certainly seems to be a sensible strategy that has been employed for the defence of polymeric surfaces from bacterial colonisation; however, as is the case for all the aforementioned examples, the safety of polymers which have been modified with disinfectants should be rigorously assessed. This is particularly true of polymers that are incorporated with novel compounds, such as the azobenzene compound which was discussed in the previous section. That said, one might argue that if the disinfectant in question is covalently bound to the surface of a polymer, or if the polymer is not part of some indwelling medical device, then the potential toxicity of the antimicrobial agent towards humans is irrelevant.

1.4 Metallic disinfectants

For thousands of years, countless civilisations have utilised the antimicrobial properties of metals, such as silver, copper, and lead, in numerous applications, including water disinfection and food preservation. The Romans, for example, built their water pipes out of lead; the Phoenicians stored water in silver containers to prevent spoilage. Though these ancient civilisations may have been blissfully unaware of the existence of microbes, they can be credited with producing the earliest known antimicrobial materials. The ability of polymers containing silver/copper salts or nanoparticles to prevent bacterial contamination will be evaluated in this section.

1.4.1 Silver

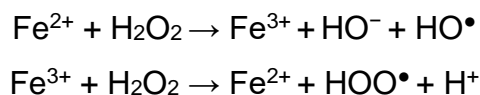
Prior to the discovery and subsequent industrial-scale production of antibiotics, silver salts were commonly used to prevent the onset of infections that can arise if an open wound becomes contaminated with bacteria.¹⁴⁴ In recent times, many research groups have begun to investigate whether silver, either in the form of a salt, or as the metal itself, is effective at preventing the microbial contamination of polymeric surfaces.¹⁴⁴⁻¹⁴⁷

Metals, such as silver, are commonly referred to as “non-essential” – that is, they have no known biological function. The observed antimicrobial activity of

silver is due to the release of Ag(I) ions, as silver itself is chemically inert. It is generally accepted that Ag(I) ions can bring about the death of a microorganism through a combination of different mechanisms, though none of these has been identified as dominant.

It has been shown by transmission electron microscopy (TEM) that Ag(I) ions interact with the cell wall of bacteria, leading to eventual loss of the cellular membrane and subsequent cell death.¹⁴⁸ One theory is that Ag(I) ions bind with sulfhydryl groups present in the cell wall, causing disruption to the bacterial electron transport chain. It has also been proposed that Ag(I) ions are able to disrupt the chemiosmotic potential of the membrane, by interfering with ion transport processes.¹⁴⁹ Either way, the end result is death of the cell in question. As well as showing binding with the cell wall, TEM has been used to demonstrate that Ag(I) ions are able to enter bacterial cells and bind with DNA, enzymes, and proteins.¹⁴⁸ The binding of Ag(I) ions to DNA, for example, causes the DNA to become densely packed, or condensed, thereby preventing replication and cell division. It should be noted, however, that it is impossible to discern whether the processes that are observed lead to cell death, or occur due to the death of the cell.¹⁴⁹

There is also evidence to suggest that reactive oxygen species (ROS), which can kill bacteria *via* a multi-site attack, accumulate in toxic amounts in the presence of Ag(I) ions, and that these have a significant effect on the antimicrobial activity. It has been shown that the antimicrobial activity of Ag(I) ions is enhanced under aerobic conditions, and diminishes when ROS scavengers are present;^{150,151} however, some research groups have obtained results that suggest that ROS contribute negligibly to the observed antimicrobial activity.^{152,153} The generation of excess ROS in the presence of Ag(I) ions is likely due to: the destruction of Fe-S clusters in the cell, which results in the release of Fe(II) ions that can partake in the Fenton reaction (Scheme 9);¹⁵⁴ and the depletion of thiol-containing anti-oxidant reserves, such as glutathione. These processes occur due to the fact that Ag(I) ions are “soft” acids, which are able to bind strongly with the sulfur-containing residues that are present within the cell.¹⁴⁹



Scheme 9. The iron-catalysed generation of hydroxyl and hydroperoxyl radicals: two potent ROS.

Up until this point, silver nanoparticles (particles which are less than 100 nm in size) have not been mentioned, as their mode of action is thought to be a little more complex. Their activity has been shown to be affected by their size,¹⁵⁵⁻¹⁵⁷ shape,¹⁵⁸ and surface charge.^{159,160} It is known that they kill bacteria by releasing Ag(I) ions from the surface, or by binding directly to the cellular sites mentioned above. They are of great interest due to the ease with which they can be embedded into polymeric matrices,¹⁶¹ and the fact that they often exhibit enhanced antibacterial properties.¹⁶²

A number of research groups have shown that pre-oxidised silver nanoparticles are more effective as antibacterial agents.^{159,163} In 2011, Xiu *et al.*¹⁶⁴ demonstrated that silver nanoparticles that were synthesised and tested under anaerobic conditions were non-toxic. Based on this discovery, they inferred that Ag(I) ions are solely accountable for any observed antimicrobial activity, regardless of whether they are released from the surface of the nanoparticle, or remain surface-bound. There are a number of proposed mechanisms for the oxidative generation of Ag(I) ions at the surface of silver nanoparticles *in situ*, which means that silver nanoparticles that haven't been pre-oxidised are still effective biocidal agents.^{153,165,166}

A number of research groups have shown that smaller silver nanoparticles are more toxic towards microorganisms than their larger counterparts. It is believed that this is due to the fact that smaller nanoparticles have a far greater surface area to volume ratio, which means that they are able to generate a higher number of Ag(I) ions by mass at the surface.^{145,159} A major concern for these research groups is the potential for aggregation of the silver nanoparticles they develop; unsurprisingly, their effectiveness as antibacterial agents diminishes with increasing aggregation.^{163,167}

A number of biomaterials incorporated with silver compounds or nanoparticles are commercially available, including wound dressings,^{168,169} endotracheal tubes,^{170,171} prostheses,¹⁷² catheters,^{45,80,173-176} vascular grafts,^{177,178} and

dental devices;¹⁷⁹ however, conflicting results regarding their effectiveness are concerning.^{144,145} Nonetheless, many research groups have developed new silver-incorporated polymeric materials, with the expectation that they should display superior antibacterial properties.^{145-147,161,180-185} One popular method that's been employed to achieve this goal involves the encapsulation of silver compounds or nanoparticles into polymeric hydrogel coatings. This results in the steady release of Ag(I) ions into the surrounding environment over time. A more advanced method involves the incorporation of the active silver agent into biodegradable coatings. The Ag(I) ions are released upon degradation of the coating, which preferably occurs in the presence of bacteria. There is also a growing interest in generating combination coatings, with a particular focus on combining silver with the previously discussed antibacterial polymer, chitosan.

Even though silver-containing polymeric materials have generally been shown to possess favourable antibacterial properties, there are concerns that silver-resistant bacterial strains could become more widespread. There are two mechanisms of resistance that are known to exist. The first involves the formation of insoluble silver compounds within the cell, including Ag₂S. In this way, toxic Ag(I) ions are effectively "mopped up", and stored as harmless salts.¹⁴⁵ The second mechanism involves the active removal of Ag(I) ions from the cell through efflux pumps.¹⁸⁶ It should be noted that neither of these mechanisms confer absolute resistance, and will be essentially useless if the Ag(I) ion concentration is too high.

In addition to the development of silver-resistant bacterial strains, there are also concerns regarding the toxicity of silver towards mammalian cells; in particular, silver nanoparticles have been shown to be toxic towards mammalian cells in *in vitro* and *in vivo* experiments.¹⁸⁷⁻¹⁹² Moreover, although Ag(I) ions are commonly regarded as being significantly less toxic towards mammalian cells than they are towards bacterial cells,¹⁹³ there is conflicting evidence that suggests that this simply isn't true.¹⁹⁴ Clearly, the toxicity of different silver compounds or nanoparticles can only be considered individually.

Like some strains of bacteria, mammalian cells can sequester Ag(I) ions, resulting in the formation of insoluble silver salts. If this occurs in the skin cells, this can result in the skin turning a greyish colour. This condition is known as argyria. Though not life-threatening, it is certainly not aesthetically pleasing either.

If the use of silver-containing polymeric materials is to be continued, then it must be demonstrated that they are both safe to use and effective. The safety of indwelling medical devices containing silver, particularly newly-developed silver nanoparticles that exhibit enhanced antibacterial properties, should be rigorously assessed to ensure that the Ag(I) ion concentration isn't toxic for mammalian cells. Moreover, the use of silver-containing polymeric materials for any application should be carefully controlled to ensure that the chance of silver-resistant bacterial strains developing is minimised.

1.4.2 Copper

Unlike silver, copper is an essential trace element in plants, animals, and aerobic microorganisms. It is required for a number of different functions, including immune response, tissue repair, and radical scavenging within cells.^{195,196} Despite its importance, it can also be fatally toxic above a certain threshold concentration, which is dependent on the organism in question. It is thought that Cu ions, particularly Cu(II) ions, are responsible for the observed antibacterial activity of copper salts and nanoparticles. Like silver, they can bind with various sulfur, oxygen, or nitrogen containing residues that are either (i) part of the cell wall, or (ii) part of various intracellular structures, such as proteins, enzymes, or DNA. If the cellular environment allows for the generation of Cu(I) ions, then these can participate in Fenton-like reactions to generate ROS. Through a combination of different mechanisms, which are very similar to those that are observed with Ag(I) ions, they are able to induce cell death (see section **1.4.1**).^{147,149}

A number of research groups have attempted to produce copper-incorporated antibacterial surfaces.¹⁴⁷ Recently, for example, Sehmi *et al.*¹⁹⁷ embedded silicone and polyurethane with copper nanoparticles *via* a swell-encapsulate-shrink process. This involved dissolving the copper nanoparticles in an

aqueous solution containing ascorbic acid, and then combining this solution with acetone in the ratio 1:9. Immersion of silicone and polyurethane films into these solutions caused swelling of the polymer matrix, which facilitated the uptake of the copper nanoparticles. Removal of the films from the solution and subsequent air-drying overnight resulted in them returning to their original size and shape, with the copper nanoparticles embedded in the polymer matrix. The copper-incorporated polymers both demonstrated potent biocidal activity against methicillin-resistant *S. aureus* and *E. coli*. In addition, recent clinical studies have shown that frequently touched surfaces that are coated with copper or copper alloys, such as door handles, bathroom fixtures, and bed rails, are effective at preventing the proliferation of microbes.¹⁹⁶

As for silver, the use of copper should be carefully controlled to ensure that copper-modified surfaces are both safe towards humans and effective at preventing microbial contamination. The incorporation of materials with copper is somewhat less well documented than for silver. This might be because silver is easier to handle as, in its metallic form, it is chemically inert. On the other hand, copper is prone to oxidation and the formation of potentially unwanted CuO. Nonetheless, further investigations into the usefulness of copper-incorporated materials is warranted, since copper is significantly cheaper and more common than silver.

1.5 Light-activated antibacterial surfaces

It has long been known that light can cause the destruction of microorganisms indirectly, *via* the activation of certain types of molecules or materials. This type of process was first reported in 1900, when Raab *et al.*¹⁹⁸ found that acridine hydrochloride exhibited antibacterial properties against *P. caudatum* in the presence of light (Figure 5). In the following sub-sections, the bactericidal properties of photocatalytic surfaces, and of surfaces containing photosensitiser molecules, will be explored.

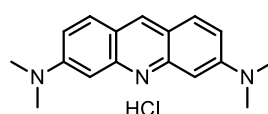
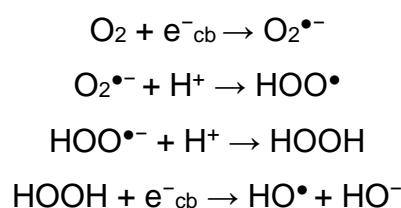


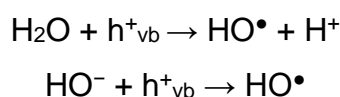
Figure 5. Acridine hydrochloride.

1.5.1 Photocatalytic surfaces

A number of semi-conductors, in particular TiO₂, have demonstrated outstanding self-sterilising properties due to their ability to kill bacteria *via* a photocatalytic mechanism. A semi-conductor has an electronic band structure: the lower energy band is filled with electrons, and is known as the valence band; the higher energy band is unfilled, and is known as the conduction band. The minimum energy required for photoexcitation of an electron from the valence band to the conduction band is known as the band gap. The result of photoexcitation is the generation of positive “holes” in the valence band (h⁺_{vb}), and the accumulation of excess electrons in the conduction band (e⁻_{cb}). These so called “electron-hole pairs” can recombine rapidly; alternatively, they can be “trapped” by suitable electron (³O₂) or positive charge (H₂O) scavengers, thus initiating photocatalytic reactions. The result of these photocatalytic reactions is the production of various ROS, including hydroxyl and hydroperoxyl radicals (Schemes 10 and 11).¹⁹⁹⁻²⁰¹

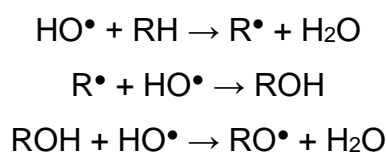


Scheme 10. The photoinduced formation of hydroxyl and hydroperoxyl radicals from oxygen.



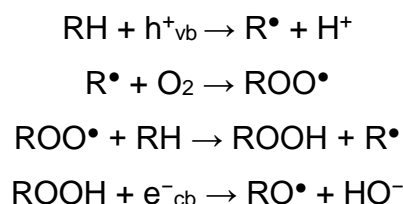
Scheme 11. The photoinduced formation of hydroxyl radicals from water.

The ROS that are generated can oxidise various organic components of bacterial cells, particularly of the cell wall or membrane, thereby inducing cell death. As numerous cellular sites are targeted, the chance of resistant bacterial strains developing is minimal (Scheme 12).^{199,202}



Scheme 12. The oxidation of organic components by hydroxyl radicals.

It has also been proposed that organic components could be directly oxidised by the electron-hole pairs (Scheme 13).²⁰²⁻²⁰⁶



Scheme 13. The oxidation of organic components by electron-hole pairs.

Over a period of time, organic matter adhered to the surface will undergo complete oxidation to form CO₂ and H₂O. This means that photocatalytic surfaces are self-cleaning, as well as being self-sterilising.^{199,202}

It is known that biomedical materials that have been manufactured with Ti alloys demonstrate excellent antibacterial and antiadhesive properties. This is due to the development of a nanometric TiO₂ layer on the surface of such alloys, which results from spontaneous oxidation.²⁰⁷ There is thus a growing interest in coating different materials, from stainless steel to silicone, with TiO₂, using numerous techniques, including a sol-gel process,²⁰⁸⁻²¹¹ anodic oxidation (Ti alloys only),²⁰⁷ electrophoretic deposition,²¹² chemical vapour deposition,^{213,214} plasma immersion ion implantation,²¹⁵⁻²¹⁸ and plasma spray.²¹⁹ In the vast majority of cases, the materials that have been produced have proven to be effective at preventing the adhesion and subsequent formation of bacterial colonies.²²⁰ Some research groups have even coated indwelling medical devices, such as catheters, with TiO₂. For example, Sekiguchi *et al.*²²¹ investigated the efficacy of TiO₂-coated catheters in an *in vivo* experiment, and found them to be highly effective with regards to preventing microbial adhesion.

The photocatalytic activity of TiO₂-coated surfaces can be altered by changing the proportions of the three main polymorphs of TiO₂ (rutile, anatase, and brookite). Although rutile has the smallest band gap, anatase is considered to be the most photochemically active phase. A number of studies have demonstrated that mixed phases (e.g. anatase and rutile, or anatase and brookite) are more active than anatase alone.^{222,223}

Another strategy to improve the photocatalytic efficacy of TiO₂-coated surfaces involves doping with another metal or non-metal.²²⁴⁻²³⁰ In particular, many research groups are interested in producing composites that have a smaller band gap than pure TiO₂ coatings, which would enable them to utilise the energy of visible light. In this area, there has been a lot of interest in N-doped TiO₂ thin films, as they are generally cheap and easy to produce.²²⁴

The ability of materials coated with photocatalytic compounds, particularly TiO₂, to prevent bacterial contamination is well documented. In the case of TiO₂, it is both inexpensive and non-toxic; therefore, it is easy to envisage its utilisation in a huge range of different applications where antibacterial and antiadhesive properties are desirable.²³¹ The mechanisms by which TiO₂-coated surfaces kill bacteria means that the likelihood of resistant bacterial strains developing is small.²⁰² Despite these advantages, the vast majority of TiO₂-coated surfaces require activation with UV light. The use of efficient UV light generating sources can be impractical, and in some cases wholly inappropriate (for example, with regards to the de-contamination of indwelling medical devices).²²⁰ Though a number of groups have tried to decrease the band gap of TiO₂ by altering the chemical properties of these materials,^{224,225} the incorporation of polymeric materials with photosensitiser molecules that absorb light in the visible region of the electromagnetic spectrum might prove to be a more sensible strategy for overcoming this limitation.

1.5.2 Surfaces incorporated with photosensitiser molecules

In 1973, Blossey *et al.*²³² reported the covalent attachment of the photosensitiser Rose Bengal to chloromethylated polystyrene beads *via* an S_N2 reaction. It should be noted, however, that the only evidence for successful covalent attachment was that the dye does not wash off the surface. This observation may simply imply that Rose Bengal is physically adsorbed to the surface. Nonetheless, in 1978 Bezman *et al.*²³³ demonstrated that polystyrene beads with covalently attached Rose Bengal moieties, as prepared by Blossey *et al.*,²³² were able to effect the photoinactivation of *E. coli* with visible light and oxygen. Since these studies were carried out, a number of research groups have investigated different methods for preparing

polymers with incorporated photosensitiser dyes, including various porphyrins, crystal violet, methylene blue, toluidine blue O, and Rose Bengal. Their findings will be discussed in detail below. These molecules tend to contain at least one heterocyclic ring, and have extensive conjugated π -systems (Figure 6).²³⁴

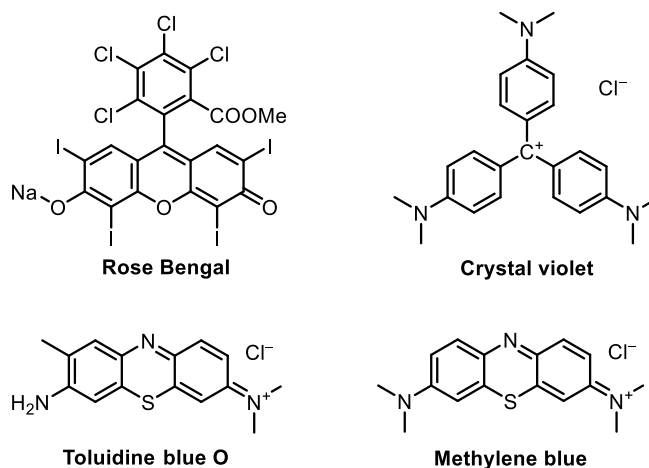


Figure 6. Examples of different types of photosensitiser molecules.

The mechanism of bacterial kill *via* the light-activation of a photosensitiser molecule is best described with the help of a Jablonski diagram (Figure 7). The first step involves absorption of a photon of light, which results in promotion of the photosensitiser molecule from its ground state (S_0) to an excited singlet state (S_1). This is immediately followed by vibrational relaxation to the lowest energy vibrational state. A radiationless process known as intersystem crossing (ISC) then occurs, which results in the molecule being in an excited triplet state (T_1). The triplet state has a longer life time as relaxation to the singlet ground state is spin forbidden. If the molecule doesn't undergo internal conversion or phosphorescence first, it can transfer an electron or energy to surrounding molecules, such as water and oxygen. Electron transfer processes are referred to as type I, while energy transfer processes are designated type II. The type I process requires the interaction of the excited state molecule with another molecular substrate, such as water. The outcome of this is the formation of a variety of ROS, like those that are generated in the TiO_2 photocatalytic process. The type II process involves quenching with molecular oxygen in the environment, which affords the very reactive singlet oxygen species. The combination of ROS, including singlet oxygen, unleashes

a multi-site attack mechanism against microorganisms. The prospect of developing bacterial resistance is therefore minimal, as the chance of bacteria developing more than one type of resistance gene simultaneously is very small.²³⁴

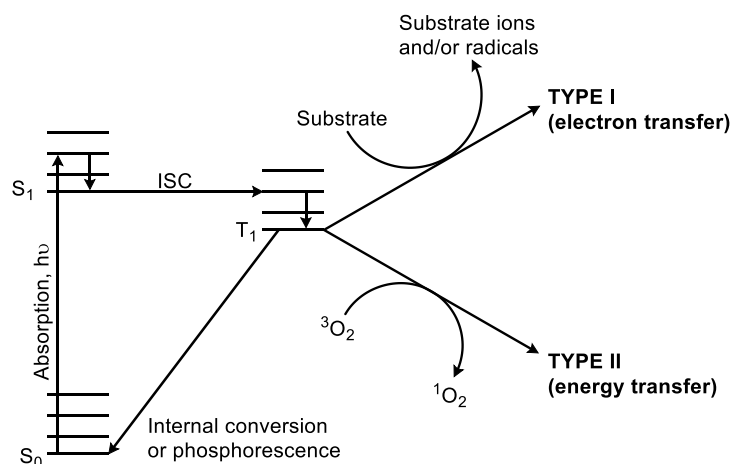


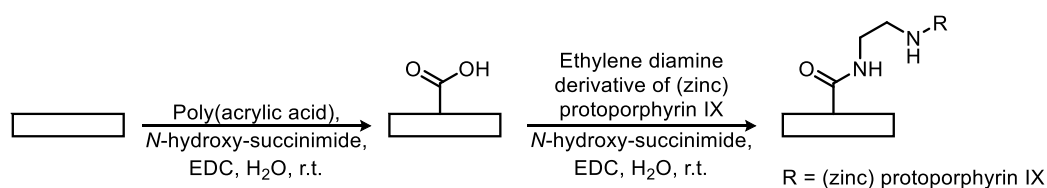
Figure 7. A Jablonski diagram outlining the mechanism of light-activation of a generic photosensitiser.

1.5.2.1 Porphyrins

Polymers with incorporated dyes have exhibited excellent bacterial kill, and have also proven to be highly successful at preventing the formation of, or destroying, bacterial biofilms on the surface when exposed to a visible light source.²³⁴ There has been a growing interest in the ability of porphyrins to protect polymeric surfaces from bacterial contamination in recent years.²³⁵ In addition, they have been utilised in a number of other applications,²³⁶ most notably photodynamic therapy.^{235,237,238}

There are several different methods by which porphyrins, amongst other dyes, might be incorporated into a polymer. In 1993, Bonnett *et al.*²³⁹ utilised three different techniques to generate a series of porphyrin-incorporated polymer films: impregnation, by immersion of the polymer in a solution of the porphyrin; co-dissolution of the polymer and the dye, followed by casting; and co-polymerisation of porphyrin containing monomers to generate polymers with covalently bound porphyrins. They noticed that the charge of the porphyrin was often important; for example, regenerated cellulose showed a greater affinity for cationic porphyrins over neutral or anionic porphyrins. Clearly, the best porphyrin in a given situation might prove to be completely ineffective in different circumstances.

In recent years, there has been increasing interest in the development of polymers with covalently bound porphyrins.²⁴⁰⁻²⁴⁹ In 2003, the Michielsen group covalently grafted protoporphyrin IX and zinc protoporphyrin IX to the surface of nylon-6,6 films.^{240,241} They first grafted poly(acrylic acid) to the surface, and then reacted the modified surface with ethylene diamine derivatives of the aforementioned porphyrins (Scheme 14). The group then demonstrated that both modified surfaces were active against *S. aureus* and *E. coli* in the presence of a light source. Of the two materials, that which contained zinc protoporphyrin IX was the more effective.



Scheme 14. The preparation of modified nylon films with covalently grafted (zinc) protoporphyrin IX, as described by Sherrill *et al.*²⁴⁰

Since 2003, many other research groups from around the world have covalently attached different types of porphyrins to a variety of different polymers. A number of groups have utilised the intrinsic reactivity of polymers such as cellulose,²⁴³⁻²⁴⁹ which contains hydroxyl groups; and chitosan,²⁴² which contains amino groups, in order to achieve their goals. Meanwhile, other research groups have conducted polymerisation reactions with,²⁵⁰ or in the presence of,^{251,252} appropriately functionalised porphyrins in order to generate the corresponding polymers. In many cases, it has been demonstrated that the resultant materials exhibit antibacterial properties in the presence of light. It has, however, been noted that porphyrin-incorporated materials are significantly more active against Gram-positive bacteria than they are against Gram-negative bacteria.²⁴¹

In 2011 Ringot *et al.*²⁴⁷ demonstrated that a surface-bound cationic porphyrin was more photoactive against *S. aureus* than a surface-bound neutral porphyrin, which was itself more active than a surface-bound anionic porphyrin. The relative effectiveness of cationic porphyrins as photobactericidal agents has been alluded to elsewhere, so this result is perhaps not entirely surprising.²⁵³⁻²⁵⁵ Though a number of different research

groups have investigated the biological activity of porphyrins with different charges, few studies have been carried out to explore the effect of more subtle structural changes.

The effect of combining porphyrins, or related compounds, with metal nanoparticles, has been investigated in recent years. For example, Lyutakov *et al.*²⁵⁶ demonstrated that polymethylmethacrylate films that were doped with *meso*-tetraphenylporphyrin and silver nanoparticles were more efficacious at killing bacteria than those which were incorporated with only one or the other.

1.5.2.2 Phenothiazinium dyes

The ability of polymers that are incorporated with dyes other than porphyrins to resist bacterial contamination has also been extensively studied. In particular, there have been a number of investigations into the usefulness of phenothiazinium dyes, such as methylene blue and toluidine blue O. These cationic dyes, which are derived from phenothiazine, have frequently exhibited excellent antibacterial properties, both in solution and when incorporated into a polymer. In 1997, Wainwright *et al.*²⁵⁷ tested the relative photobactericidal activities of the following phenothiazinium dyes: toluidine blue O, methylene blue, methylene green, and dimethyl methylene blue. They compared the activities of these dyes with two acridine photosensitisers: acridine orange and proflavine. They discovered that, in general, the photobactericidal activities of the phenothiazinium dyes were more pronounced. Of the phenothiazinium dyes, toluidine blue O was shown to be the most effective photosensitiser against the following strains of bacteria: *P. aeruginosa*, *E. coli*, and *E. faecalis*.

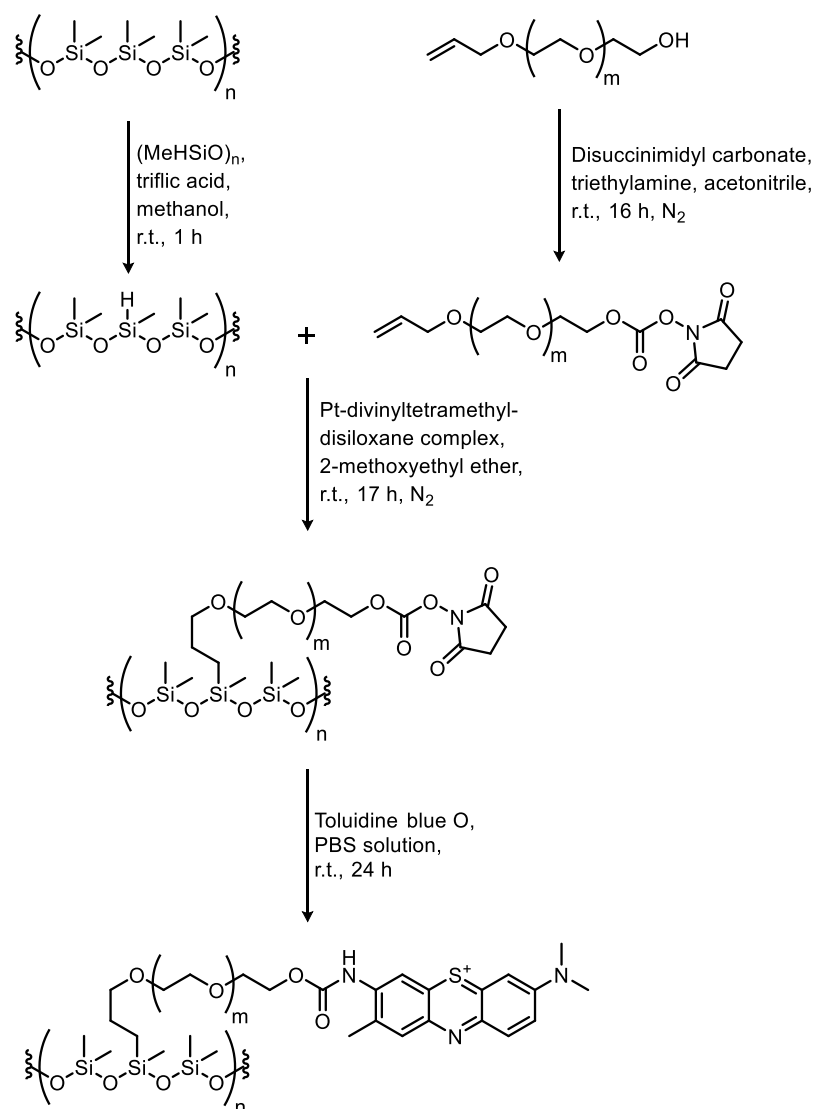
In 2003, Wilson *et al.*²⁵⁸ demonstrated that cellulose acetate films which were incorporated with toluidine blue O were effective at killing *S. aureus* and *P. aeruginosa* after one day of white light illumination. Three years later, the same group incorporated cellulose acetate with a combination of toluidine blue O and Rose Bengal, an anionic dye.²⁵⁹ It was shown that cellulose acetate films containing toluidine blue O and Rose Bengal could reduce the viable count of several different bacterial strains (*S. aureus*, methicillin-resistant *S. aureus*, *C. difficile*, and *E. coli*) to below the detection limit after white light illumination for up to sixteen hours. They were also effective at killing suspensions of *S.*

aureus that were sprayed onto the surface.²⁶⁰ Further studies have demonstrated the ability of cellulose acetate coatings that contain toluidine blue O and Rose Bengal to reduce the levels of bacterial contamination in a clinical environment.²⁶¹

In 2009, the photobactericidal properties of silicone films incorporated with combinations of either methylene blue and gold nanoparticles, or toluidine blue O and gold nanoparticles, were investigated.^{262,263} It should be noted that gold nanoparticles do not display any antibacterial properties; moreover, unless otherwise stated, the gold nanoparticles that were used were 2 nm in diameter. The Parkin group found that gold nanoparticles enhanced the ability of methylene blue-incorporated silicone films to kill bacteria in the presence of light, but that this effect was not observed with silicone films that were incorporated with toluidine blue O. It was, however, apparent that silicone films that were incorporated with toluidine blue O were vastly more effective at killing bacteria than those which contained methylene blue, with or without gold nanoparticles. The latter observation is perhaps not surprising when one takes into consideration the previous observations of Wainwright *et al.*,²⁵⁷ discussed above. The observation that methylene blue in the presence of gold nanoparticles displays enhanced light-induced antibacterial properties is rather more intriguing, and has been the subject of further studies. In 2012, Noimark *et al.*²⁶⁴ conducted a series of time-resolved electron paramagnetic resonance experiments with PVC films that had been incorporated with methylene blue and gold nanoparticles. The results suggested that methylene blue triplet state production is enhanced by the presence of the gold nanoparticles. Further studies have shown that larger gold nanoparticles (5 nm or 20 nm) do not enhance the activity of methylene blue.²⁶⁵ In addition, silicone films that were embedded with a combination of methylene blue and gold nanoparticles were effective at preventing the formation of bacterial biofilms,²⁶⁶ killing *S. aureus* when illuminated with a white light source (as opposed to a laser light of a particular wavelength),²⁶⁷ and preventing the bacterial contamination of hospital surfaces in a clinical trial.²⁶⁸

In all the previously discussed examples, toluidine blue O or methylene blue was incorporated into the polymer in question *via* a swell-encapsulate-shrink

process, and was thus physically adsorbed to the polymeric matrix. In 2009, Piccirillo *et al.*²⁶⁹ produced two different silicone polymers with covalently bound methylene blue, or toluidine blue O, moieties. They first functionalised the surface of silicone with $(\text{MeHSiO})_n$ in the presence of triflic acid. This afforded them a polymer with Si-H bonds, which was then reacted with a functionalised PEG linker containing an allyl ether in a hydrosilylation reaction. The resultant polymer was treated with methylene blue or toluidine blue O in PBS solution (Scheme 15). The dye-functionalised polymers exhibited excellent photobactericidal activities against *E. coli* and *S. epidermidis*. Unfortunately, the use of expensive and/or harsh reagents throughout this synthesis, such as platinum-divinyltetramethyldisiloxane complex or triflic acid, means that it is not industrially viable. There is thus an interest in developing new and improved routes towards light-activated antibacterial surfaces with covalently bound phenothiazinium dyes.



Scheme 15. The synthesis of a silicone polymer with covalently attached toluidine blue O moieties, as described by Piccirillo *et al.*²⁶⁹

1.5.2.3 Crystal violet

In 2013, Noimark *et al.*²⁷⁰ incorporated silicone with crystal violet, and when they exposed the resultant polymer to laser light, discovered that it was significantly more effective at killing bacteria (*S. epidermidis* and *E. coli*) than silicone which was incorporated with methylene blue and gold nanoparticles. As with methylene blue, they found that gold nanoparticles enhanced the photobactericidal properties of crystal violet. More recently, it was also demonstrated that a crystal violet-incorporated silicone film was able to kill *S. aureus* and *E. coli* in the presence of a white light source.²⁷¹ A year later, Noimark *et al.*²⁷² produced a silicone film which was incorporated with a combination of crystal violet, methylene blue, and gold nanoparticles. They

showed that it was even more potent at killing bacteria (*S. epidermidis* and *E. coli*) than a silicone film which contained only crystal violet and gold nanoparticles. Moreover, they found that this new polymer could kill bacteria in the dark, although it was markedly less efficacious under these conditions. The usefulness of this polymer has been demonstrated practically: Page *et al.*²⁷³ developed photobactericidal mobile phone and tablet screen protectors by incorporating them with methylene blue, crystal violet, and gold nanoparticles.

In further studies, the ability of zinc nanoparticles to improve the antibacterial properties of crystal violet-incorporated silicone films was investigated.^{274,275} It was found that the film containing both crystal violet and zinc nanoparticles was more effective than films containing only crystal violet or zinc nanoparticles. In 2015, Sehmi *et al.*²⁷⁶ observed similar results with crystal violet-incorporated polyurethane films; however, they also found that the polymer containing crystal violet and zinc nanoparticles killed 99.9% of *S. aureus* (after two hours) and *E. coli* (after four hours) in the dark. The polymer demonstrated even more impressive kill rates when exposed to white light. Considering the outstanding performance of this polymer, and the excellent activity that has been observed when crystal violet is combined with methylene blue and gold nanoparticles, it would surely be prudent to assess the photobactericidal properties of polymers containing the following combinations: (i) crystal violet, methylene blue, and zinc nanoparticles; and (ii) crystal violet, methylene blue, zinc nanoparticles, and gold nanoparticles.

Although crystal violet has been incorporated into different polymers on a number of separate occasions, it has never been covalently attached to a polymer surface. The main reason for this is that crystal violet does not contain any reactive functional groups that enable its modification; therefore, to enable its covalent attachment to a polymer surface, one would have to synthesise a suitably functionalised crystal violet derivative.

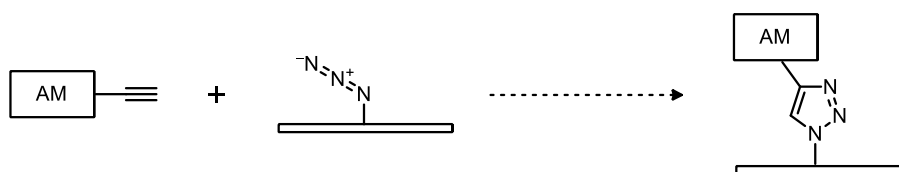
The effectiveness of various light-activated antibacterial agents at reducing the bacterial load on surfaces has been highlighted in this section. As they are able to kill bacteria by the generation of ROS when illuminated, there are no

concerns regarding the development of bacterial strains that are resistant to this method of eradication; however, ROS can oxidise the dye molecules themselves, in a process which is known as photobleaching.²⁷⁷ That said, photobleaching has not been reported as being a problem with the previously described dye-incorporated polymer systems; therefore, the incorporation of polymers with light-activated antibacterial agents would appear to be an excellent strategy to combat bacterial contamination.

2 Results and discussion

One of the main goals of this project was to covalently attach small organic dye molecules, which exhibit antibacterial activity by light-activation, to the surface of a polymer. It was proposed that there would be two major advantages associated with having dyes covalently attached to a polymer surface, instead of them being physically adsorbed; both of which are due to the fact that the dye should not be lost from the surface over time. Firstly, the toxicity of various dyes towards mammalian cells would be irrelevant. Secondly, one would expect that the antibacterial lifetime of the surface should be greatly extended. Of course, a major disadvantage could be that chemical modification of a polymer surface might give it undesirable physical properties; however, if only a small percentage of the surface is modified it is thought that any changes would have a negligible effect on the physical properties of the bulk polymer.²⁷⁸

There are a number of reports in the literature describing the covalent linkage of alkyne or azide containing molecules to the surface of an appropriately functionalised polymer surface, *via* a 1,3-dipolar cycloaddition reaction (Scheme 16).^{9,103,246,248,279-284}



Scheme 16. A generic 1,3-dipolar cycloaddition reaction between an azide-functionalised polymer surface and an alkyne-functionalised antimicrobial molecule (AM).

It was felt that this approach could be utilised for the preparation of antimicrobial polymers with covalently bound photosensitiser molecules of the triarylmethane and phenothiazine classes, such as crystal violet and methylene blue respectively. In the past, compounds such as these have been shown to be highly effective at preventing the bacterial colonisation of various polymeric surfaces.²³⁴ There is, however, only one known publication that describes the covalent attachment of both methylene blue and toluidine blue O to the surface of a silicone polymer. The disadvantages of the route used by Piccirillo *et al.*²⁶⁹ are described extensively in the introduction (See section

1.5.2.2). At the time of writing, there are no known examples describing the covalent grafting of crystal violet, or closely related analogues, to the surface of any polymer.

2.1 Preparation of alkyne-functionalised dyes, and their antibacterial activities

In the following sections, the attempts to synthesise a variety of analogues of methylene blue, toluidine blue O and crystal violet are described. In every case, it was intended that the final product would contain an alkyne substituent that would allow for its covalent attachment to a pre-modified polymer which contained azide functionality. It was felt that alkyne-containing small molecules would be easier to handle than those containing azides, which have the potential to be explosive.

The direct chemical modification of dyes such as crystal violet and methylene blue was not deemed to be a feasible approach. These compounds have no reactive functional groups that could be manipulated to generate analogues containing alkyne substituents. In addition, it was decided that a good approach would involve the formation of the charged, modified dye in the final step of the synthesis. This is because both methylene blue and crystal violet are water soluble, thus it was felt that the purification of the modified dyes might prove to be challenging.

2.1.1 Methylene blue analogues

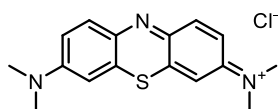
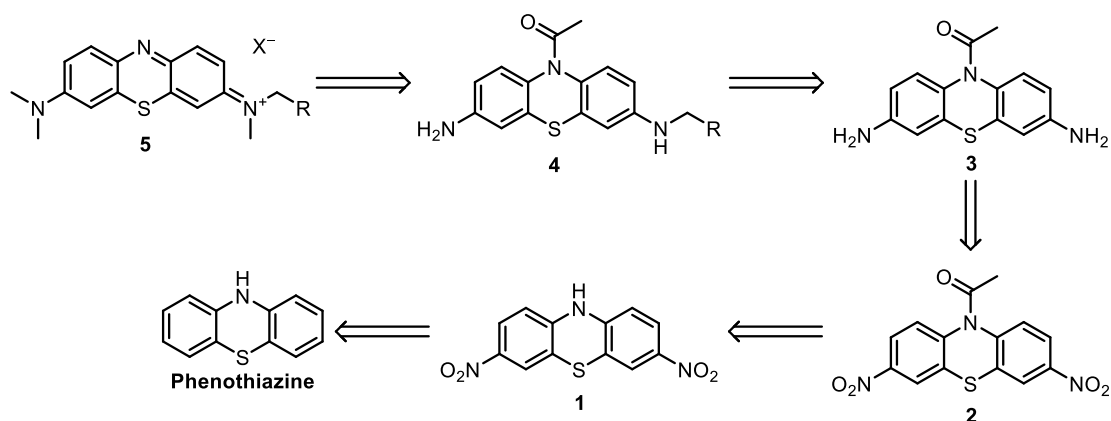


Figure 8. Methylene blue.

In 2007, Wischik *et al.*²⁸⁵ described the synthesis of a number of different phenothiazine salts, as well as their precursors. It was thus postulated that a variety of methylene blue analogues could be accessed by the following route, which is outlined in the retrosynthetic analysis below (Scheme 17).

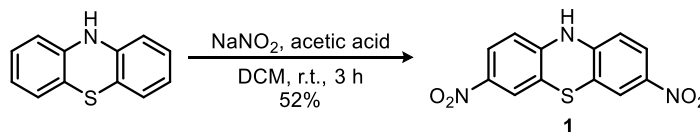


Scheme 17. The proposed synthetic route towards different methylene blue analogues.

The first step of the proposed synthesis involves the di-nitration of commercially available phenothiazine to give di-nitro compound **1**. This is followed by acetylation to give the corresponding acetylated di-nitro compound **2**, and then reduction of the nitro substituents to generate diamine **3**. It was hoped that mono-alkylation at one of the amino positions could then be achieved, with a pre-prepared or commercially available alkyne, to give mono-alkylated diamine **4**. Finally, methylation of the remaining positions, deacetylation, and oxidation would afford methylene blue analogue **5**. In theory, methylene blue analogue **5** could be covalently attached to an azide-functionalised polymer surface by a 1,3-dipolar cycloaddition, as described above. Of course, the reduced form of the methylene blue analogue in question could be linked to a pre-functionalised polymeric surface before undergoing oxidation, if the former approach was unsuccessful.

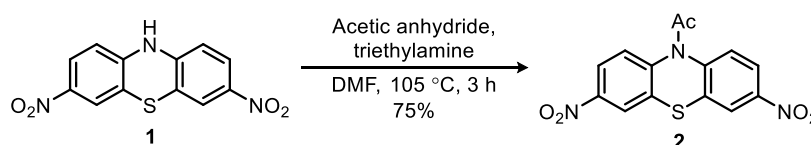
The di-nitration of phenothiazine with NaNO_2 in acetic acid and dichloromethane (DCM) to give 3,7-dinitrophenothiazine **1** did not work as described by Wischik *et al.*²⁸⁵ initially. When the reaction was left for three hours, as specified in the literature, the crude yield of di-nitro compound **1** was only 20%. It was thought that this was due to the reaction not going to completion, as only di-nitro compound **1** was expected to precipitate out of the reaction mixture (See section 4.2). Further experiments were thus attempted, where the number of equivalents of NaNO_2 was increased from six to eight, and the reaction time was extended to six hours. No notable increase in product yield was obtained, so the original reaction conditions were re-

investigated. In this instance, more satisfactory yields of up to 52% were obtained (Scheme 18).²⁸⁵



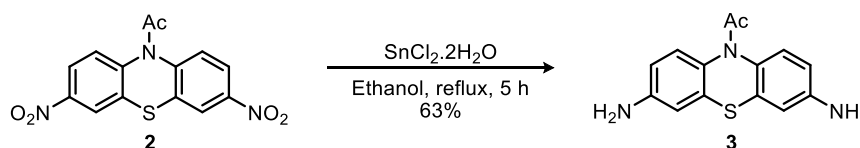
Scheme 18. Di-nitration of phenothiazine.

The acetylation of di-nitro compound **1** using acetic anhydride in *N,N*-dimethylformamide (DMF) with triethylamine gave the corresponding acetylated di-nitro compound **2** in yields of up to 75% (Scheme 19).²⁸⁶



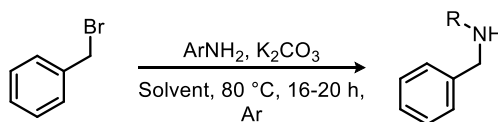
Scheme 19. Acetylation of di-nitro compound 1.

The reduction of acetylated di-nitro compound **2** with $\text{SnCl}_2 \cdot 2\text{H}_2\text{O}$ in ethanol afforded diamine **3** in moderate yields of up to 63% (Scheme 20).²⁸⁵



Scheme 20. Reduction of acetylated di-nitro compound 2.

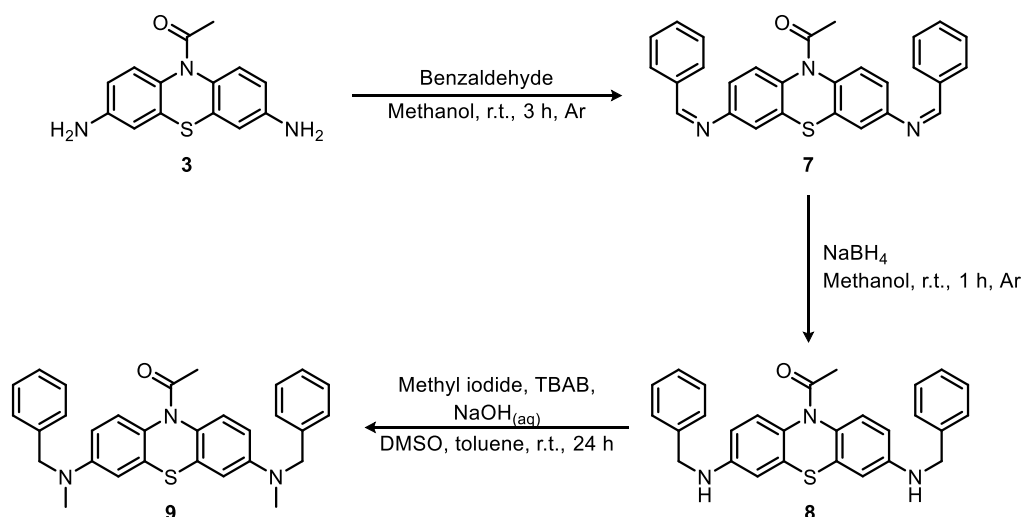
Prior to attempting to attach an alkyne motif to diamine **3**, two model systems were tested to try to discern the best method for mono-alkylation of one or both of the amine substituents.^{287,288} The $\text{S}_{\text{N}}2$ reactions of aniline and 4-aminobenzoic acid with benzyl bromide were investigated: low to moderate yields were obtained in all cases. The di-alkylated product was always observed, along with other unidentifiable by-products. Sadly, the attempted alkylation of diamine **3** gave complex mixtures under two different sets of conditions (Table 1).



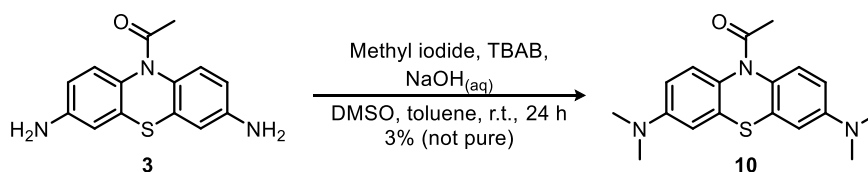
ArNH ₂	Solvent	Yield
Aniline	Acetonitrile	< 37%, 13% isolated, 6
Aniline	DMSO	< 59%, 24% isolated, 6
4-aminobenzoic acid	Acetonitrile	< 26%
4-aminobenzoic acid	DMSO	< 44%
Diamine 3	Acetonitrile	complex mixture
Diamine 3	DMSO	complex mixture

Table 1. Attempted mono-alkylation of aniline, 4-aminobenzoic acid, and diamine **3**.

It was proposed that a slightly different approach might overcome this problem. In theory, the conversion of diamine **3** to an imine, followed by reduction and then methylation, would give the corresponding leucomethylene blue analogue. The reaction between diamine **3** and benzaldehyde to give the corresponding imine **7**, followed by reduction with sodium borohydride to give secondary diamine **8**, and finally methylation with methyl iodide to give leucomethylene blue analogue **9**, was attempted, and gave a complex mixture (Scheme **21**). Unfortunately, it was not possible to isolate any of the intermediates.

Scheme 21. Attempted reductive alkylation of diamine **3**.

Finally, the formation of 10-acetyl-3,7-bis(dimethylamino)phenothiazine **10** was attempted, as described in the literature, but only a 3% crude yield of the desired product was obtained (Scheme **22**).²⁸⁵ At this point, attempts to prepare alkyne-functionalised methylene blue analogues were abandoned.

Scheme 22. Attempted synthesis of 10-acetyl-3,7-bis(dimethylamino)phenothiazine **10**.

2.1.2 Toluidine blue O analogues

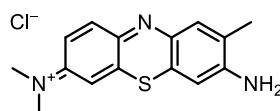
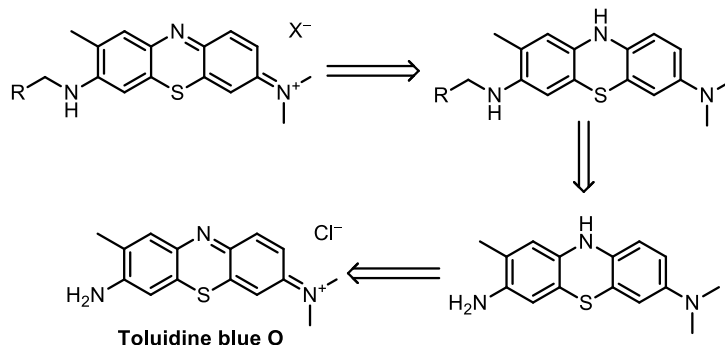


Figure 9. Toluidine blue O.

Considering the difficulties encountered in the attempted synthesis of methylene blue analogues, and the fact that both methylene blue and toluidine blue O contain the same phenothiazine motif, the proposed route to synthesise analogues of toluidine blue O was by starting with the dye itself (Scheme 23). In this instance, it was felt that direct functionalisation might be possible because toluidine blue O contains a primary aniline substituent, which can participate in chemical reactions.



Scheme 23. Proposed synthesis of toluidine blue O analogues.

The reduction of toluidine blue O to form the corresponding leuco dye **11** was attempted using two different methods, but no product was obtained in either case (Table 2).^{286,289}

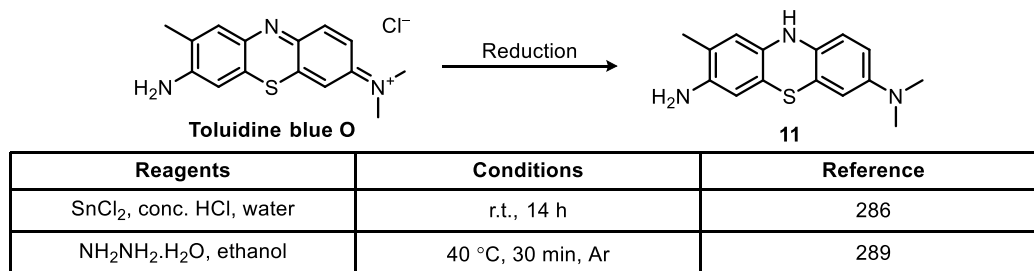
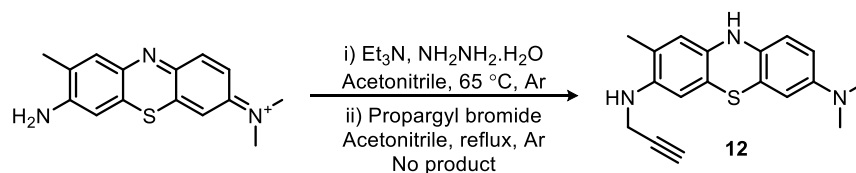


Table 2. Attempted reduction of toluidine blue O.

Instead of trying to isolate leuco dye **11**, a one-pot reaction was attempted where reduction under basic conditions was followed immediately by alkylation with propargyl bromide to give mono-alkylated leuco dye **12** (Scheme 24).²⁸⁶ Once again, the desired product was not obtained.

Scheme 24. Attempted synthesis of mono-alkylated leuco dye **12**.

Rather than continuing to investigate phenothiazine based dyes, it was decided to attempt the formation of alkyne-functionalised crystal violet analogues. In a recent publication, Noimark *et al.*²⁷⁰ had showed that crystal violet incorporated into medical grade silicone exhibited excellent photobactericidal properties, and also induced significant reduction in the numbers of bacterial colonies in the dark.

2.1.3 Crystal violet analogues via a Grignard reaction

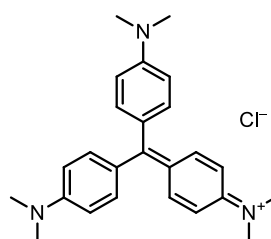
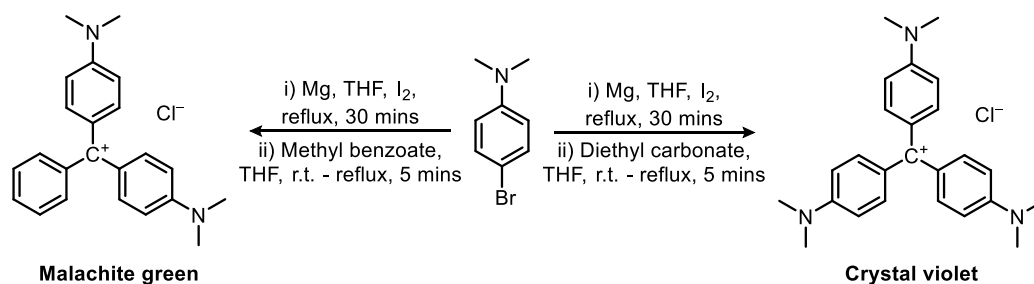
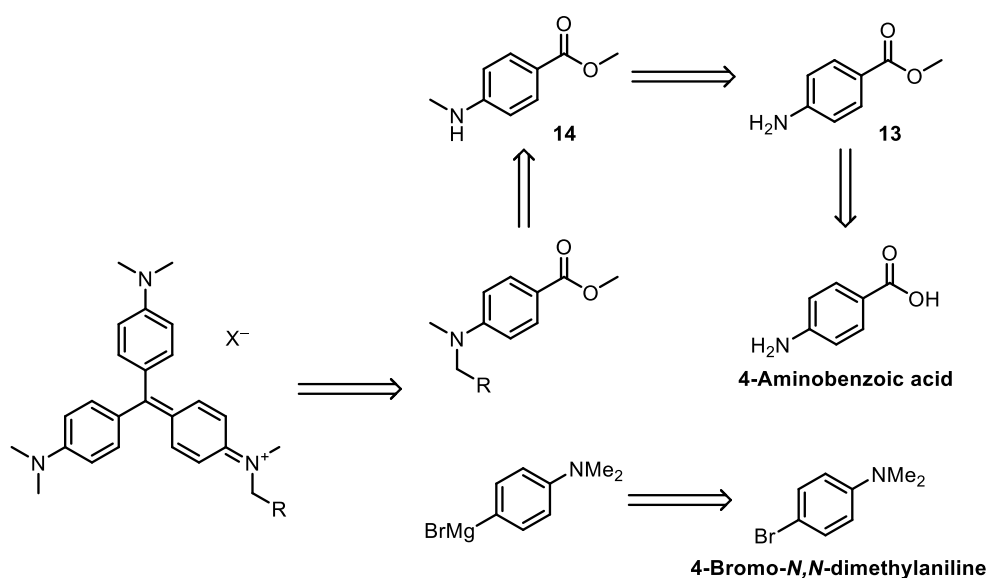


Figure 10. Crystal violet.

In 1996, Taber *et al.*²⁹⁰ demonstrated that it was possible to synthesise crystal violet and malachite green *via* a Grignard reaction (Scheme 25).

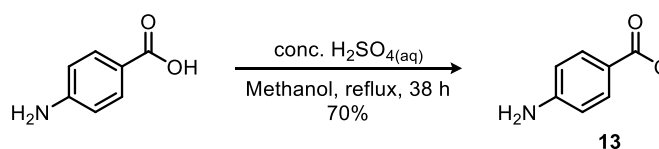
Scheme 25. Synthesis of malachite green and crystal violet, as described by Taber *et al.*²⁹⁰

It was postulated that similar conditions could be used to synthesise an alkyne-containing crystal violet analogue. To achieve this, the synthesis of an alkyne-functionalised tertiary amino benzoate was proposed. This could then be reacted with the Grignard reagent, 4-(*N,N*-dimethylamino)phenyl magnesium bromide, which is prepared from commercially available 4-bromo-*N,N*-dimethylaniline, to give the desired crystal violet analogue. The aminobenzoate could be prepared in three steps, beginning with the esterification of 4-aminobenzoic acid to give methyl 4-aminobenzoate **13**. This would be followed by mono-methylation of the amino position to give methyl 4-(methylamino)benzoate **14**. Finally, alkylation with an alkyne-containing alkyl halide would give the desired alkyne-functionalised tertiary aminobenzoate. The retrosynthetic analysis is detailed below (Scheme 26).



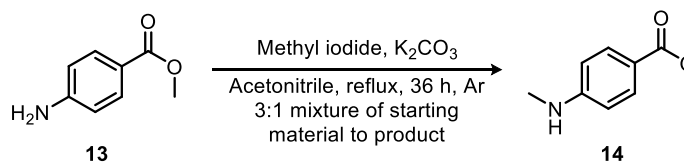
Scheme 26. Proposed synthesis of crystal violet analogues.

The first step involved the acid-catalysed esterification of 4-aminobenzoic acid with methanol to give methyl 4-aminobenzoate **13** in yields of up to 70% (Scheme 27).²⁹¹

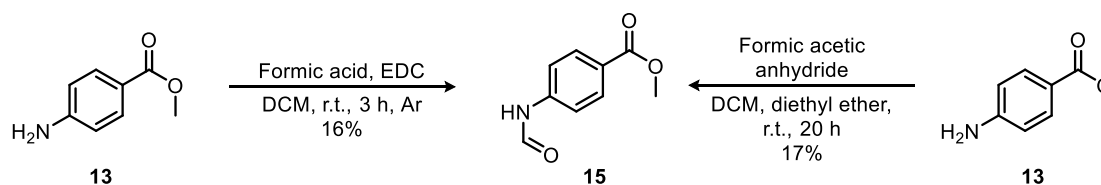


Scheme 27. Esterification of 4-aminobenzoic acid.

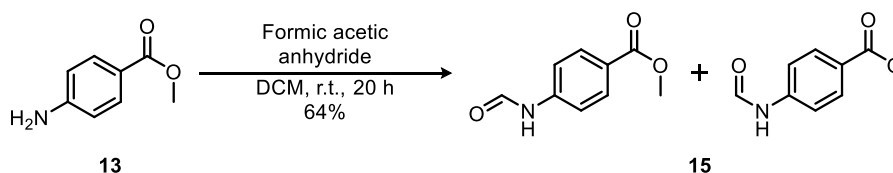
The most direct route towards an alkyne-functionalised crystal violet analogue would have involved mono-methylation of the primary amino substituent in the next step. The conditions of Gray *et al.*²⁸⁷ did not give as good a yield of methyl 4-(methylamino)benzoate **14** as hoped (Scheme **28**). The reaction was sluggish: even after thirty-six hours a 3:1 mixture of starting material to product was obtained. Another issue that was encountered was that the addition of extra methyl iodide gave rise to methyl 4-(dimethylamino)benzoate exclusively: an undesired by-product.

Scheme 28. Attempted mono-methylation of methyl 4-aminobenzoate **13**.

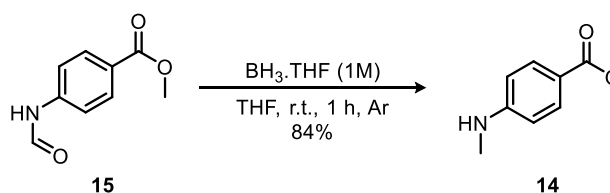
Instead, a two-step route towards methyl 4-(methylamino)benzoate **14**, involving reductive amination, was investigated. The first step involved formylation of methyl 4-aminobenzoate **13** to afford the corresponding formamide **15**. Initially, two sets of conditions were explored for this reaction: one involved the use of 1-ethyl-3-(3-dimethylaminopropyl)carbodiimide hydrochloride (EDC), a carboxyl activating agent, with formic acid; the other involved the formation of formic acetic anhydride by the reaction of formic acid and acetic anhydride, which was then reacted with methyl 4-aminobenzoate **13**. Unfortunately, both reactions gave low yields of 16% and 17% respectively (Scheme **29**).

Scheme 29. Formylation of methyl 4-aminobenzoate **13**.

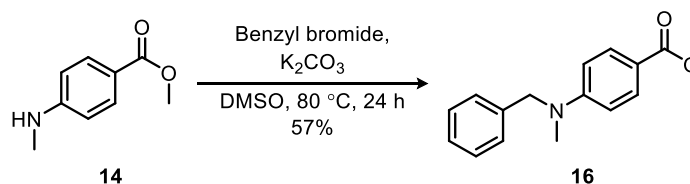
As EDC is quite expensive relative to acetic anhydride and formic acid, attempts to optimise the latter reaction were undertaken. In the above reaction, diethyl ether was added to formic acetic anhydride, and methyl 4-aminobenzoate **13** was added to this mixture as a solution in DCM. It was decided to repeat the reaction in DCM instead of using diethyl ether. Once the reaction was complete, the reaction mixture was concentrated *in vacuo*, before removal of any impurities by dissolution of the residue in diethyl ether and subsequent removal of insoluble impurities by filtration. This gave vastly improved yields of up to 64% (Scheme 30). In some cases, where it proved difficult to remove residual acetic acid, the resultant product was washed with water. The desired product was obtained as a mixture of rotamers in a ratio of 3:1.

Scheme 30. Synthesis of formamide **15**.

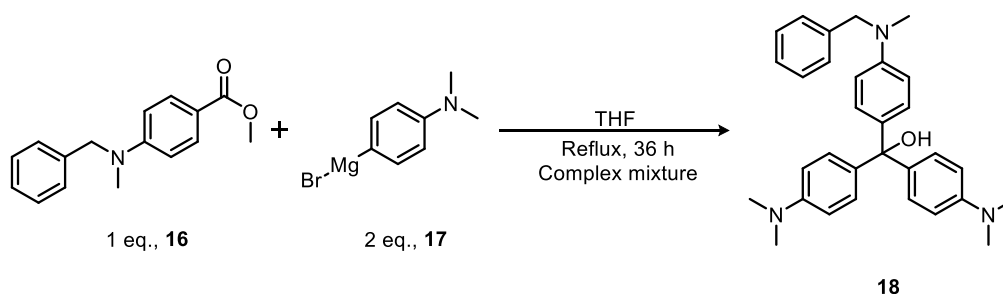
The reduction of formamide **15** using $\text{BH}_3\text{-THF}$, dissolved in tetrahydrofuran (THF), gave methyl 4-(methylamino)benzoate **14** in yields of up to 84% (Scheme 31). It was found that the intermediate boron species was quenched by the dropwise addition of methanol, and that refluxing this species in 6M HCl (the method used by another research group for a much more complex compound), gave no product.²⁹²

Scheme 31. Reduction of formamide **16**.

The next step in the synthesis required the alkylation of methyl 4-(methylamino)benzoate **14** with a pre-synthesised, or commercially available, alkyne motif. The alkylation was tested using benzyl bromide and the conditions of Srivastava *et al.*,²⁸⁸ and tertiary aminobenzoate **16** was obtained in a moderate yield of 57% (Scheme 32).

Scheme 32. Alkylation of methyl 4-(methylamino)benzoate **14**.

The proposed double-Grignard reaction was attempted with tertiary aminobenzoate **16**: 4-bromo-*N,N*-dimethylaniline was reacted with magnesium turnings in THF to generate the Grignard reagent **17**, to which was added tertiary aminobenzoate **16** (Scheme 33).

Scheme 33. Attempted synthesis of crystal violet analogue **18**.

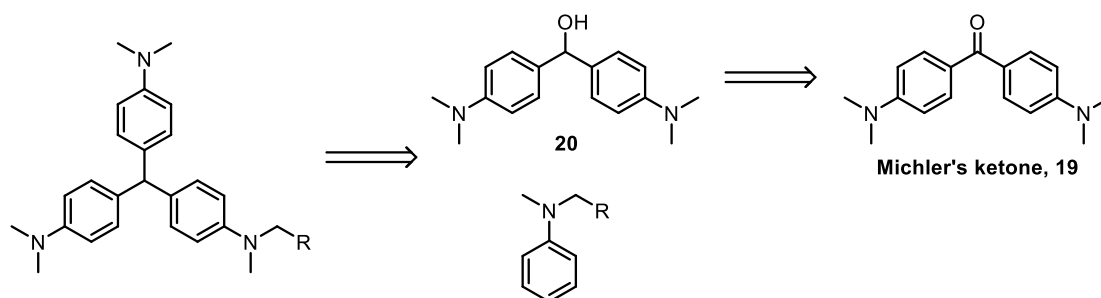
It was not possible to isolate the product **18** from this reaction, if it was formed at all. After an aqueous work-up, a small amount of blue solid was isolated, which was an unidentifiable mixture of compounds. At this stage, another route towards alkyne-functionalised crystal violet analogues had been identified, and was deemed to be worthy of further exploration.

2.1.4 Leucocrystal violet analogues from Michler's hydrol

A different route, involving the synthesis of a leucocrystal violet analogue, was postulated as being a better method for preparing a variety of crystal violet analogues. It was proposed that the leuco dye could be attached to the surface before being oxidised to the photoactive coloured form. Any difficulties associated with the purification of charged dyes would thus be overcome as, in theory, any by-products from the oxidation reaction could simply be washed from the surface.

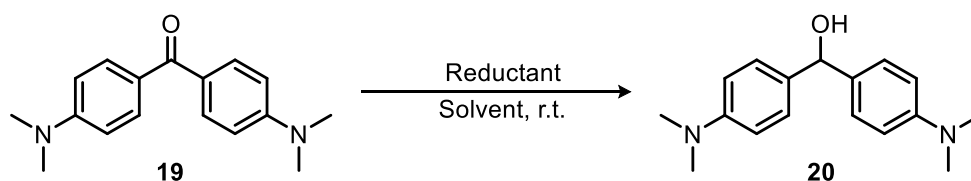
The proposed synthesis of a variety of different leucocrystal violet analogues involved two steps, not including the formation of an appropriately functionalised tertiary aniline. Firstly, bis(4-(dimethylamino)phenyl)methanone

(Michler's ketone) **19** would be reduced to bis(4-(dimethylamino)phenyl)methanol (Michler's hydrol) **20**. Secondly, an acid-catalysed reaction between Michler's hydrol **20** and a pre-prepared tertiary aniline alkyne motif would give the corresponding leucocrystal violet analogue (Scheme **34**).^{293,294}



Scheme **34**. Proposed synthesis of leucocrystal violet analogues.

The preparation of Michler's hydrol **20** was more problematic than originally anticipated. Costero *et al.*²⁹⁵ previously claimed that the reduction of Michler's ketone **19** with NaBH₄ gave Michler's hydrol **20** in an excellent yield of 95%. The reaction was attempted as described, and also with subtle changes to the reaction conditions. In addition, other reducing agents were tested, but only conversions of up to 40% were achieved (Table **3**).



Reductant ^a	Solvent	Time	Relative concentration	% Conversion
NaBH ₄ ⁽¹⁾ , 10 eq.	Methanol	18 hours	1	0
NaBH ₄ ⁽²⁾ , 10 eq.	Methanol	18 hours	1	10
NaBH ₄ ⁽²⁾ , 10 eq.	Methanol	18 hours	1	0 ^b
NaBH ₄ ⁽³⁾ , 10 eq.	Methanol	18 hours	1	10
NaBH ₄ ⁽²⁾ , 10 eq.	Ethanol	18 hours	1	40
NaBH ₄ ⁽²⁾ , 10 eq.	Methanol	18 hours	5	0
NaBH ₄ ⁽²⁾ , 20 eq.	Methanol	18 hours	1	30
NaBH ₄ ⁽²⁾ , 20 eq.	Methanol	96 hours	1	30
NaBH ₄ ⁽²⁾ , 10 eq.	Methanol	18 hours	2	0
NaBH ₄ ⁽⁴⁾ , 10 eq.	Methanol	18 hours	10	0
NaBH ₄ ⁽⁴⁾ , 10 eq.	Methanol	18 hours	10	20 ^c
NaBH ₄ ⁽⁴⁾ , 10 eq.	THF	18 hours	10	0 ^c
LiBH ₄ , 10 eq.	Methanol	18 hours	10	40
NaBH ₄ ⁽⁴⁾ , 10 eq.	Methanol	10 minutes	10	55 ^d
Li(Et) ₃ H, 2 eq.	THF	1 hour	10	Complex mixture
LiAlH ₄ , 5 eq.	THF	1 hour	1	100 ^e

^a Superscript numbers denote different batches of NaBH₄ used.

^b The reaction mixture was refluxed.

^c Reaction was performed under an inert atmosphere of argon.

^d CeCl₃·8H₂O used as an additive; crude yield was only 19%.

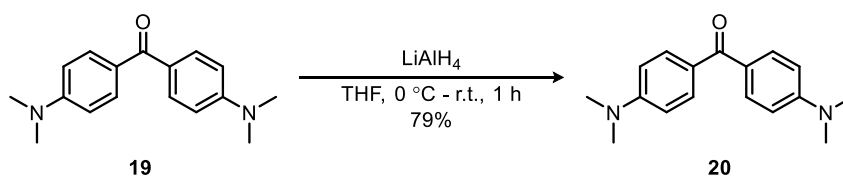
^e The addition of Michler's hydrol was done at 0 °C; afterwards, the reaction mixture was allowed to warm to r.t.

Table 3. Reduction of Michler's ketone 19.

The results indicate that the reaction was very sensitive to the batch of NaBH₄ that was used. Moreover, the concentration of the reaction mixture, as well as the presence or absence of air, were found to be important factors. The use of ethanol seemed to improve the % conversion significantly over the use of methanol or THF. The greater reactivity of LiBH₄ over NaBH₄, due to the more

strongly polarising Li^+ ion that coordinates with the carbonyl in the rate determining step, was apparent.

Fortunately, it was discovered that the powerful reducing agent, LiAlH_4 , gave complete conversion after one hour. The crude product could be recrystallized from benzene to give Michler's hydrol **20** in yields of up to 79%; however, the capricious nature of this reaction meant that the purity of the crude product was variable and thus yields could vary quite dramatically (Scheme 35).



Scheme 35. Reduction of Michler's ketone **19** using LiAlH_4 .

Having successfully synthesised Michler's hydrol **20**, two different alkyne-containing tertiary anilines **21** and **22** were identified as target compounds (Figure 11). One of the substrates contains an alkyne moiety that is conjugated with an aromatic ring, the other contains an isolated alkyne. It was hypothesised that they would both therefore have differing levels of reactivity when, in the future, attempts would be made to react them with an azide-functionalised surface.

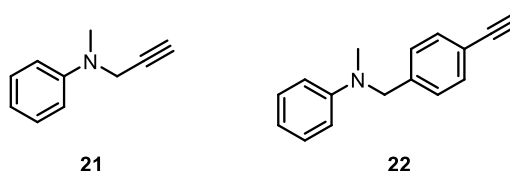
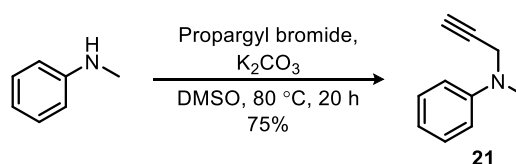


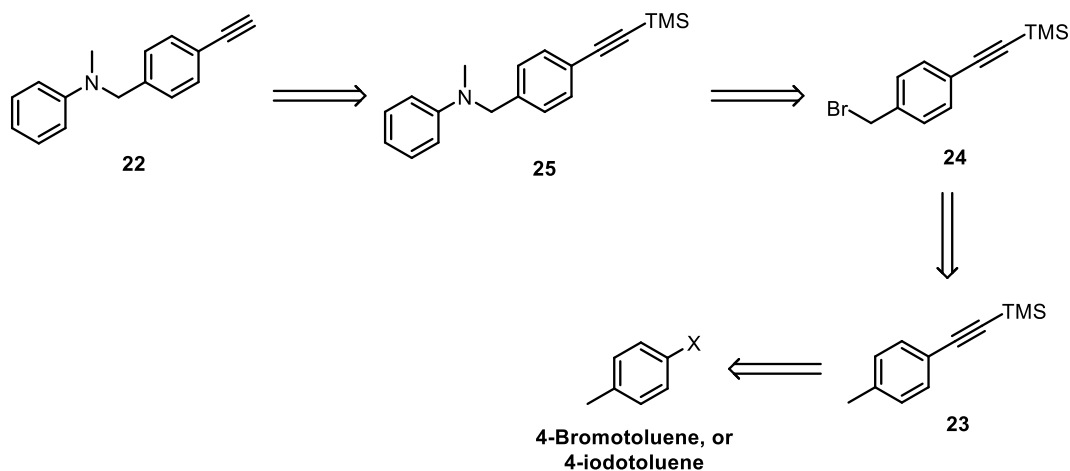
Figure 11. Two tertiary anilines **21** and **22**, that were identified as target compounds.

The reaction between *N*-methylaniline and propargyl bromide in dimethyl sulfoxide (DMSO) with potassium carbonate gave the corresponding tertiary aniline **21** in yields of up to 75%. Once again, the procedure of Srivastava *et al.*²⁸⁸ was used (Scheme 36).



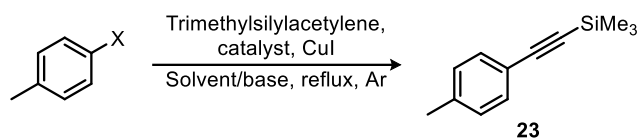
Scheme 36. Synthesis of tertiary aniline **21**.

It was proposed that the other tertiary aniline **22** could be prepared in four steps *via* the following route (Scheme 37).



Scheme 37. Proposed synthesis of tertiary aniline **22**.

The first step of the synthesis involved a Sonogashira cross-coupling reaction between an aryl halide and trimethylsilylacetylene to give the corresponding trimethylsilyl-protected alkyne **23**. Initially, 4-bromotoluene was reacted with trimethylsilylacetylene in different solvent systems, and with two different palladium catalysts: Pd(PPh₃)₄ and Pd(PPh₃)₂Cl₂. It was found, however, that the yield of trimethylsilyl-protected alkyne **23** was always less than or equal to 10% after two days of heating under reflux (Table 4; see the first seven entries). It was decided that the issue was the poor reactivity of 4-bromotoluene, so instead 4-iodotoluene was employed as the coupling partner. It is known that 4-iodotoluene is more reactive than 4-bromotoluene due to the C-I bond being weaker than the C-Br bond. Once again, both Pd(PPh₃)₄ and Pd(PPh₃)₂Cl₂ were tested as catalysts, but only the dichloride showed a reasonable level of activity. In addition, various amines were screened as solvents, and the best proved to be triethylamine, which consistently gave rise to yields of greater than 50% (Table 4; see the final six entries). Further improvements to the experimental procedure meant that yields of up to 89% could be achieved for this reaction.



X	Solvent/base	Catalyst	Time / h	Yield
Br	THF/triethylamine	Pd(PPh ₃) ₄	48	No reaction
Br	Triethylamine	Pd(PPh ₃) ₄	36	Trace
Br	Triethylamine	Pd(PPh ₃) ₂ Cl ₂	36	Trace
Br	DMF/triethylamine	Pd(PPh ₃) ₄	48	No product
Br	DMF/triethylamine	Pd(PPh ₃) ₂ Cl ₂	48	10%
Br	Triethylamine	Pd(PPh ₃) ₄	48	6%
Br	Triethylamine	Pd(PPh ₃) ₂ Cl ₂	48	<6% (crude)
I	Triethylamine	Pd(PPh ₃) ₄	24	Trace
I	Piperidine	Pd(PPh ₃) ₂ Cl ₂	18	Trace
I	Pyrrolidine	Pd(PPh ₃) ₂ Cl ₂	18	No product
I	Diisopropylamine	Pd(PPh ₃) ₂ Cl ₂	24	54%
I	Triethylamine	Pd(PPh ₃) ₂ Cl ₂	18	58%

Table 4. Sonogashira cross-coupling reaction to form trimethylsilyl-protected alkyne **23**.

In nearly every case, the Glaser coupling product **26** was observed in the crude ¹H NMR spectra and is represented by a singlet at 0.18 ppm,²⁹⁶ but it was easily separated from the product by flash column chromatography (Figure **12**). The Glaser coupling is facilitated by copper (I) salts in the presence of oxygen, so the reaction was performed under an inert atmosphere of argon. In addition, trimethylsilylacetylene was used in excess to accommodate for the occurrence of the Glaser coupling.

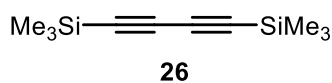
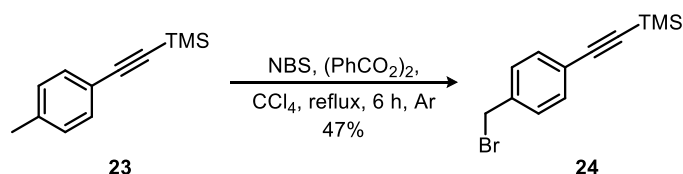
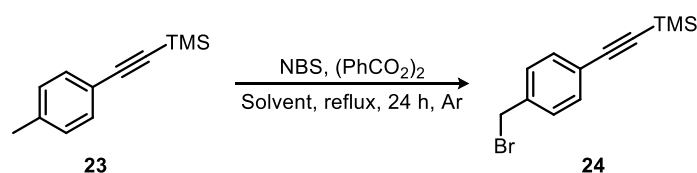


Figure 12. Glaser coupling product **26**.

Having successfully synthesised trimethylsilyl-protected alkyne **23**, monobromination at the benzylic position was attempted. Initially, the reaction was performed in carbon tetrachloride with *N*-bromosuccinimide (NBS) as the brominating agent, and dibenzoyl peroxide as the radical initiator (Scheme **38**).

Scheme 38. Mono-bromination of trimethylsilyl-protected alkyne **23**.

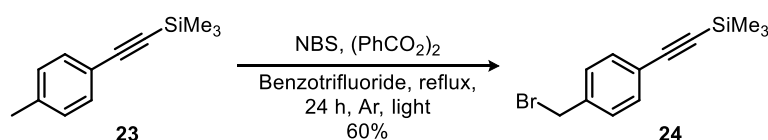
It was soon decided that it would be beneficial to find a more suitable solvent system for this reaction, due to restrictions in place that make it difficult to obtain carbon tetrachloride: it is highly toxic and known to effect ozone depletion. Several solvents were screened and the best proved to be benzotrifluoride, both in terms of % conversion and with regards to its low toxicity (relative to 1,2-dichloroethane, for example). Therefore, benzotrifluoride was used in place of carbon tetrachloride for all future repeats of this reaction (Table 5).



Solvent	% Conversion
Acetonitrile	No reaction
Chloroform	22%
Benzotrifluoride	76%
1,2-Dichloroethane	60%
1,1,2-Trichloroethane	Complex mixture

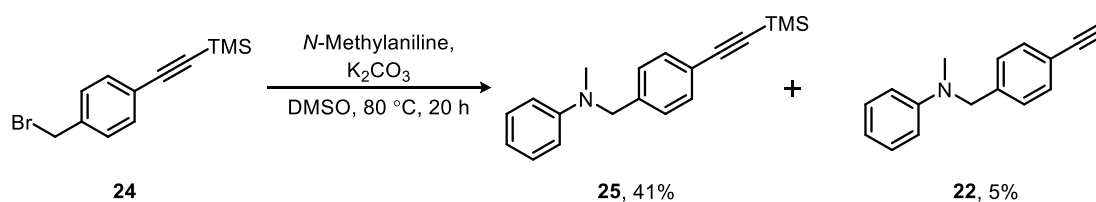
Table 5. Mono-bromination reaction to form benzylic bromide **24**.

It was later established that performing this reaction in the presence of an IQ group floodlight in addition to heating under reflux gave rise to isolated yields of up to 60%, as opposed to 30% in the absence of a light source (Scheme 39).

Scheme 39. Synthesis of benzylic bromide **24**.

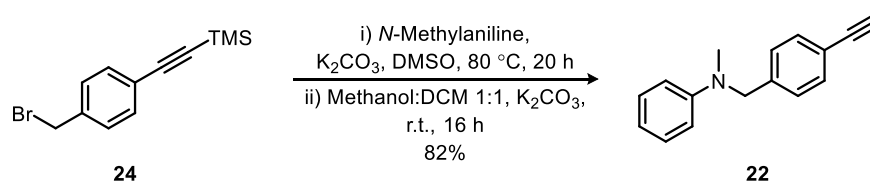
The S_N2 reaction between benzylic bromide **24** and *N*-methylaniline in DMSO with potassium carbonate gave a mixture of trimethylsilyl-protected tertiary

aniline **25** and the desired final product, tertiary aniline **22** (Scheme 40). Once again, the procedure of Srivastava *et al.*²⁸⁸ was used.



Scheme 40. Alkylation of mono-brominated, trimethylsilyl-protected alkyne **24**.

Instead of attempting to isolate trimethylsilyl-protected tertiary aniline **25**, which was inseparable from tertiary aniline **22** by flash column chromatography, the crude product was subjected to proto-desilylation conditions. The overall yield across the two steps was 82% (Scheme 41).

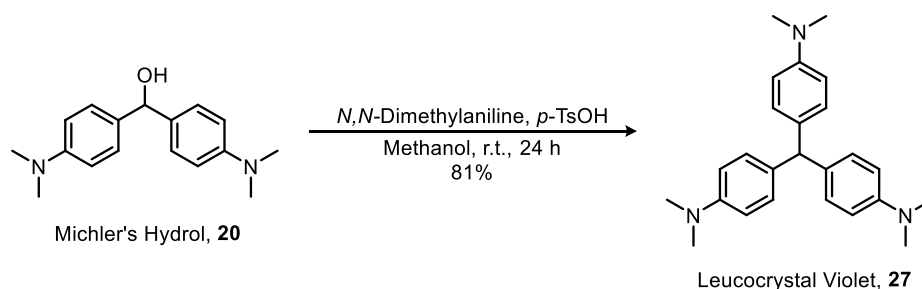


Scheme 41. Two-step synthesis of tertiary aniline **22**.

Having synthesised all the required precursors, the preparation of tris(4-dimethylaminophenyl)methane (leucocrystal violet) **27** was investigated. The procedure of Yang *et al.*²⁹⁴ was tried to begin with, and involved the reaction between Michler's hydrol **20** and *N,N*-dimethylaniline in toluene in the presence of an acid catalyst, *p*-toluenesulfonic acid. Unfortunately, leucocrystal violet **27** was not isolated using these conditions. The procedure was investigated and modified, with adjustments being made to the number of equivalents of Michler's hydrol **20** relative to *N,N*-dimethylaniline, or the crude work up.

By chance, it was noticed that some of the purple solid that was obtained from one experiment appeared to be partially soluble in methanol. Immersion of the solid in methanol resulted in the formation of a purple solution and an insoluble, colourless solid. It transpired that the colourless solid was in fact pure leucocrystal violet **27**. Based on this discovery, the reaction was attempted in methanol as opposed to toluene. The desired product precipitated out of the reaction mixture as it formed. It was isolated by filtration, washed with methanol, and dried under suction in the dark. It was found that

no further purification was necessary, and the reaction gave yields of up to 81% (Scheme 42).



Scheme 42. Synthesis of leucocrystal violet **27**.

Using the same conditions, Michler's hydrol **20** was reacted with tertiary aniline alkyne precursors **21** and **22**, to afford the corresponding leucocrystal violet analogues **28** and **29** (Figure 13).

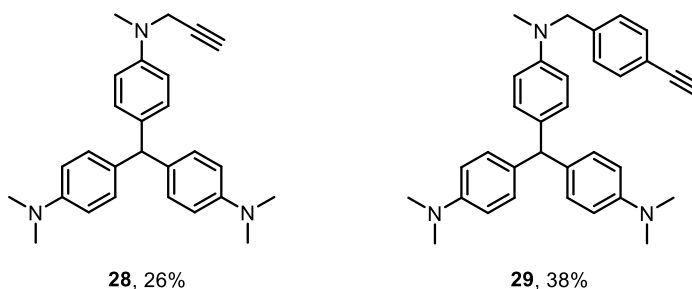


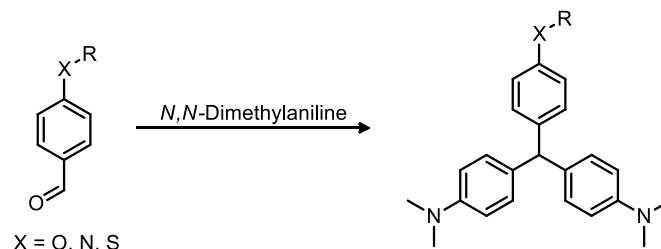
Figure 13. Novel leucocrystal violet analogues **28** and **29**.

The yield for both reactions was poor, which might be because leucocrystal violet analogues **28** and **29** are more susceptible to various decomposition pathways than leucocrystal violet **27** itself. It is not clear why this should be, though. Alternatively, leucocrystal violet analogues **28** and **29** might be more soluble in methanol than leucocrystal violet **27**; however, none of the compounds appeared to dissolve when attempts were made to solubilise them.

2.1.5 Leucocrystal violet analogues from aryl aldehydes

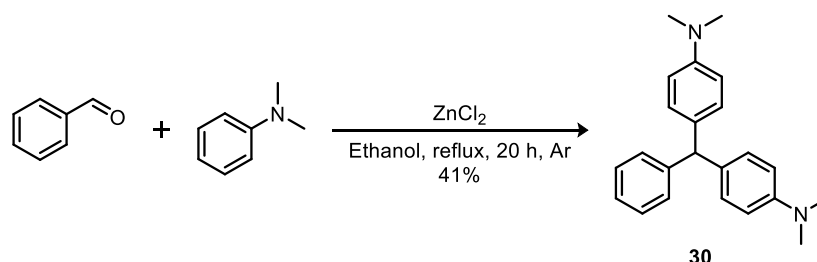
Having successfully synthesised two novel leucocrystal violet analogues, it was decided that it would be interesting to replace one of the nitrogen atoms with another heteroatom (for example, O or S). It was anticipated that this would give rise to a crystal violet analogue with a significantly different UV-Vis absorption profile compared to that of crystal violet itself, thus one would expect it to demonstrate altered photobactericidal properties.

A different route was investigated, involving a reaction between an aryl aldehyde and two equivalents of *N,N*-dimethylaniline to afford the corresponding leucocrystal violet motif (Scheme 43).¹²⁷



Scheme 43. A different approach towards leucocrystal violet analogues.

Initially, the literature reaction between *N,N*-dimethylaniline and benzaldehyde to give bis(4-dimethylaminophenyl)phenylmethane (leucomalachite green) **30** was repeated as proof of principle.²⁹⁷ The reaction gave a complex mixture when attempted in air, but gave leucomalachite green **30** in a 41% yield when conducted under an inert atmosphere of argon (Scheme 44).



Scheme 44. Synthesis of leucomalachite green **30**.

Having synthesised leucomalachite green **30**, two aryl aldehyde alkyne motifs were identified as suitable synthetic targets (Figure 14). They were chosen since they are structurally similar to the tertiary anilines **21** and **22**, that were prepared previously.

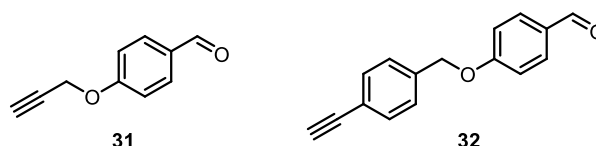
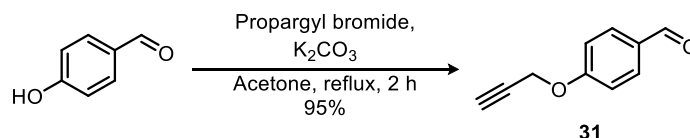


Figure 14. Two alkyne-functionalised aryl aldehydes **31** and **32**, that were chosen as synthetic targets.

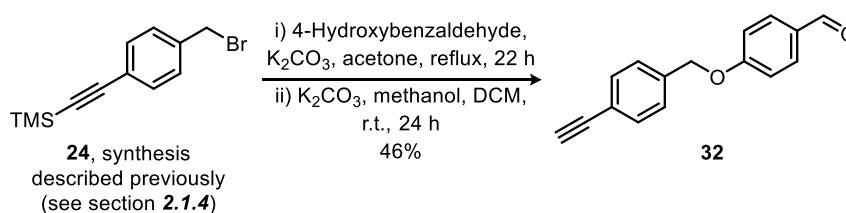
The synthesis of the first aryl aldehyde **31** proceeded as reported in the literature by Hoogendoorn *et al.*,²⁹⁸ with yields of up to 79% obtained after purification by flash column chromatography. The crude product could,

however, be used without purification; crude yields were up to 95% (Scheme 45).



Scheme 45. Synthesis of aryl aldehyde **31**.

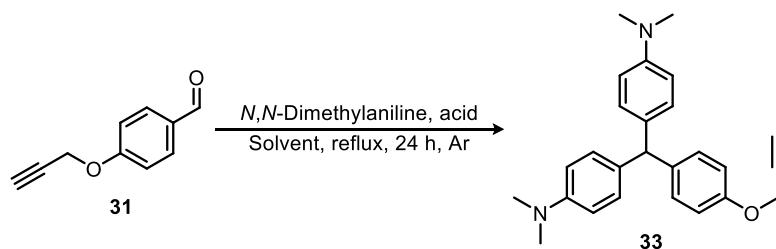
The synthesis of aryl aldehyde **32** was analogous to that which successfully yielded tertiary aniline **22** (See section 2.1.4). The previously synthesised benzylic bromide **24** was reacted with 4-hydroxybenzaldehyde and potassium carbonate in acetone, as described by Hoogendoorn *et al.*²⁹⁸ The crude product was then subjected to basic conditions to remove the trimethylsilyl-protecting group. The desired product, aryl aldehyde **32**, was obtained in yields of up to 46% over the two steps (Scheme 46).



Scheme 46. Two-step preparation of aryl aldehyde **32**.

Having successfully synthesised the desired aryl aldehyde alkyne motifs **31** and **32**, attention was turned to the production of the two corresponding leucocrystal violet analogues.

Initially, the conditions of Szent-Gyorgyi *et al.*²⁹⁷ were used for the preparation of leucocrystal violet analogue **33**, which was obtained in a low yield of 34%. The reaction was attempted using different conditions to try and improve the yield (Table 6).



Solvent	Acid	Yield
Ethanol	ZnCl ₂ (2 eq.) ^a	34%
Ethanol	ZnCl ₂ (2 eq.)	15%
Methanol	ZnCl ₂ (2 eq.)	No product
Ethanol	ZnCl ₂ (2 eq.), AcCl (0.01 eq.)	48%
Ethanol	AcCl (0.01 eq.)	21% (conversion)
Ethanol	AcCl (2 eq.)	62%

^a An old bottle of ZnCl₂ was used.

Table 6. Synthesis of leucocrystal violet analogue **33**.

Intriguingly, it was found that a higher yield was obtained when an old bottle of ZnCl₂ was used, instead of a freshly opened one (Table 6; see the first two entries). The old “ZnCl₂” that was used was very obviously wet, due to the absorption of water from the atmosphere over time. Its improved reactivity may have been due to the fact that it was predominantly composed of highly acidic tetrahedral ZnCl_x(OH)_{2(4-x)} complexes, which are essentially a source of H⁺ ions and are thus Brønsted acids.²⁹⁹ The reaction was therefore attempted with a catalytic amount of acetyl chloride, which was expected to react with ethanol to generate hydrochloric acid in situ, in addition to ZnCl₂. Under these conditions an improved yield of 48% was obtained. The reaction was also attempted with a catalytic amount of acetyl chloride only, but poor conversion (21%) was achieved after one day. The reaction was then attempted with two equivalents of acetyl chloride and the desired product, leucocrystal violet analogue **33**, was obtained in a moderate yield of 62% (Table 6). These conditions were thus used in future repeats of the above reaction.

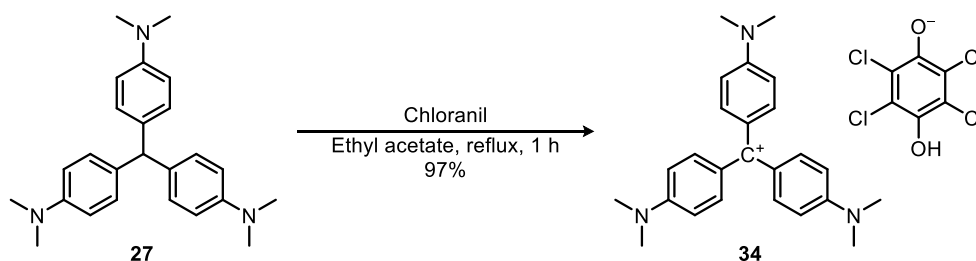
Attempts to synthesise the other desired leucocrystal violet analogue from aryl aldehyde **32** via an analogous reaction with *N,N*-dimethylaniline were not initially successful. Unfortunately, the attempted attachment of the previously synthesised leucocrystal violet analogues to the surface of a polymer had failed at this time (See section 2.2). It was decided to focus on oxidising the

leucocrystal violet analogues that had already been prepared, and to subsequently assess their efficacy as light-activated antimicrobial compounds.

2.1.6 Oxidation of leucocrystal violet analogues

Oxidation of the three alkyne-functionalised leucocrystal violet analogues **28**, **29**, and **33** was explored. The photobactericidal properties of the resultant crystal violet analogues were assessed when incorporated into polyurethane.

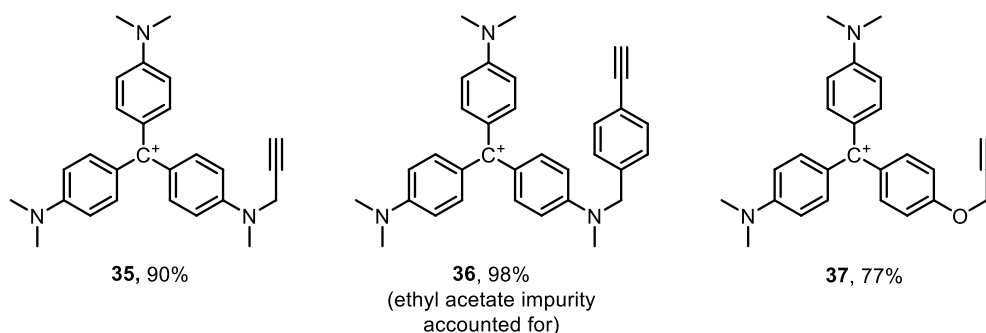
Initially, the oxidation of leucocrystal violet **27** was investigated, as this can be synthesised easily from Michler's hydrol **20** and *N,N*-dimethylaniline (See section **2.1.4**). In preliminary studies, it was found that the use of a mild oxidant, MnO_2 , was unsuccessful: no product was obtained using various conditions and work-up procedures. Instead, a modified procedure of Szent-Gyorgyi *et al.*,²⁹⁷ who oxidised another crystal violet analogue in ethyl acetate with chloranil, gave the desired product, crystal violet analogue **34** (Scheme **47**).



Scheme **47**. Synthesis of crystal violet analogue **34**.

It was found that extraction with ethyl acetate was not necessary as, upon cooling the reaction mixture to r.t., the product precipitated out of the reaction mixture. Simply washing the resultant solid with cold ethyl acetate (0 °C) and diethyl ether afforded the desired product.

Having successfully synthesised crystal violet analogue **34**, the other crystal violet analogues **35-37** were prepared from the corresponding leuco dyes **28**, **29**, and **33** using the same conditions (Figure **15**). Unfortunately, it was found that one of the products, crystal violet analogue **36**, contained ethyl acetate as an irremovable impurity (<3% by mass).

Figure 15. Crystal violet analogues **35-37**.

The counter-ion, 2,3,5,6-tetrachloro-4-hydroxyphenolate, doesn't give a ^1H NMR signal; however, it was identified by negative ion mass spectrometry for each of the crystal violet analogues. Signals corresponding to other possible anions such as chloride, which was reported as being the counter-ion by Szent-Gyorgyi *et al.*,²⁹⁷ were not observed.

Each of the above compounds was dissolved in ethanol (1×10^{-5} M); UV-Vis absorbance spectra were acquired, and are shown below (Figure 16). Unsurprisingly, crystal violet analogues **34-36** each give rise to near identical spectra: one peak with a poorly defined shoulder is observed, and the absorbance maximum arises between 589-590 nm in each instance. It should be noted that the spectra recorded correlate well with those obtained for crystal violet itself in the past (λ_{max} at 590 nm in ethanol, for example).³⁰⁰ For the other crystal violet analogue **37**, where one of the nitrogen atoms is substituted with an oxygen atom, a spectrum with two distinct peaks is obtained: one of the peaks is red-shifted with an absorbance maximum at 611 nm; the other is blue-shifted with an absorbance maximum at 459 nm. The drastically different spectrum obtained for the latter compound is not unexpected as one would expect the introduction of a different heteroatom to have a pronounced effect on the electronic properties of the triarylmethyl cation segment of the molecule.

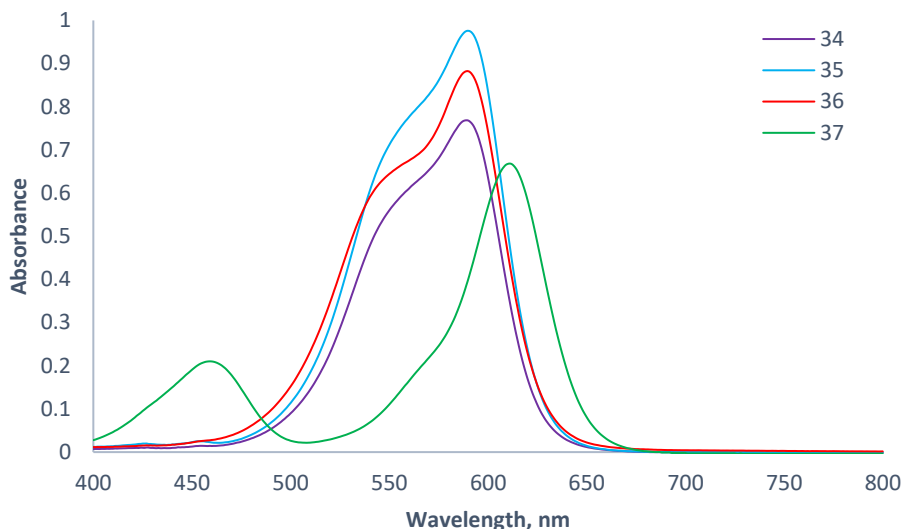


Figure 16. UV-Vis absorbance spectra of crystal violet analogues **34-37** dissolved in ethanol.

2.1.7 Physical and biological characterisation of crystal violet-polyurethane samples

Three crystal violet analogues **35-37**, whose syntheses are described in the previous sections, were incorporated into polyurethane using a simple dip-coating technique, which had been used previously by Noimark *et al.*²⁷⁰ This involved immersing 1 cm × 1 cm films, which had been cut from a sheet of polyurethane, in aqueous solutions of each dye (1×10^{-3} M), and leaving them for four days in the dark. The samples were then washed with distilled water, dried with paper towels, and air dried in the dark overnight (Figure 17).

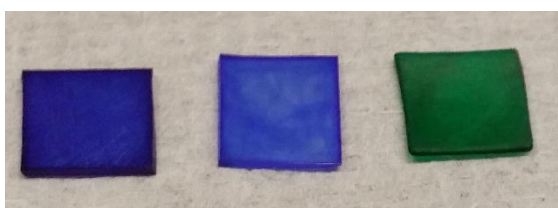


Figure 17. Polyurethane samples that were incorporated with crystal violet analogues **35**, **36**, and **37** (from left to right).

The dye-incorporated samples were analysed by FT-IR and UV-Vis absorbance spectroscopy.

No significant differences between the FT-IR spectra of unmodified polyurethane, and of the dye-incorporated polymer samples, were observed. This indicates that the incorporation process did not result in any significant changes to the chemical structure of the polyurethane. Only peaks associated

with the polyurethane polymer matrix were observed. The absence of peaks corresponding to the presence of the dye molecules can be attributed to the low concentration of dye present relative to the bulk polymer.

The UV-Vis absorbance spectra of the dye-incorporated polymer samples were obtained (Figure 18). As expected, unmodified polyurethane does not absorb visible light. The polyurethane samples incorporated with crystal violet analogues **35** and **36** gave rise to peaks with absorbance maxima at 600 ± 5 nm. Additionally, shoulder peaks at roughly 550 nm can be seen. For the sample incorporated with crystal violet analogue **37**, a stronger absorption maximum at 620 ± 5 nm was observed, along with a smaller peak at 465 ± 5 nm. The spectral values obtained are close to those obtained from the solution phase measurements for each of the dyes dissolved in ethanol (See section 2.1.6). A bathochromic shift of roughly 10 nm was observed in each instance for the dyes when incorporated into polyurethane.

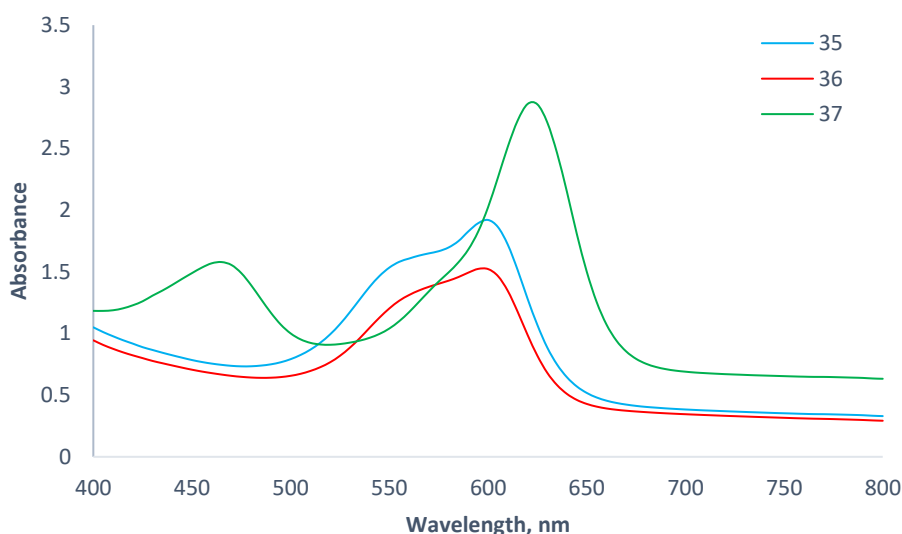


Figure 18. UV-Vis absorbance spectra of polyurethane samples that were incorporated with crystal violet analogues **35-37**.

Further physical and biological characterisation was carried out by Ekrem Ozkan. The contact angles of the unmodified and dye-incorporated polyurethane samples are displayed below (Table 7). The surface of unmodified polyurethane is moderately hydrophobic, with a water contact angle of 103.2° . The incorporation of crystal violet analogues **35** and **36** did not cause any significant change in the hydrophobicity of the surface; however,

a more hydrophilic surface, with a water contact angle of 91.2° , was obtained when polyurethane was incorporated with crystal violet analogue **37**.

Polyurethane sample	Water contact angle, °
Unmodified control	103.2 ± 1.0
35	101.7 ± 1.1
36	101.1 ± 0.9
37	91.2 ± 2.8

Table 7. Water contact angles for each of the polymer samples (\pm SD).

The photobactericidal activities of the samples were investigated against a Gram-positive bacterium, *S. aureus* 8325-4. A General Electric 28 W Watt Miser™ T5 2D compact fluorescent lamp, like those commonly found in UK hospitals, was used as the light source. In addition, a set of control samples were incubated in the dark, to determine whether any antibacterial activity observed was photoinduced.

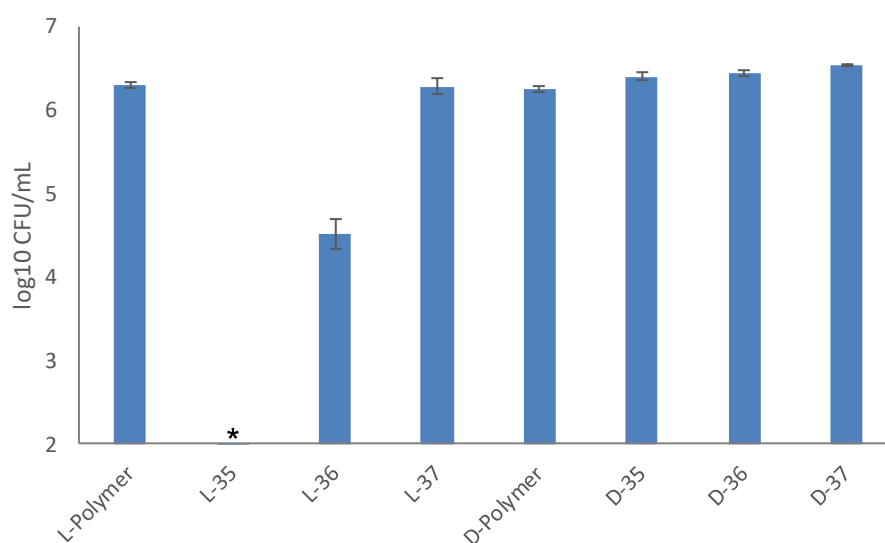


Figure 19. The number of *S. aureus* colony forming units (CFU) per mL on the surfaces of the polymer samples after white light illumination, or incubation in the dark for 3 hours. D = dark, L = light; * indicates that the bacteria count was below the detection limit of 100 CFU mL^{-1} .

As expected, none of the polymer samples tested caused a reduction in the numbers of bacteria after incubation in the dark for three hours (Figure 19). In addition, no bacterial kill was observed for the unmodified polyurethane (L-Polymer), or for the sample incorporated with crystal violet analogue **37** (L-37) after irradiation with white light for three hours. Illumination of the sample incorporated with crystal violet analogue **36** (L-36), however, produced an

almost two log reduction ($P = 0.004$) in the number of viable bacteria after three hours. The sample that was incorporated with crystal violet analogue **35** (L-**35**) was highly effective at killing *S. aureus* after three hours of white light illumination, reducing bacterial numbers to below the detection limit (> 4 log reduction; $P = 0.002$). The differences between the antibacterial activities of the polymers incorporated with crystal violet analogues **35-37** could be attributed to the variation in the amount of dye present on the surface in each sample, as well as intrinsic chemical and/or physical differences between the dyes.

In this study, it was established that the crystal violet analogue **35**, when incorporated into polyurethane, was the most effective photosensitiser of the three analogues that were tested.

2.2 Attempted grafting of alkyne-functionalised dyes to a variety of polymer surfaces

Three synthetic routes towards polymer surfaces with covalently attached photosensitiser molecules were proposed, which all involved a 1,3-dipolar cycloaddition as a key step: a reaction between an azide-functionalised polymer surface with an alkyne-functionalised dye; a reaction between an azide-functionalised poly(ethylene glycol) (PEG) linker with an alkyne-functionalised dye, followed by attachment of the linker to a polymer surface; and a reaction between an azide-functionalised PEG linker with a polymer surface, followed by attachment of an alkyne-functionalised dye (Figure **20**).

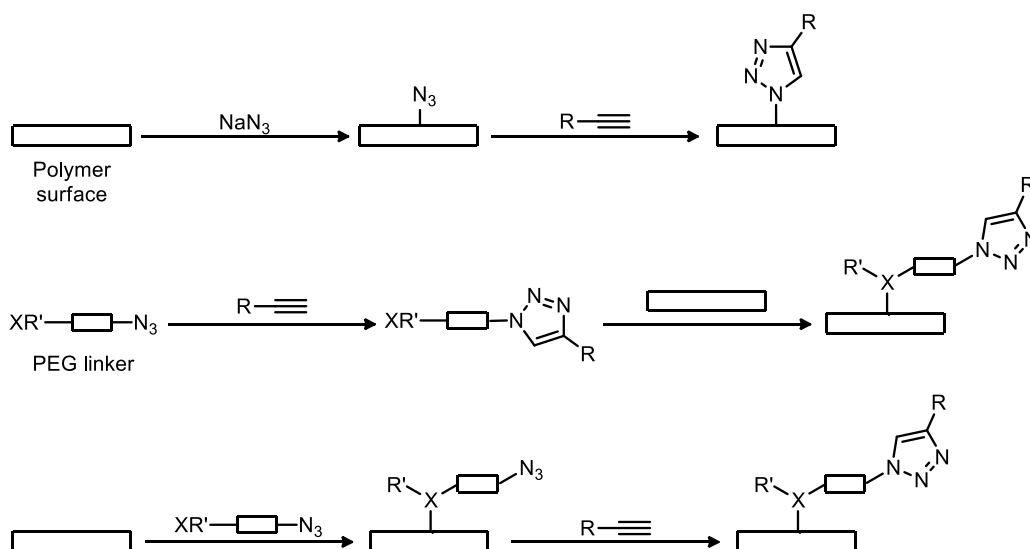


Figure 20. Proposed routes towards a functionalised polymer surface.

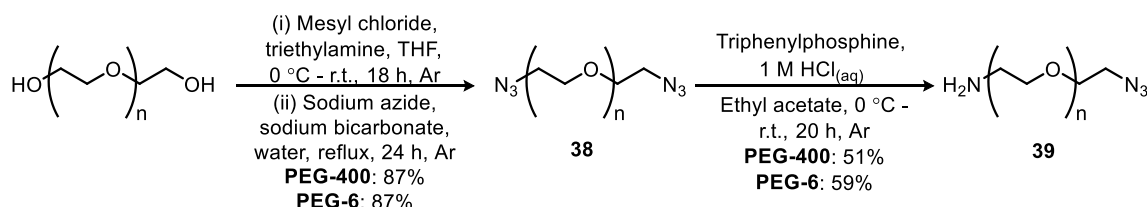
It was felt that the use of a PEG linker could be beneficial, as various types have been shown to resist the adhesion of bacteria and other biological material in the past.^{1,13} Moreover, the use of a polymeric spacer might prevent the aggregation of the surface-bound antibacterial agent. On the other hand, the PEG linker might prove to be highly susceptible to oxidative degradation, which could result in bond cleavage and subsequent loss of the covalently attached photosensitiser to the surrounding medium.

In the following sections, all the proposed routes towards functionalised polymer surfaces are explored in the quest to prepare a photobactericidal polymer film.

2.2.1 Synthesis of a mono-amine, mono-azide-terminated PEG linker

The synthesis of a suitable PEG linker that could be attached to a polymer surface and subsequently undergo a 1,3-dipolar cycloaddition with an alkyne-functionalised dye molecule, or vice versa, was proposed. In 2009, Susumu *et al.*³⁰¹ successfully synthesised a mono-amine, mono-azide-terminated PEG linker **39** via a two-step sequence, starting from PEG. The first step involved mesylation of the two hydroxyl substituents, followed by displacement via an S_N2 reaction with sodium azide to afford the corresponding di-azide-terminated PEG compound **38**. The di-azide-terminated PEG compound **38** was then reacted with triphenylphosphine in a bi-phasic mixture of 1M $HCl_{(aq)}$ and ethyl acetate. The Staudinger reduction only occurs at one end of the PEG

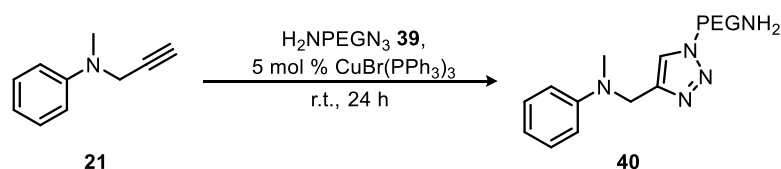
chain as the ammonium salt formed under acidic conditions dissolves into the aqueous phase and is effectively removed from the reaction mixture. Two mono-amine, mono-azide-terminated PEG linkers **39** were synthesised in accordance with the literature protocol (Scheme 48): one that was polydisperse, from PEG-400; and another that was monodisperse, from PEG-6.



Scheme 48. Synthesis of mono-amine, mono-azide-terminated PEG linker **39**.

2.2.2 Attempted 1,3-dipolar cycloaddition reaction between a PEG linker and an alkyne-functionalised dye

Initially, the 1,3-dipolar cycloaddition reaction between *N*-methyl-*N*-phenyl-propargylamine **21**, synthesised previously (See section 2.1.4), and PEG linker **39** was investigated. A brief review of the literature uncovered $\text{CuBr}(\text{PPh}_3)_3$ as a suitable catalyst, particularly because of its solubility in various organic solvents.³⁰² A number of different solvents and conditions were screened (Table 8).



Solvent	Atmosphere	% Conversion
Acetone	Air	0% ^a
Acetone	Ar	0% ^a
None	Air	50%
None	Ar	84%
None	Ar	85% ^b
Acetone	Ar	69%
DCM	Ar	86%
Acetonitrile	Ar	38%
Isopropanol	Ar	complex mixture

^a The reaction mixture was 10 times more dilute.

^b The reaction was terminated after 5 hours.

Table 8. 1,3-dipolar cycloaddition reaction between alkyne **21** and PEG linker **39**.

The best solvent was found to be DCM, and performing the reaction under an inert atmosphere of argon was found to be important. The latter observation is perhaps not surprising, as oxidation of the active Cu(I) species is undesirable. The crude ^1H NMR spectra showed that a single isomer was present, presumably the 1,4-disubstituted product, which is the expected product of any Cu(I)-catalysed 1,3-dipolar cycloaddition reaction.³⁰²⁻³⁰⁴ The attempted purification of the resultant triazole **40** *via* flash column chromatography led to partial conversion to another product with very similar ^1H NMR characteristics. It was speculated that the new compound, which was obtained as the major product in a 2:1 ratio, may be one of the structural isomers shown below (Figure 21). There is, however, no literature precedent for isomerisation occurring with molecules of this type, and the mechanism for this transformation is not clear. Moreover, it was not possible to assign fully the connectivity of any of the compounds that were formed.

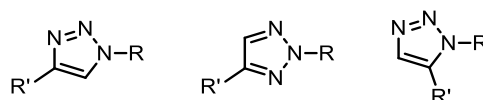
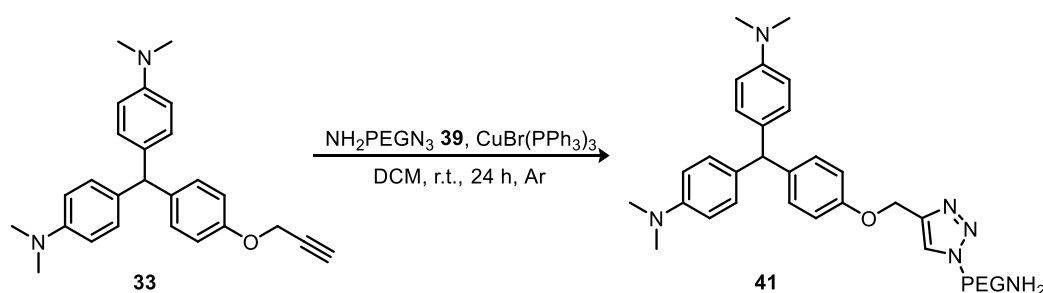


Figure 21. Three possible structural isomers of a generic 1,2,3-triazole.

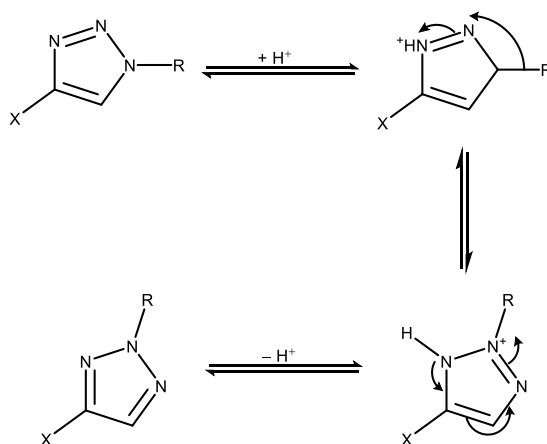
Nonetheless, attempts were made to react PEG linker **39** with leucocrystal violet analogue **33**, which was synthesised previously (See section 2.1.5). The reaction was tried in both DCM and acetone; once again DCM proved to be the superior alternative (86% versus 71% conversion). The attempted purification of triazole **41** by flash column chromatography resulted in complete isomerisation of the original product this time around. The resultant product was not pure and so a yield hasn't been quoted (Scheme 49).



Scheme 49. Attempted synthesis of triazole **41**.

It was discovered that leaving the original isomer open to the air on the bench for one day did not result in any isomerisation occurring. On the other hand,

isomerisation was found to occur to some extent after one day of being dissolved in deuterated chloroform, or after exposure to silica gel. It can thus be inferred that the isomerisation that is occurring might be acid-catalysed, and a mechanism has been suggested below (Scheme 50). The first step involves protonation of one of the nitrogen atoms to give a positively charged species. This allows the migration of the PEG linker onto an adjacent nitrogen. Finally, de-protonation gives rise to a new isomeric form. As far as this writer is aware, the acid-catalysed isomerisation of 1,4-disubstituted 1,2,3-triazoles has not been reported elsewhere.



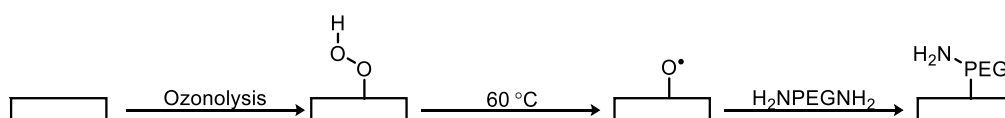
Scheme 50. Suggested mechanism for the acid-catalysed isomerisation of a general 1,2,3-triazole. A similar mechanism can be invoked to explain the migration of the “R” substituent onto any N atom.

The attempted oxidation of triazole **41** with chloranil in ethyl acetate was unsuccessful, and gave a complex mixture of products.²⁹⁷ Considering the problems encountered, it was decided that performing the 1,3-dipolar cycloaddition on the surface of a polymer would be a better approach as, in theory, any un-wanted by-products could simply be washed from the surface using an appropriate solvent system.

2.2.3 Attempted modification of silicone

The possibility of covalently attaching a modified dye molecule to the surface of a silicone elastomer was investigated. The use of silicone elastomers in various medical and pharmaceutical applications is well documented because of their chemical inertness and biocompatibility.³⁰⁵ Despite this, there are various methods for introducing reactive groups to the surface, including ozonolysis, and plasma treatments.³⁰⁶⁻³⁰⁸ Ozonolysis was particularly

appealing due to its relative simplicity, low cost, and easy access to an ozone generator. Ozonolysis treatment gives rise to peroxide groups on the surface of the polymer, which collapse to form highly reactive oxygen radicals with sufficient heating (60 °C).³⁰⁷ Previously, di-amine-terminated PEG has been covalently grafted to the surface of ozonolysed polyurethane and silicone films *via* a two-step coupling reaction (Scheme 51).³⁰⁷ It was thus hypothesised that if mono-amine, mono-azide-terminated PEG linker **39** could be attached to the surface of silicone using this method, then covalent attachment of an alkyne-functionalised dye could proceed *via* a 1,3-dipolar cycloaddition reaction.



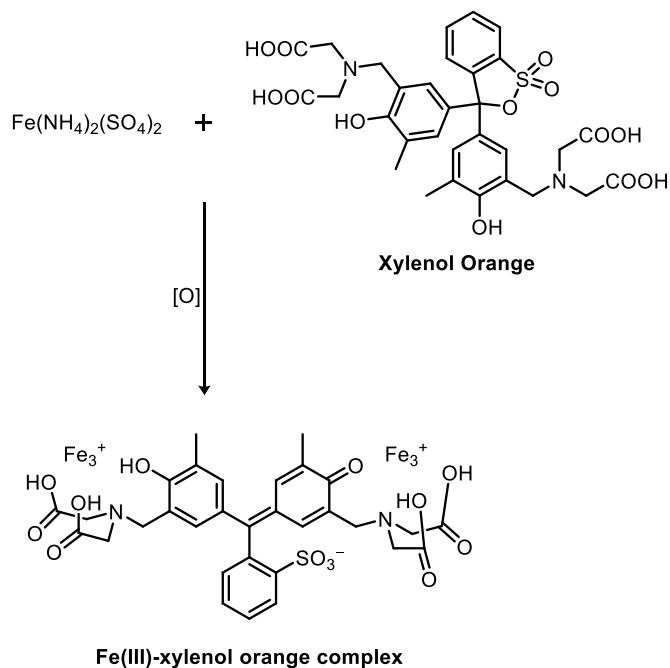
Scheme 51. Coupling of di-amine-terminated PEG to the surface of silicone or polyurethane, as described by Ko *et al.*³⁰⁷

Sheets of medical grade silicone were cut into discs using a standard sized hole punch, and ozone was passed over the discs for varying periods of time (up to one hour). After treatment, the films were put under vacuum overnight to remove any traces of ozone trapped within the polymer matrix.

To begin with, experiments were performed to establish the number of peroxides introduced as a result of ozone treatment, if any. One way of measuring the number of peroxides present is *via* the iodometric method. This involves suspending the polymer films in a mixture of sodium iodide and a catalyst, such as ferric chloride, in a mixture of benzene and isopropanol at 60 °C for ten minutes, with occasional swirling.³⁰⁸ The oxidation of I^- to I_3^- is effected by peroxides, and the concentration of I_3^- can be measured by UV-Vis absorbance spectroscopy ($\lambda_{max} = 360$ nm). Unfortunately, no λ_{max} signal indicating the presence of I_3^- was detected. It was concluded that the iodometric method was not sensitive enough and so a different colorimetric assay was investigated.

When a solution of ammonium ferrous sulfate and xylenol orange in acidified methanol comes into contact with peroxides, Fe(II) is oxidised to Fe(III). The formation of a purple coloured Fe(III)-xylenol orange complex ensues

(Scheme 52). The concentration of this complex can be elucidated by using UV-Vis absorbance spectroscopy ($\lambda_{\text{max}} = 560 \text{ nm}$).³⁰⁹



Scheme 52. Formation of the Fe(III)-xylenol orange complex.

The number of peroxides present in a test sample can be calculated from a plot of A_{560} against the number of moles of *tert*-butyl hydroperoxide in a series of calibration experiments. A known amount of *tert*-butyl hydroperoxide was mixed with an excess of the Fe(II)/xylenol orange reagent for thirty minutes, and this was repeated for a number of different concentrations of *tert*-butyl hydroperoxide. The UV-Vis absorbance spectrum of each sample was then obtained and the corresponding values for A_{560} were plotted against the number of nmoles of *tert*-butyl hydroperoxide per reaction volume (Figure 22). A measurement of the UV-Vis absorbance spectrum of the Fe(II)-xylenol orange reagent after exposure to the test sample should give a value for A_{560} which corresponds to a point on the curve. The number of moles of peroxides present in the test sample can then be deduced.

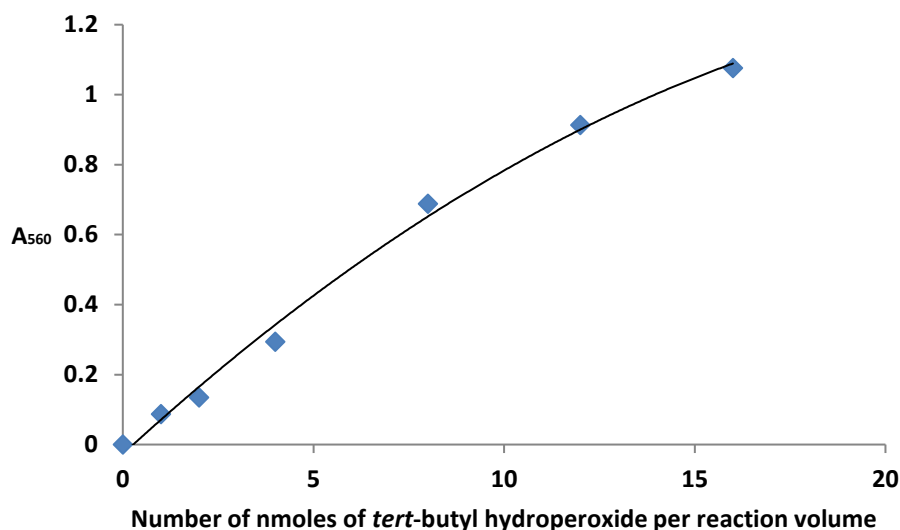
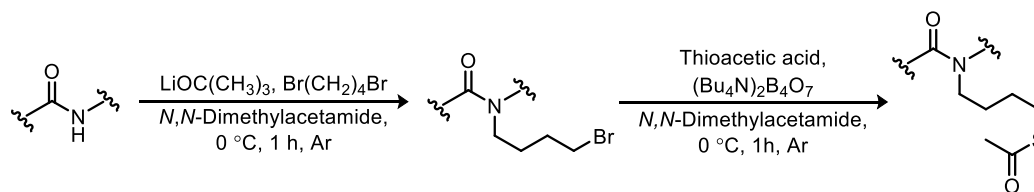


Figure 22. Graph of A_{560} against the number of nmoles of *tert*-butyl hydroperoxide per reaction volume.

Once again, silicone discs were exposed to ozone for varying periods of time (up to one hour), after which they were put under vacuum overnight, before being exposed to the Fe(II)-xylenol orange reagent. The control samples that had not been exposed to ozone gave the same amount of oxidation of Fe(II) to Fe(III) as those samples which had supposedly undergone ozonolysis. This indicates that the ozonolysis was unsuccessful, and at this stage, the investigation into the functionalisation of polyurethane was begun.

2.2.4 Attempted modification of polyurethane

There are a number of examples of polyurethane modification in the literature, most of which involve ozonolysis or plasma treatment, as discussed above.^{307,308,310} In addition to these techniques, deprotonation of the amide moiety of polyurethane followed by an S_N2 reaction with an appropriate electrophile can give rise to a variety of modified surfaces. For example, Alferiev *et al.*³¹¹ successfully attached acetylthio groups to the surface of polyurethane *via* treatment with $\text{LiOC}(\text{CH}_3)_3$ and 1,4-dibromobutane in *N,N*-dimethylacetamide, followed by S_N2 displacement of the remaining bromide with thioacetic acid (Scheme 53).

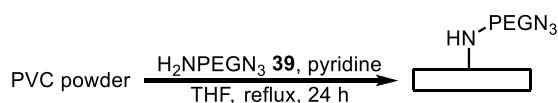
Scheme 53. Chemical modification of polyurethane, as described by Alferiev *et al.*³¹¹

It was proposed that the above conditions could be used to produce modified polyurethane with pendant PEG or azide groups, by using the previously synthesised PEG linker **39** or sodium azide instead of thioacetic acid in the second step.

Initially, a solution of polyurethane in *N,N*-dimethylacetamide was treated with $\text{LiOC}(\text{CH}_3)_3$ and 1,4-dibromobutane, using the conditions previously described. According to the ^1H NMR spectrum of the modified polyurethane in $\text{DMF-}d_6$, no bromobutyl groups were present. Moreover, the polyurethane film that was obtained did not bear any structural or visual resemblance to the starting material prior to being solubilised in *N,N*-dimethylacetamide: rather than being hard and flexible, the product was much softer and more brittle. The reaction was thus tried in toluene instead of *N,N*-dimethylacetamide, as it was felt that using a solvent that only swelled the polymer and didn't dissolve it would give a product that bore a greater resemblance to the starting material. This was indeed the case, and was unsurprising with hindsight since no reaction had occurred according to the ^1H NMR spectrum of the product dissolved in $\text{DMF-}d_6$.

2.2.5 Attempted covalent attachment of a PEG linker to PVC

Recently, Ameer *et al.*³¹² claimed that they reacted PVC with a variety of different amines to afford the corresponding modified polymers. The previously synthesised PEG linker **39** (See section 2.2.1) was subjected to the same reaction conditions (Scheme 54). It was hoped that a PEG-functionalised PVC film could be obtained by simply removing the solvent *in vacuo*.



Scheme 54. Attempted generation of PEG-functionalised PVC.

The FT-IR spectrum of the resultant polymer did not contain any peaks that were attributable to the presence of any azide moieties, which indicated that the reaction hadn't been successful.

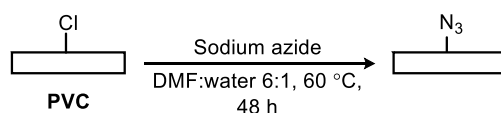
The reaction was then tried with a PVC film (See section **4.3.2** for preparation) in the presence of potassium carbonate, and in a variety of solvents, including isopropanol, ethanol, methanol, and acetonitrile. In every instance, no peaks in the FT-IR spectrum of the product corresponding to the presence of any azide moieties were detected. Moreover, it was noticed that the films were highly discoloured in every instance, presumably due to dehydrochlorination.³¹³

To try and overcome this problem, the reaction was attempted at a lower temperature of 60 °C, with the same solvents that had been used previously. In addition, the concentration of PEG linker **39** was doubled. Unfortunately, none of these alterations resulted in the covalent attachment of PEG linker **39** to the surface of a PVC film, and attempts to produce a PEG-functionalised PVC film were not pursued.

2.2.6 Modification of PVC with sodium azide

In 1969, Takeishi *et al.*³¹⁴ demonstrated that by reacting a solution of PVC with sodium azide in DMF at 60 °C, it was possible to generate PVC with covalently bound azide moieties. Later, Sacristán *et al.*³¹⁵ showed that the reaction could be done heterogeneously with a PVC film in a mixture of DMF and water. It was shown that the degree of chloride displacement by sodium azide was dependent on the ratio of DMF:water used. It was also claimed that the azide groups were homogeneously distributed throughout the polymer film when this technique was used, so one might expect chemical modification of the bulk polymer as well as the surface.

Initially, modification of a piece of PVC catheter was attempted, using the conditions of Sacristán *et al.*³¹⁵ The PVC was immersed in a solution of sodium azide (0.5 M) in DMF:water (6:1) for two days at 60 °C (Scheme **55**).

Scheme 55. Formation of azide-functionalised PVC.³¹⁵

The FT-IR spectrum of the resultant polymer did not contain any peaks that corresponded to the presence of an azide moiety; therefore, the reaction was tried using PVC powder instead of the catheter polymer film. A prominent peak in the FT-IR spectrum at 2105 cm^{-1} was observed, which was indicative of the presence of azide; however, it was impossible to discern whether or not this was covalently bound to the polymer matrix.³¹⁵ The reaction was then tried with a PVC film, which was generated from PVC powder (See section 4.3.2): once again azide functionality was detectable by FT-IR. The absence of any azide moieties when the modification was attempted with the catheter segment is hard to explain, as the exact chemical composition of the catheter segment that was used isn't known.

It was noticed that the reaction was not particularly reliable: in every instance the PVC film that was generated was a different colour, from pale yellow to dark brown. It was decided that the issue might be the concentration of the sodium azide solution, so a 0.1 M solution was used instead of a 0.5 M solution. This appeared to improve the consistency as visually similar PVC films were obtained from every separate reaction performed.

Having solved the issue with visual consistency, a more rigorous washing sequence was implemented as DMF was still present in the previously prepared PVC samples (as indicated by the presence of a peak at 1672 cm^{-1} in the FT-IR spectrum). Instead of simply rinsing the samples with water and diethyl ether, the azide containing PVC films were immersed in solutions of acetone:water 6:4 for one day, and the process was repeated three times. The acetone:water solution caused polymer swelling, so it was hoped that any unreacted sodium azide and DMF trapped in the polymer matrix would be removed in the washing process.

It was found that the DMF was removed from the polymer matrix, but was replaced by acetone (as indicated by a peak at 1710 cm^{-1} in the FT-IR spectrum). Moreover, the presence of acetone instead of DMF caused a shift

in the peak corresponding to the presence of azide to 2110 cm^{-1} (from 2105 cm^{-1}). This can be attributed to changes in the physical properties of the polymer film due to the incorporation of acetone instead of DMF.

Having improved the washing technique, evidence was obtained to confirm that the azide was covalently linked to the polymer film. An FT-IR spectrum of the azide-functionalised film was obtained prior to washing: two peaks corresponding to the presence of azide were observed at 2110 and 2027 cm^{-1} (Figure 23).

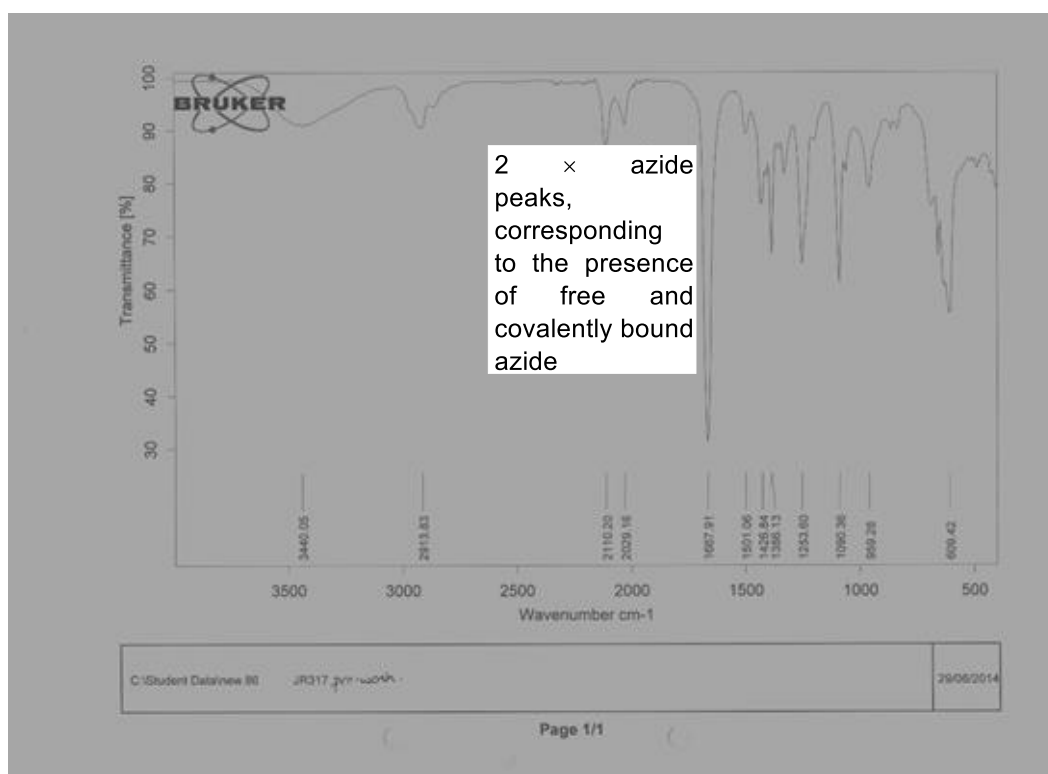


Figure 23. The FT-IR spectrum of an azide-functionalised PVC film prior to washing.

After washing, only the peak at 2110 cm^{-1} was present (Figure 24). It can thus be deduced that the peak at 2027 cm^{-1} corresponds to the presence of free, unbound sodium azide, which is removed in the washing process.

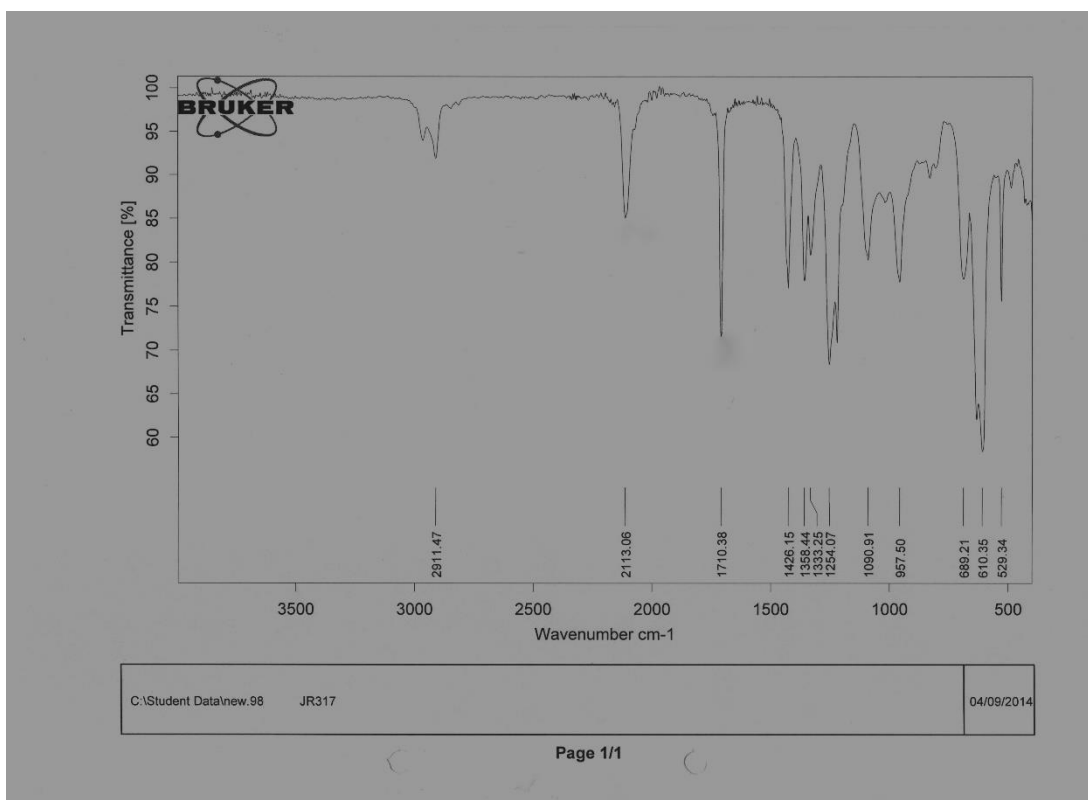


Figure 24. The FT-IR spectrum of the same azide-functionalised PVC film after washing.

Although the visual consistency of the resultant product had been improved by altering the reaction conditions, some data to quantify the amount of azide present was desired. Lafarge *et al.*¹⁰³ used X-ray photoelectron spectroscopy (XPS) to ascertain the percentage substitution of chloride substituents with azide moieties. The relative intensity of the peaks corresponding to the presence of N and Cl atoms was used to calculate the percentage of chloride displacement, using the formula shown below:

$$\% (\text{Chloride displacement}) = \frac{\frac{\%N}{3}}{\%Cl + \frac{\%N}{3}} \times 100$$

The effect on the consistency of the reaction was investigated by making alterations to the scale, as well as the concentration of sodium azide (from 0.1-0.5 M). It was found that the reaction was very inconsistent: even films immersed in the same reaction solution were subject to vastly different levels of chloride displacement, which was particularly noticeable when the reaction was scaled up (Table 9). It was felt that one issue could have been the amount of time each PVC disc spent in contact with the wall of the reaction vessel.

According to Sacristán *et al.*,³¹⁵ however, sodium azide is able to penetrate the polymer bulk, so this shouldn't have an effect in theory.

Concentration of sodium azide	Relative scale	% of chloride displacement values for each PVC film
0.1 M (a)	1	5.4, 11.1
0.1 M (b)	1	5.9, 14.8
0.2 M (a)	1	10.2, 12.3
0.2 M (b)	1	21.5, 10.8
0.3 M (a)	1	22.3, 23.7
0.3 M (b)	1	24.2, 19.0
0.4 M (a)	1	23.9, 22.6
0.4 M (b)	1	16.3, 17.6
0.5 M (a)	1	4.6, 24.5
0.5 M (b)	1	32.9, 28.2
0.1 M (a)	2	14.4, 19.4, 15.6, 11.0
0.1 M (b)	2	5.8, 1.7*, 0*, 8.5
0.1 M (a)	4	0*, 11.9, 1.5*, 13.0, 15.6, 15.6, 7.8, 4.4
0.1 M (b)	4	8.9, 10.1, 13.4, 11.1, 5.9, 9.9, 12.6, 10.4

Note: Two repeat experiments were conducted for each different concentration of sodium azide used (denoted "a" and "b"); values marked with an asterisk have a large associated error.

Table 9. Percentage of chloride displacement values for each polymer film.

It was felt that using PVC powder instead of a film might result in the reaction being more consistent, so a similar set of experiments were tried. For each powder sample, spread evenly across carbon fibre tape, the XPS spectrum was measured five times at different locations. The average percentage of chloride displacement under different reaction conditions is shown below, along with the original five measurements for each sample (Table 10).

Concentration of sodium azide	% of chloride displacement measurements	Average % of chloride displacement
0.05 M (a)	0*, 2.7, 2.9, 2.8, 2.8	2.8
0.05 M (b)	3.5, 1.5, 0*, 0*, 3.8	2.9
0.1 M (a)	4.0, 8.1, 6.4, 3.8, 4.1	5.3
0.1 M (b)	5.7, 4.7, 4.8, 4.9, 6.4	5.3
0.2 M (a)	1.9, 0*, 0*, 0*, 2.3	2.1
0.2 M (b)	0*, 3.8, 3.3, 0*, 2.4	3.2
0.3 M (a)	3.7, 2.9, 3.4, 3.8, 4.1	3.6
0.3 M (b)	3.6, 3.2, 2.9, 4.3, 3.1	3.4
0.4 M (a)	16.3, 14.1, 14.7, 13.4, 14.3	14.6
0.4 M (b)	14.6, 15.2, 15.4, 14.6, 12.7	14.5
0.5 M (a)	16.8, 18.6, 18.1, 15.7, 16.1	17.0
0.5 M (b)	15.1, 14.2, 14.1, 14.7, 14.3	14.5

Note: Two repeat experiments were conducted for each different concentration of sodium azide used (denoted "a" and "b"); values marked with an asterisk have a large associated error and are therefore not included in the average calculations.

Table 10. Average percentage of chloride displacement as calculated from the XPS data that was obtained.

The peak corresponding to N in the XPS spectrum was barely visible when the concentration of sodium azide was less than or equal to 0.3 M. The calculated values for percentage of chloride displacement have a large associated error for these samples. When PVC powder was exposed to higher concentrations of sodium azide (0.4 and 0.5 M), the percentage of chloride displacement was measured as being anywhere between 13% and 16%, and 14% and 19% respectively.

Of course, as might be expected, the PVC powders that had been exposed to more concentrated solutions of sodium azide were highly discoloured, which was not desirable. Moreover, the reaction had not been shown to be remarkably consistent at these concentrations, and it's impossible to suggest whether the reaction is more consistent at lower concentrations as the XPS data for these samples is unreliable. Nonetheless, attempts to graft various

alkynes to an azide-functionalised PVC film, as prepared in this section, are described below.

2.2.7 Attempted grafting of an alkyne to an azide-functionalised PVC film via a 1,3-dipolar cycloaddition

As discussed at the beginning of the results and discussion (Section 2.1), a number of groups have utilised the 1,3-dipolar cycloaddition reaction to covalently graft a variety of compounds or polymers to a polymer surface. A few of these groups have described the covalent attachment of various alkyne-functionalised moieties to azide-functionalised PVC.^{9,103,279-281}

Initially the physical properties of the PVC film that had been generated (See section 4.3.2) were investigated after immersion in a range of different solvents. A solvent that induced swelling without permanent changes to the size and physical properties of the polymer was desired as a medium for the proposed 1,3-dipolar cycloaddition reaction. It was found that the structure of the film was unaltered, and no swelling was induced, after immersion in water, alcoholic solvents, and diethyl ether. On the other hand, solvents such as DCM, chloroform, acetone, and DMSO effected significant swelling, which resulted in the permanent deformation of the polymer film. In addition, DMF and THF were found to dissolve PVC. It was found that acetonitrile, as well as toluene, caused only minor swelling and after drying the polymer film returned to its original size and shape. The more volatile solvent, acetonitrile, was chosen for most of the experiments.

To produce the azide-functionalised PVC used in these reactions, PVC films were immersed in 0.1 M solutions of sodium azide. The XPS data obtained cannot be relied upon extensively, but it was apparent that chloride displacement by sodium azide was significantly less than 10% when the reaction was conducted at this concentration. It was therefore decided that the amount of coupling partner that was required should be calculated on the basis that the percentage of chloride displacement was 10%. Moreover, to drive the reaction to completion with respect to azide consumption, 1.5 equivalents of alkyne-functionalised leucocrystal violet analogue **28** (See section 2.1.4) were used. The complete disappearance of the azide peak in the FT-IR spectrum

of the resultant polymer would be indicative of a successful reaction. Conversely, if the dye was used as the limiting reagent, it would be more difficult to prove that it was covalently bound to the polymer and not just physically adsorbed to the surface, as an azide peak would still be present in the FT-IR spectrum even if the reaction were successful.

The reaction between azide-functionalised PVC and leucocrystal violet analogue **28** was tried predominantly in acetonitrile with a variety of different copper catalysts: $\text{CuSO}_4 \cdot 5\text{H}_2\text{O}$ /sodium ascorbate, CuI , CuBr , CuCl , $\text{CuBr}(\text{PPh}_3)_3$, $\text{Cu}(\text{OAc})_2 \cdot \text{H}_2\text{O}$ /sodium ascorbate, $\text{Cu}(0)$ powder, and $\text{CuSO}_4 \cdot 5\text{H}_2\text{O}/\text{Cu}(0)$ powder. In every instance the reaction was performed in the presence of triethylamine. Control reactions were tried in the absence of triethylamine, and in toluene instead of acetonitrile, with the catalyst $\text{CuBr}(\text{PPh}_3)_3$. In addition, a control reaction with no copper catalyst was conducted (Table 11).

Catalyst	Solvent	Base	Colour after "click"	Colour after oxidation
$\text{CuSO}_4 \cdot 5\text{H}_2\text{O}$, sodium ascorbate	Acetonitrile	Triethylamine	Blue-Purple	Purple
CuI	Acetonitrile	Triethylamine	Pale Blue	Purple
CuBr	Acetonitrile	Triethylamine	Green-Grey	Purple
CuCl	Acetonitrile	Triethylamine	Light Brown	Purple
$\text{CuBr}(\text{PPh}_3)_3$	Acetonitrile	Triethylamine	Purple	Purple
$\text{CuBr}(\text{PPh}_3)_3$	Toluene	Triethylamine	Purple	Purple
$\text{CuBr}(\text{PPh}_3)_3$	Acetonitrile	None	Purple	Purple
$\text{Cu}(\text{OAc})_2 \cdot \text{H}_2\text{O}$, sodium ascorbate	Acetonitrile	Triethylamine	Purple	Purple
$\text{Cu}(0)$ powder	Acetonitrile	Triethylamine	Purple	Purple
$\text{CuSO}_4 \cdot 5\text{H}_2\text{O}$, $\text{Cu}(0)$ powder	Acetonitrile	Triethylamine	Purple	Purple
None	Acetonitrile	Triethylamine	Pale Purple	Purple

Table 11. Attempted 1,3-dipolar cycloaddition reaction between azide-functionalised PVC and leucocrystal violet analogue **28**.

Once the PVC discs had been subjected to the above-mentioned conditions for one day, they were immersed in acetonitrile with the intention of washing away any unbound components. The latter process was repeated three times,

after which nothing else appeared to be removed. The discs from nearly all the reactions exhibited a deep purple colouration, indicative of the presence of the oxidised form of leucocrystal violet analogue **28** (Table 11). This was a cause for optimism, as it would negate the need to subject the discs to oxidative conditions to generate the desired crystal violet analogue **35**.

The presence of crystal violet analogue **35** in the PVC discs was confirmed by UV-Vis absorbance spectroscopy: the absorbance maxima were observed at, or close to, 593 nm. Unfortunately, the FT-IR spectra still contained prominent peaks in the azide region in every case, so it was not possible to say whether any of crystal violet analogue **35** present was covalently bound. Moreover, a ^1H NMR spectrum was obtained in $\text{DMF-}d_7$ for one of the samples which appeared to contain a higher concentration of crystal violet analogue **35**. It was not possible, however, to detect any peaks that might have been attributable to the presence of a triazole proton in the aromatic region of the spectrum.³¹⁶

The PVC films were subjected to oxidative conditions (chloranil in acetonitrile) to convert any of the reduced form of crystal violet analogue **35** that might still be present. The polymer samples were then washed by immersion in solutions of acetone:water (3:2). This solvent system was chosen because it can both induce swelling of the PVC samples and dissolve crystal violet analogue **35**. It was felt that if crystal violet analogue **35** did not leach from the polymer in a solution that caused swelling, then this would be strong evidence to suggest that it was in fact covalently bound.

Sadly, extensive leaching of crystal violet analogue **35** from the polymer samples was observed, even after ten wash cycles in some instances. With no further ideas for proving that any crystal violet analogue **35** was covalently bound to the polymer, this area of research was not pursued any further.

With hindsight, perhaps it was not reasonable to expect that all the polymer bound azide could undergo a reaction purely due to steric demand. It may be impossible for leucocrystal violet analogue **28** to penetrate the bulk polymer, or for it to react with two azide moieties in close proximity. The latter issue could perhaps be overcome by reducing the percentage of surface-bound azide relative to chloride. It then becomes even more difficult to quantify to any

extent the amount of azide that is present, though. In any case, it has not been possible to show that the azide moieties are uniformly distributed throughout the polymer, so this is still no guarantee of success.

2.3 Ethyl violet as an alternative to crystal violet?

The use of crystal violet as an antibacterial agent, either when illuminated or in the dark, is very well documented in the literature and is discussed extensively in the introduction. There are, however, issues relating to the toxicity of crystal violet: it is known to persist in the environment and is a potent carcinogen.¹³⁵ Though this is not envisaged as being a problem in cases where the compound is embedded in a polymer matrix,²⁷⁰⁻²⁷² there is clearly scope for elucidating less hazardous alternatives.

The commercially available compound ethyl violet has a very similar structure to crystal violet, with the only difference being the exchange of the methyl groups attached to the amine in crystal violet with ethyl groups (Figure 25).

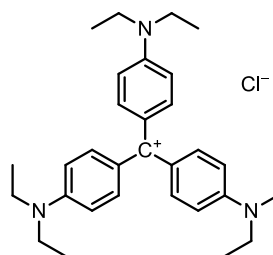


Figure 25. Ethyl violet.

In 2001, Mellish *et al.*³¹⁷ described the synthesis of a variety of methylene blue analogues, where the dimethyl- substituents were replaced with longer alkyl chains. The group observed that the photosensitising ability of the compounds was reduced as the alkyl chain length increased. The differences observed were small when the alkyl chain length was four carbons or less. For longer alkyl chain lengths, the photosensitising ability of the corresponding compounds was greatly reduced. Interestingly, in the study conducted, all the compounds except for methylene blue were excluded from the nucleus of the tumour cells they were incubated with, thus reducing the mutagenic potential of these compounds.

Importantly, unlike crystal violet, ethyl violet has not been classified as a hazardous compound. One might reasonably assume that its potential as a mutagen would be less than that of crystal violet, due to it being more hydrophobic and based on the observations of Mellish *et al.*³¹⁷ In essence, ethyl violet might prove to be a better alternative to crystal violet in the future due to it being a less hazardous substance, even if its efficacy as a photosensitiser was shown to be less than that of crystal violet.

In the following sections, the efficacy of ethyl violet as a photosensitiser is assessed. Its photobactericidal activity was compared to that of crystal violet in the light, and in the dark.

2.3.1 Preparation and characterisation of dye-incorporated polymer samples

Initially, crystal violet and ethyl violet were incorporated into medical grade silicone using a “swell-encapsulate-shrink” technique, previously reported by Ozkan *et al.*²⁷¹ A sheet of silicone was cut into 1 cm × 1 cm squares, which were immersed in solutions of each dye (1×10^{-3} M) in chloroform for three days in the dark. After this time, the samples were rinsed with distilled water, dried with paper towels, and allowed to air dry in the dark overnight (Figure 26).

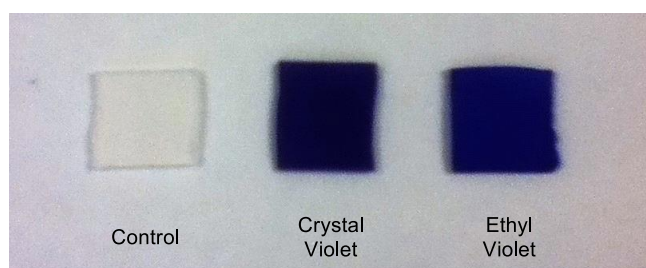


Figure 26. Polymer samples after the incorporation process.

The dye-incorporated samples were analysed by FT-IR and UV-Vis absorbance spectroscopy. In addition, leaching tests were performed in PBS solution.

The FT-IR spectra of the silicone samples incorporated with ethyl violet and crystal violet were obtained, and compared to the spectrum of an unmodified control sample. The spectra were identical in appearance, which indicates that

no significant chemical change occurs during the incorporation process. Moreover, new peaks corresponding to the presence of crystal/ethyl violet were not observed. One can therefore conclude that the physical and chemical properties of the bulk polymer are largely unaffected by the introduction of crystal/ethyl violet.

The UV-Vis absorbance spectra of the samples were obtained, and are shown below (Figure 27). The peaks corresponding to the presence of ethyl violet and crystal violet are poorly resolved, due to the low percentage of light transmission through the intensely coloured polymer samples. For this reason, it is impossible to ascertain the consistency of dye uptake of samples from the same incorporation batch and of samples subjected to the same conditions in different batches. In addition, the spectrum of the polymer sample containing ethyl violet is red-shifted relative to that of the one with crystal violet incorporated, but it is not possible to determine an absorbance maximum for either.

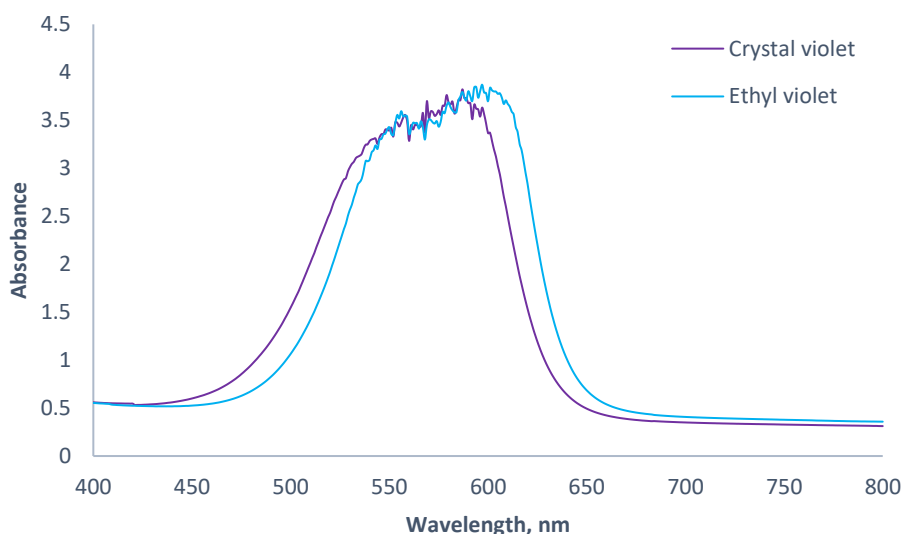


Figure 27. UV-Vis absorbance spectra of the dye-incorporated polymer samples.

The polymer samples incorporated with crystal/ethyl violet were immersed in PBS solution for a period of one week. The UV-Vis spectra of the resultant solutions were recorded after this time, as well as at various time intervals in-between. After one week, no loss of crystal/ethyl violet from the polymer into solution due to leaching was observed.

2.3.2 Antibacterial activity of dye-incorporated polymer samples

The following study was carried out by Sandeep Sehmi. The antibacterial activity of the polymer samples was tested against *E. coli*, a Gram-negative bacterium. As expected, the unmodified control samples exhibited no activity after incubation in the dark for five hours or after five hours of illumination with a 6000-lux white light source. The samples containing crystal/ethyl violet had no appreciable effect on the numbers of bacterial colonies after incubation in the dark for five hours. The samples incorporated with ethyl violet (~1 log reduction in CFU) proved to be less efficacious than those that contained crystal violet (~1.5 log reduction in CFU), when exposed to the white light source (Figure 28).

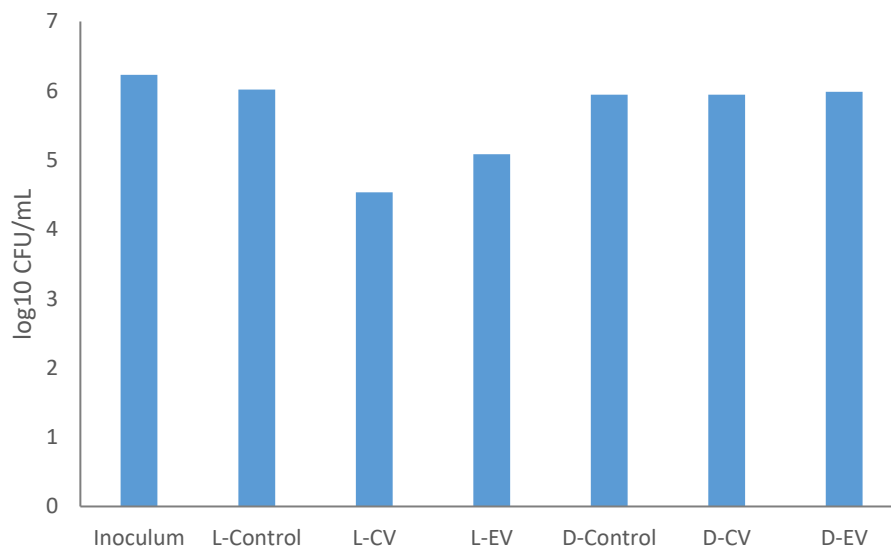


Figure 28. The number of *E. coli* CFU per mL on the surfaces of the polymer samples after white light illumination, or incubation in the dark for 5 hours. D = dark, L = light; CV = crystal violet, EV = ethyl violet.

In this section, ethyl violet has been shown to be less effective at preventing the colonisation of polymer surfaces by *E. coli* than crystal violet. Though this result is disappointing, the ability of ethyl violet to function as a photosensitiser has been demonstrated and, as previously discussed, it may prove to be a less toxic, more environmentally friendly alternative to crystal violet in future applications where this is desirable.

2.4 Assessment of the antibacterial activity and physical properties of silicone incorporated with different porphyrins

The use of porphyrins in photodynamic therapy and, to a lesser extent, in the preparation of antibacterial surfaces is extremely well documented, and is discussed extensively in the introduction. It was apparent that in nearly all instances, the antibacterial activity was assessed for only one or two porphyrins in the same microbiological assay. It is thus difficult to infer what chemical modifications could be used to improve the antibacterial activity of a porphyrin.

In the following sections, the syntheses of several different analogues of *meso*-tetraphenylporphyrin (TPP) **42** are described. The porphyrins were incorporated into medical grade silicone *via* a swell-encapsulate-shrink process. For the resultant polymers, FT-IR, UV-Vis, and fluorescence spectra were obtained. Unfortunately, no microbiologists were available to test the antibacterial activity of the films before this thesis was written.

2.4.1 Synthesis of related analogues of *meso*-tetraphenylporphyrin (TPP)

The structures of 8 different porphyrins, identified as synthetic targets and all closely related to TPP **42**, are shown below (Figure **29**).

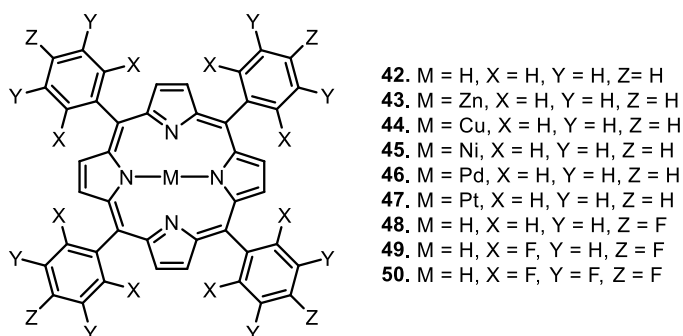
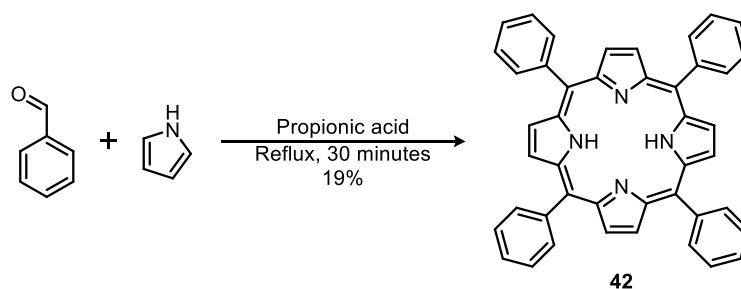
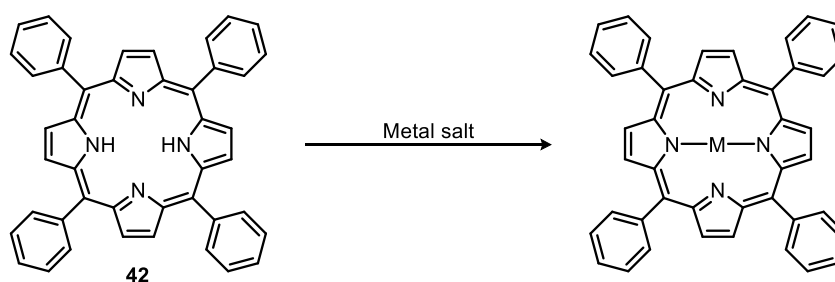


Figure **29**. Compounds **42-50** that were identified as synthetic targets.

Initially, TPP **42** was prepared by reacting pyrrole with benzaldehyde in refluxing propionic acid.³¹⁸ The desired product was obtained in yields of 18-19%, which are in accordance with the reported literature values (Scheme **56**).

Scheme 56. Synthesis of TPP **42**.

The reaction between TPP **42** and various metal salts afforded the resultant metalloporphyrins in reasonably good yields (Table 12).



Metal salt	Solvent	Temperature	Time	Yield
Zn(OAc) ₂	Chloroform	R.t.	1 h	69%, 43
Cu(OAc) ₂	Chloroform	Reflux	3 h	73%, 44
Ni(acac) ₂	Toluene	Reflux	72 h	69%, 45
Pd(OAc) ₂	Chloroform	Reflux	96 h	74%, 46
PtCl ₂	Benzonitrile	Reflux	24 h	76%, 47

Table 12. Synthesis of metalloporphyrins **43-47**.

The reaction between Zn(OAc)₂ or Cu(OAc)₂ with TPP **42** was found to proceed much more rapidly than the analogous reaction between TPP **42** and Ni(acac)₂, Pd(OAc)₂ or PtCl₂. This is because complexes of Cu(II) and Zn(II) are almost invariably tetrahedral, whereas group 10 metal (II) complexes are nearly always square planar. It is well known that d⁸ square planar complexes are highly stable as the unfilled d(x² – y²) orbital is strongly anti-bonding, and the filled d orbitals are virtually non-bonding in nature (Figure 30).

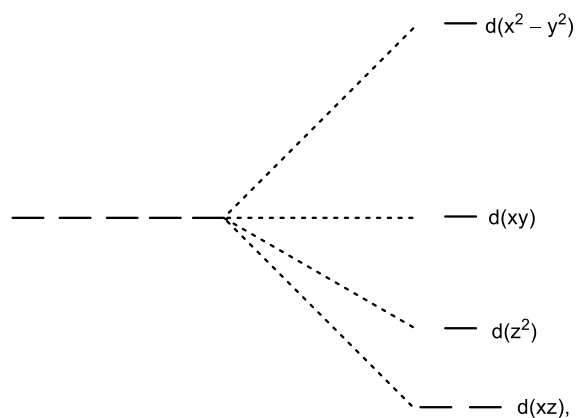
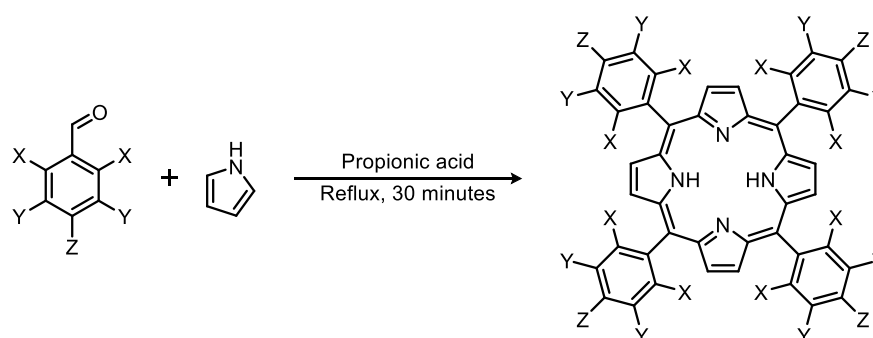


Figure 30. Crystal field splitting diagram of a square planar complex.

It was found that the isolation of NiTPP **45** proved to be somewhat troublesome due to its relatively low solubility in toluene. It was quickly established that filtering a mixture of NiTPP **45** and Na_2SO_4 in toluene, obtained in the aqueous crude work up, resulted in a substantial loss of the desired product. The drying step was not carried out in future experiments and thus good yields were obtained.

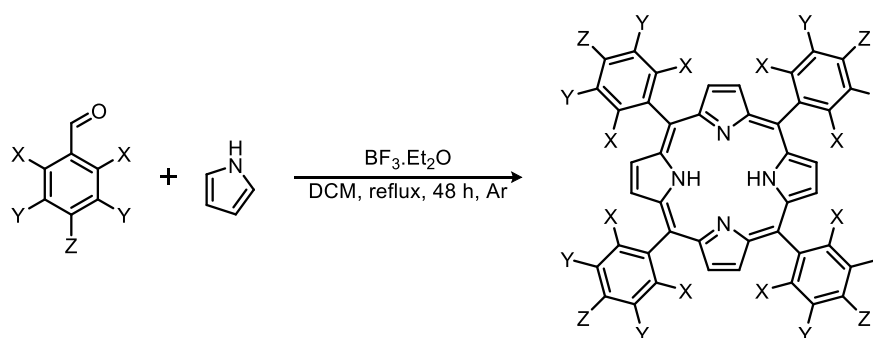
Having successfully synthesised a set of metalloporphyrins, attempts to prepare three different tetraphenylporphyrins with varying degrees of fluorination were begun. Initially, the porphyrin syntheses were attempted using the conditions of Adler *et al.*³¹⁸ (Table 13). It was quickly discovered that these conditions were not suitable for the syntheses of the more soluble porphyrins, *meso*-tetra(pentafluorophenyl)porphyrin (F_{20}TPP) **48** and *meso*-tetra(2,4,6-trifluorophenyl)porphyrin (F_{12}TPP) **49**, which were not isolated. On the other hand, the method employed afforded *meso*-tetra(4-fluorophenyl)porphyrin (F_4TPP) **50** in a yield of 24%. It was discovered, however, that the product was highly insoluble in chloroform, as well as in other solvents, so it was not possible to obtain NMR spectra for this compound. This observation is in agreement with the results published that were previously by Fleischer *et al.*³¹⁹ in 1973.



Substrate	Yield
X = Y = Z = F	Not isolated, 48
X = Z = F, Y = H	Not isolated, 49
X = Y = H, Z = F	24%, 50

Table 13. Attempted synthesis of the fluorinated tetraphenylporphyrins **48-50** by the method of Adler *et al.*³¹⁸

The method of Adler *et al.*³¹⁸ is generally preferred for ease of purification of the desired product, but can only be used to access a relatively limited number of porphyrins. In addition, the reaction conditions that are employed are fairly harsh. The method of Dommaschk *et al.*,³²⁰ based on the work of Lindsey *et al.*,³²¹ was tried with boron trifluoride as the acid-catalyst. These conditions are much milder and so it is possible to synthesise a greater range of porphyrins. The desired porphyrins, F₂₀TPP **48** and F₁₂TPP **49**, were synthesised, and obtained in yields of 17% and 20% respectively (Table 14).



Substrate	Yield
X = Y = Z = F	17%, 48
X = Z = F, Y = H	20%, 49

Table 14. Synthesis of F₂₀TPP **48** and F₁₂TPP **49** by the method of Dommaschk *et al.*³²⁰

Unfortunately, F₁₂TPP **49** was only successfully prepared once. Future attempts to make this compound proved to be fruitless, and so it was only used in the preliminary optimisation studies of the incorporation process.

For each of the porphyrins dissolved in chloroform (1×10^{-5} M), UV-Vis absorbance and fluorescence spectra were recorded and are shown below (Figures 31 and 32).

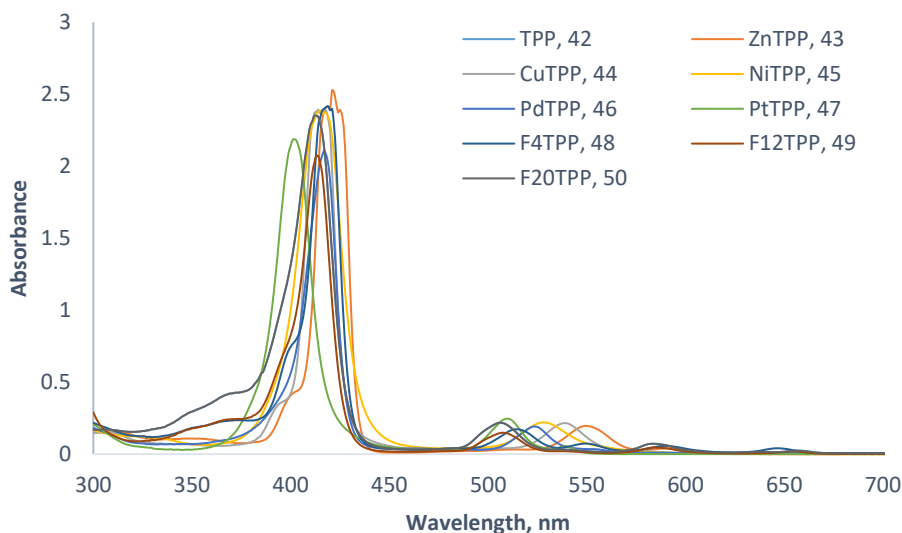


Figure 31. UV-Vis absorbance spectra of porphyrins **42-50** dissolved in chloroform.

The UV-Vis absorbance spectra of each of the above porphyrins can be considered in terms of two separate sections: the near UV region containing a high intensity Soret or B band, which corresponds to an $S_0 \rightarrow S_2$ transition; and the visible region that contains one or more lower intensity Q bands, which correspond to the $S_0 \rightarrow S_1$ transition.³²²

The spectra of the more symmetric metalloporphyrins contain up to two visible Q bands, whereas for the less symmetric free-base porphyrins up to four Q bands can be observed. This is because the electronic dipole transitions in the x and y directions are equivalent for metalloporphyrins. The electronic absorptions of PtTPP **47** are subject to a significant hypsochromic shift. This is predominantly a result of increased metal $d\pi$ to porphyrin π^* back-bonding, which increases the HOMO-LUMO gap of the system. This effect is also seen, to a lesser extent, in the spectra of the copper, nickel, and palladium tetraphenylporphyrins (**44**, **45**, and **46**), when compared to the spectrum of ZnTPP **43**.^{323,324}

The fluorinated tetraphenylporphyrins **48-50** gave spectra that were not markedly different to the spectrum of TPP **42**. There were two oddities, though, the first being that the peak that was expected at roughly 550 nm was only

clearly visible in the spectrum of F₄TPP **50**. The second observation was that the extinction coefficient obtained for F₁₂TPP **49** in chloroform was markedly lower than that of the other fluorinated variants (**48** and **50**) and TPP **42**. There is no obvious reason for these unusual findings; however, they are of little consequence.

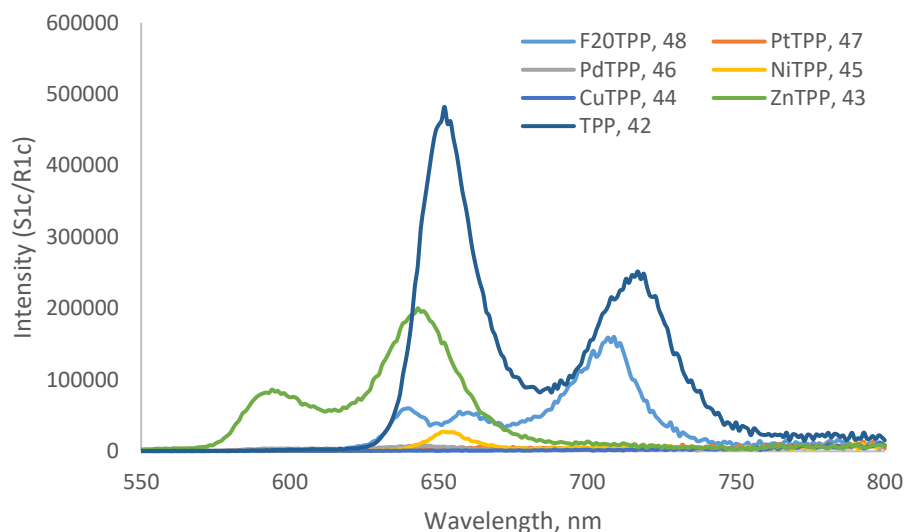


Figure 32. Fluorescence spectra of porphyrins **42-48** dissolved in chloroform.

The fluorescence spectrum of each of the samples was obtained (Figure 32). While the fluorescence spectra of the polymer films that were incorporated with TPP **42** and ZnTPP **43** contained two clear peaks, the polymer samples containing the other metalloporphyrins **44-47** were virtually inactive. In the case of PtTPP **47**, and to a lesser extent PdTPP **46**, the presence of a heavy metal atom results in increased spin-orbit coupling, which makes spin-forbidden ISC to an excited triplet state more favourable.³²⁵ In addition, ISC is relatively favourable for CuTPP **44** due to the fact that it is a paramagnetic species.³²⁵ The excited triplet state molecule can transfer its energy to another nearby molecule, such as oxygen or water, to generate ROS; alternatively, it can undergo phosphorescence or some other non-radiative energy transfer in order to return to the ground state. On the other hand, the excited singlet state of NiTPP **45** is low in energy, which means that the molecule can return to ground state *via* internal conversion.³²⁶ Intriguingly, the polymer film that was incorporated with the free-base porphyrin, F₂₀TPP **48**, gave rise to a spectrum with three fluorescence peaks, despite the fact that only two peaks were

anticipated. It is felt that this is due to peak splitting, which results from vibronic coupling; however, it is strange that this effect hasn't been noted previously.³²⁷

2.4.2 Preparation and characterisation of porphyrin-incorporated polymer films

To begin with, optimisation studies were carried out to establish the best conditions for the incorporation process. The experiments were carried out with TPP **42** dissolved in toluene, which was chosen because it can both solubilise the porphyrins that had been synthesised and effect the swelling of silicone. In addition, all the experiments were carried out in the dark, to prevent photocatalytic oxidation of the porphyrins in solution. Firstly, the effect of porphyrin concentration was investigated: solutions containing different amounts of TPP **42** were prepared, and 1 cm × 1 cm silicone films were immersed in these solutions for three days. The resultant films were rinsed with distilled water, before being air-dried in the dark for one day. An image of the resultant films is shown below (Figure **33**).

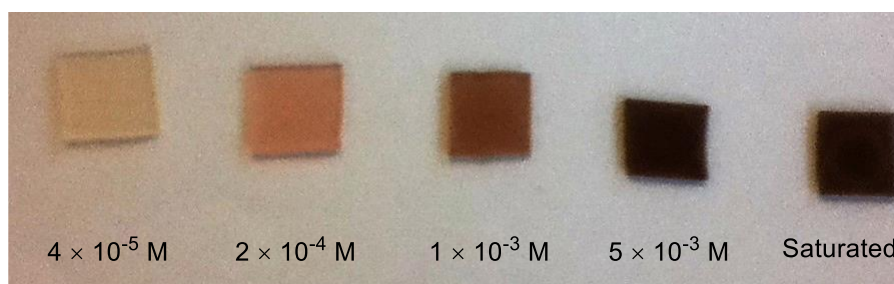


Figure **33**. Silicone films that had been exposed to solutions of TPP **42** of varying concentration for three days.

When the concentration of the porphyrin solution was less than 4×10^{-5} M, the porphyrin was not visible in solution. The incorporation process appeared to work best for the silicone film that was exposed to a 5×10^{-3} M solution of TPP **42**; therefore, this concentration was selected for all further experiments.

Having identified the most suitable concentration, the effect of immersion time was investigated. In this case, 1 cm × 1 cm silicone films were submerged in 5×10^{-3} M porphyrin solutions for varying periods of time, after which they were washed and dried as described above. An image of the films that were produced is shown (Figure **34**).

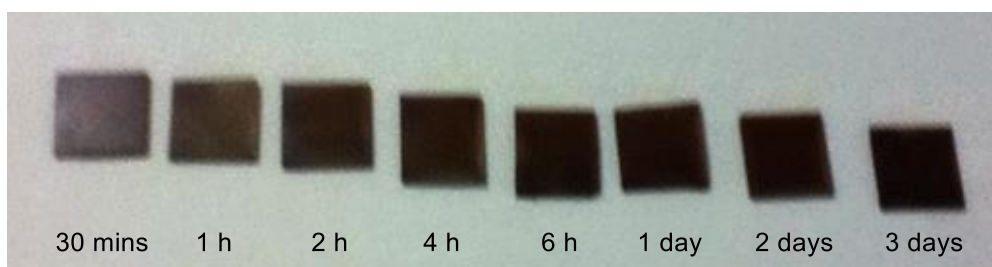


Figure 34. Silicone films that had been exposed to solutions of TPP **42** for varying periods of time.

By looking at the above image, it is not altogether obvious what the optimal immersion time is; however, on closer inspection, it does seem that longer immersion times give rise to greater dye uptake (Figure 35). On that basis, it was decided that the incorporation time would be three days for all further experiments.

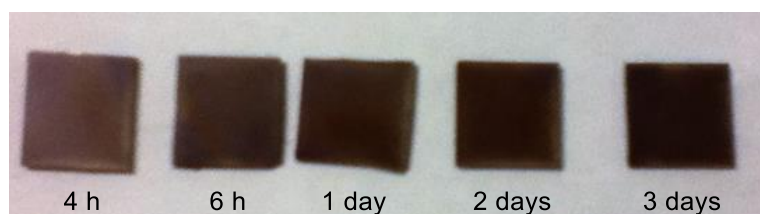


Figure 35. Silicone films that had been exposed to solutions of TPP **42** for longer periods of time.

The optimised conditions were used to incorporate the previously synthesised porphyrins **42-50** into 1 cm × 1 cm silicone films. In this instance, fifteen polymer squares were immersed in the same solution of porphyrin in toluene (5×10^{-3} M) for three days. Unfortunately, several problems were encountered at various stages of the incorporation process. It was immediately found that both NiTPP **45** and F₄TPP **50** were very poorly soluble in toluene. Once the incorporation process was complete, a number of samples, including the ones incorporated with TPP **42**, were observed to have extensive porphyrin aggregation (Figure 36). Moreover, samples that were incorporated with the same porphyrin were found to exhibit obvious visual differences, indicating that the process was inconsistent.

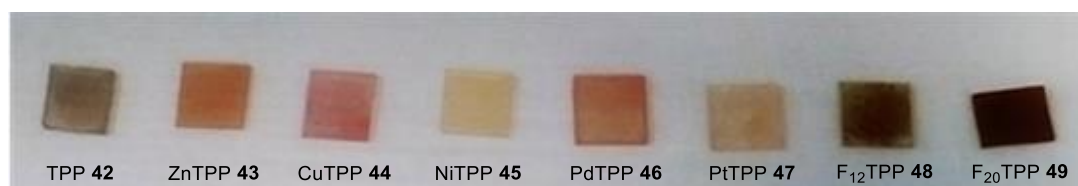


Figure 36. Silicone films that had been exposed to different porphyrin solutions for three days.

It was hypothesised that one issue might be the fluxional temperature within the lab. To test this, two 1 cm × 1 cm silicone films were immersed in identical, yet separate, solutions of TPP **42** in toluene. One experiment was kept in the fridge, while the other was kept on the bench. No appreciable difference between the two resultant samples was observed, although dye uptake appeared to be greater for the experiment that was carried out on the bench (Figure **37**).

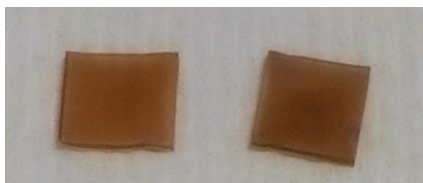


Figure 37. Silicone films that had been immersed in solutions of TPP **42**, which had been left in the fridge (left) and on the bench (right), for three days.

It was noticed that toluene was ineffective at solubilising some dyes, so a new solvent system needed to be considered. Moreover, doubts were had about the effectiveness of the washing process, and whether this was a cause of some of the problems that were being encountered. Finally, the incorporation process appeared to be markedly more uniform when only one silicone film was immersed in a porphyrin solution, and that things tended to go wrong when multiple samples were immersed in the same solution at the same time.

To try to resolve the first two issues, four experiments were devised to ascertain whether chloroform would be a more suitable solvent system than toluene for the incorporations, and whether the washing process had a negative effect. To start with, two 1 cm × 1 cm silicone films were immersed in separate solutions of TPP **42** in chloroform, while another two samples were immersed in separate solutions of the same porphyrin in toluene. Of the four silicone films that were incorporated with TPP **42**, two that were subjected to different incorporation conditions were washed with distilled water before drying, while the remaining two samples were only dried (Figure **38**).

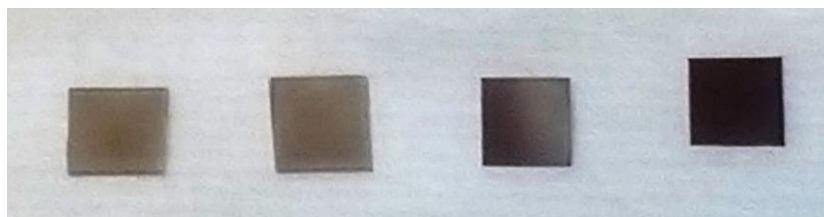


Figure 38. Silicone films that were incorporated with TPP **42** via different procedures. From left to right: toluene, no wash; toluene, washed; chloroform, no wash; and chloroform, washed.

Clearly, the sample that had been immersed in a solution of TPP **42** in chloroform, and rinsed with distilled water once the incorporation process was terminated, appeared to have the most uniform dye distribution. These conditions were thus used to for the preparation of a batch of fifteen silicone samples that were immersed in the same incorporation solution at the same time. Unfortunately, the resultant films displayed signs of porphyrin aggregation, as TPP **42** was unevenly distributed on the surface (Figure 39).

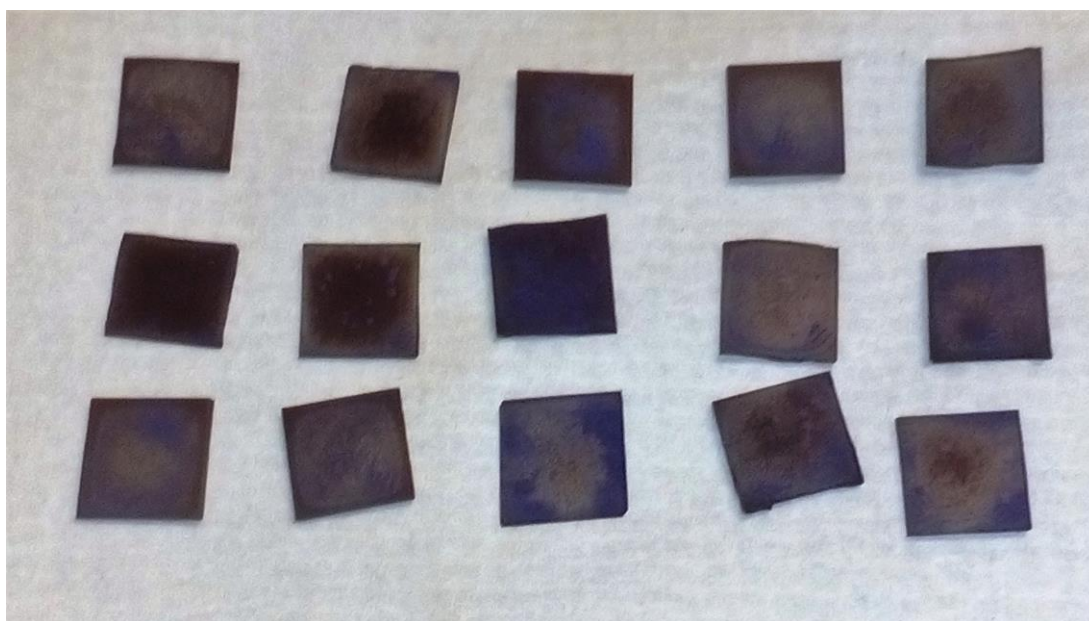


Figure 39. The fifteen 1 cm x 1 cm silicone films that were incorporated with TPP **42**.

Having established that the incorporation of every polymer sample had to be done individually, and that chloroform appeared to be a more suitable solvent system than toluene, new experiments were designed to incorporate 1 cm x 1 cm silicone films with porphyrins **42-48**. The porphyrin concentration was lowered from 5×10^{-3} M to 1×10^{-3} M, to preserve precious material in case this set of experiments did not go according to plan. It was felt that using this concentration would still give a sufficient level of dye uptake, as can be seen above (Figure 38). Thankfully, the dye-incorporated polymer films that were

obtained from these experiments exhibited no signs of porphyrin aggregation, and samples that were incorporated with the same compound appeared to display similar colouration, at least by eye (Figure 40).



Figure 40. Silicone films that had been exposed to different porphyrin solutions for three days.

The FT-IR spectra of the porphyrin-incorporated silicone samples were obtained, and compared to the spectrum of an unmodified control sample. The spectra were identical in appearance, which indicates that no significant chemical change occurs during the incorporation process. Moreover, new peaks corresponding to the presence of porphyrins **42-48** were not observed. One can therefore conclude that the physical and chemical properties of the bulk polymer are largely unaffected by the introduction of porphyrins **42-48**.

The UV-Vis absorbance spectra of the samples were obtained, and are shown below (Figure 41). The sample containing fluorinated porphyrin **48** is intensely absorbing, whereas the samples containing the other porphyrins **42-47** are very weakly absorbing. In fact, the samples containing ZnTPP **43** and NiTPP **45** have barely discernible absorbance maxima. Of the samples that do give rise to spectra with clearly defined absorbance maxima, the UV-Vis spectra correlate closely with the previously obtained spectra for each of the porphyrins dissolved in chloroform.

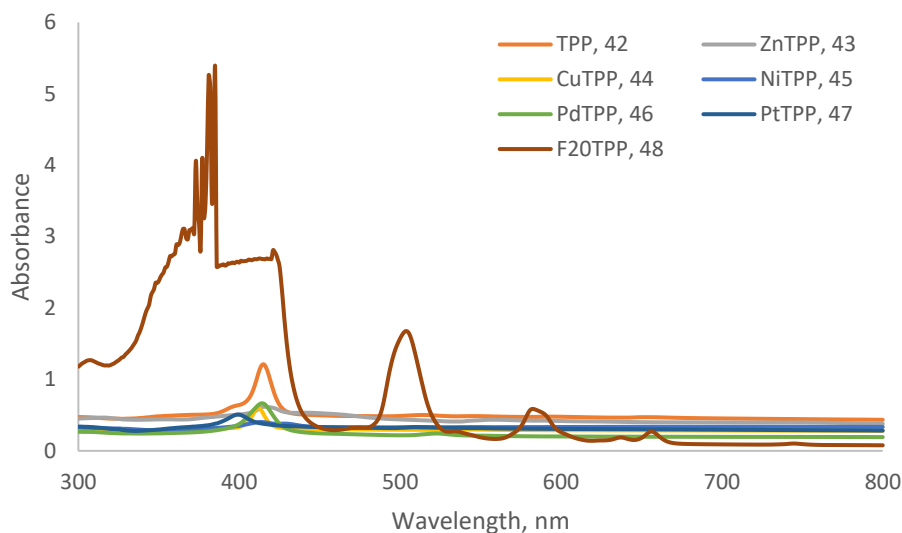


Figure 41. UV-Vis absorbance spectra of 1 cm x 1 cm silicone films incorporated with porphyrins **42-48**.

The fluorescence spectra of the samples were obtained (Figure 42). Except for ZnTPP **43**, every porphyrin-incorporated sample gave rise to a fluorescence spectrum which was almost identical to that which was recorded for each of the porphyrins when dissolved in chloroform. For the sample that was incorporated with ZnTPP **43**, the anticipated peak at 600 nm was non-existent, while the peak at 650 nm now appeared to have a shoulder peak at roughly 640 nm. Moreover, a broad peak at around 710 nm was observed, which wasn't seen previously. It can be concluded that the properties of ZnTPP **43** have been altered by the incorporation process, or by virtue of it being encapsulated within silicone.

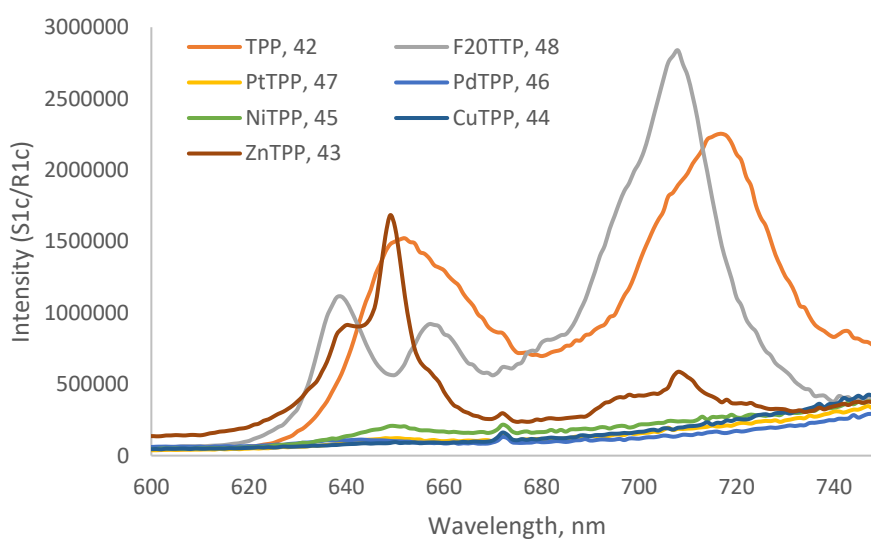


Figure 42. Fluorescence spectra of 1 cm x 1 cm silicone films incorporated with porphyrins **42-48**.

Having prepared and analysed a series of silicone films incorporated with porphyrins **42-48**, the next stage is to run microbiological experiments to ascertain their effectiveness at killing bacteria both in the light and in the dark. Unfortunately, due to time constraints and a lack of available trained microbiologists, these studies have been put on hold for the foreseeable future.

2.5 Attempted formation of polyurethane with a covalently attached crystal violet analogue via a polymerisation reaction

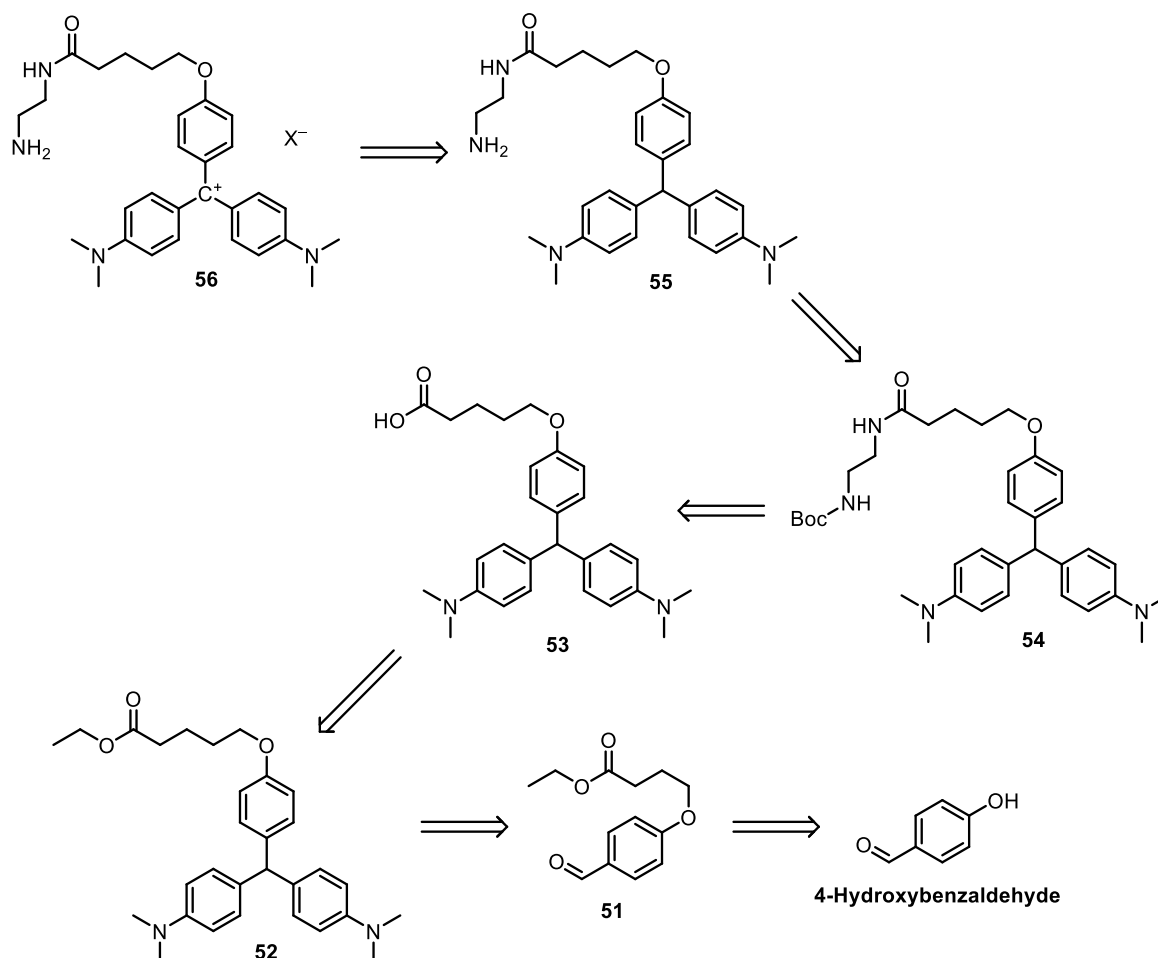
Previously, attempts to covalently link small molecules to a pre-functionalised polymer surface, *via* a 1,3-dipolar cycloaddition reaction, were unsuccessful (See section **2.2**). Issues were encountered when the modified polymer was dissolved in the reaction solvent, or when the reaction was attempted heterogeneously. In this section, the attempted synthesis of a polymer from monomeric units, with the simultaneous covalent attachment of an appropriately functionalised crystal violet analogue, is described.

In 2014, Felgenträger *et al.*²⁵² described the preparation of a polyurethane coating containing a covalently attached porphyrin, 5-(4-hydroxyphenyl)-10,15,20-triphenylporphyrin. The polyurethane was prepared by dissolving the porphyrin in a mixture of polyvalent alcohols, which was then combined with a “hardener”, presumably diisocyanates of some kind. In addition, Chung *et al.*^{328,329} describe the preparation of polyurethanes with a variety of covalently bound dyes by a similar method. They react poly(tetramethylene glycol) (poly(THF)), 4,4'-methylenebis(phenylisocyanate) (MDI), and 1,4-butanediol in the presence of commercially available dyes such as rhodamine and fluorescein to afford the resultant dye-incorporated polymers. These studies were the inspiration for considering the covalent attachment of a crystal violet analogue.

2.5.1 Attempted preparation of an amine-functionalised crystal violet analogue

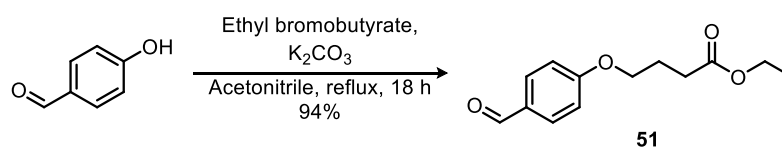
The synthesis of two PEGylated amine-functionalised crystal violet analogues had already been described by Szent-Gyorgyi *et al.*²⁹⁷ in 2008. A synthetic

route based on their methodology was devised and is shown below (Scheme 57).



Scheme 57. Proposed synthetic route towards an amine-functionalised crystal violet analogue.

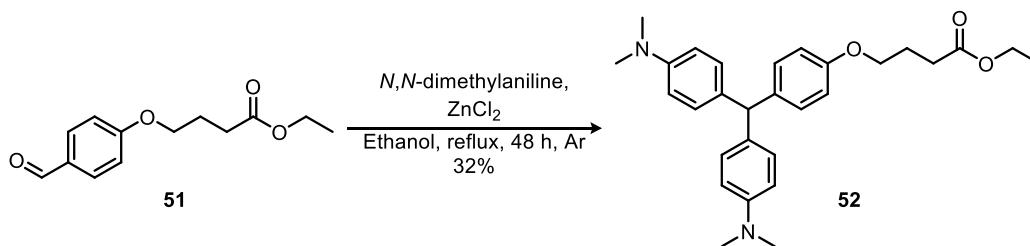
The first step involved an S_N2 reaction between 4-hydroxybenzaldehyde and ethyl bromobutyrate in acetonitrile. The desired aryl aldehyde **51**, was obtained in yields of up to 94% (Scheme 58).³³⁰



Scheme 58. Synthesis of aryl aldehyde **51**.

The reaction of aryl aldehyde **51** with 2 equivalents of *N,N*-dimethylaniline to give the corresponding leucocrystal violet analogue **52**, using the conditions of Szent-Gyorgyi *et al.*,²⁹⁷ was capricious. The numbers of equivalents of all the reagents were frequently adjusted, as was the concentration. After

numerous attempts the desired leucocrystal violet analogue **52** was obtained in a yield of 32% (Scheme 59).



Scheme 59. Synthesis of leucocrystal violet analogue **52**.

Attempts to cleave the ester group were unsuccessful in acetone with both $\text{NaOH}_{(\text{aq})}$ and $\text{KOH}_{(\text{aq})}$, using the procedure of Szent-Gyorgyi *et al.*²⁹⁷ In addition, the reaction was tried in ethanol with $\text{KOH}_{(\text{aq})}$ but again the desired product was not obtained.

2.5.2 Preparation of a modified polyurethane film

Initially, a commercially available polyurethane-making kit was used, which included a mixture of poly-alcohols, and a “hardener”. The intention was to optimise the amount of dye required to generate a polymer film without any aggregation of the dye, but with sufficient colouration so that it would be expected to exhibit antibacterial activity in the presence of a light source.

To the poly-alcohol mixture was added commercially available crystal violet. The amount of crystal violet that was used was varied, and ranged between 0.01%-0.30% by mass. The polyurethane was made by adding the hardener to the poly-alcohol mix, before pouring the resultant mixture into a silicone ice cube tray and allowing the desired polymer film to form. Although the polymers generated were robust and consistently had the same properties, aggregation of crystal violet was observed in every experiment. As the exact composition of the polyurethane-making kit was not known, it was decided that a more rigorous approach would involve preparation of the polymer from known starting materials.

The conditions of Chung *et al.*^{328,329} were used, but modified slightly owing to availability of equipment. The chain-extender, 1,4-butanol, was added to a mixture of poly(THF) and MDI in THF (instead of DMF). The amounts of each component were varied, and are noted in the table below (Table 15).

Poly(THF)	1,4-butanediol	MDI	Comments
2	3	5	Done in petri dish - unable to remove polymer.
2	3	5	Polymer was very soft and brittle.
1	4	5	Polymer fairly soft.
1	4	5	Polymer brittle and soft.
3	7	10	Polymer very brittle.
1	9	10	Polymer quite hard, but extremely brittle.

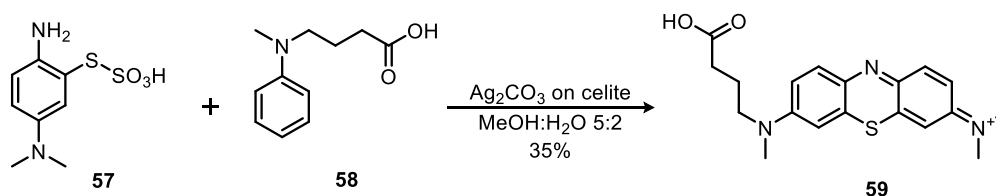
Table 15. The various conditions that were used for the preparation of different polyurethane films. The relative numbers of equivalents of each component are indicated.

The resultant mixture from each experiment was poured into segments of a silicone ice cube tray, instead of into a petri dish; the solvent was then allowed to evaporate in air which resulted in the generation of the desired polymer film, as opposed to carrying out this process in a vacuum oven. None of the polymer films that were produced were fit for purpose: they were either too brittle or soft, or both. Moreover, some of these experiments were repeated and the properties of the films generated were seen to vary substantially.

Considering the difficulties encountered up until this point, and having had little success with trying to synthesise the desired crystal violet analogue, no further experiments were tried and this project was abandoned.

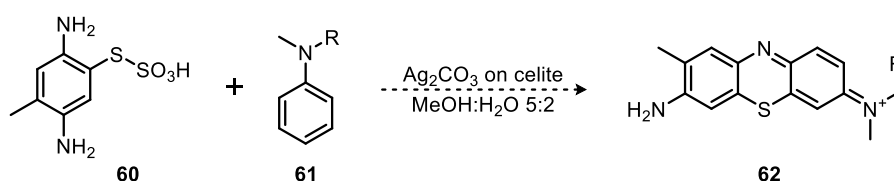
3 Conclusions and future work

The syntheses of alkyne-functionalised analogues of methylene blue, toluidine blue O, and crystal violet, were investigated. It was not possible to synthesise any analogues of methylene blue or toluidine blue O. One of the major problems with the attempted synthesis of methylene blue analogues was the susceptibility of every product to oxidation, making their purification difficult. The attempted alkylation of 10-acetyl-3,7-diaminophenothiazine **3** proved to be particularly troublesome, and the synthesis was abandoned at this point. In 2014, Murray *et al.*³³¹ synthesised methylene blue analogue **59** by reacting 2-amino-5-(dimethylamino)phenylthiosulfonic acid **57** with tertiary aniline **58** (Scheme **60**). One might synthesise, and use, an alkyne-functionalised tertiary aniline in place of tertiary aniline **58**, and expect a similar outcome.



Scheme **60**. Synthesis of methylene blue analogue **59**, as described by Murray *et al.*³³¹

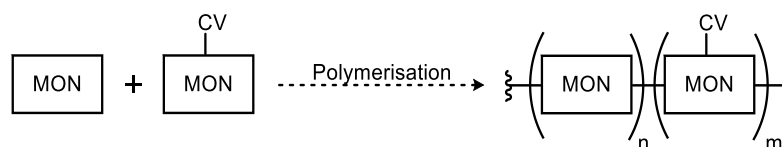
By using the same methodology, it might be possible to access a range of toluidine blue O analogues. In this case, arylthiosulfonic acid **60** would need to be synthesised (Scheme **61**).



Scheme **61**. Proposed synthesis of toluidine blue analogue **62**.

The syntheses of three different crystal violet analogues **35-37** are described. Of the four, three contain alkyne substituents that should allow them to participate in further chemical reactions. It was hypothesised that these compounds might be able to undergo a copper-catalysed 1,3-dipolar cycloaddition reaction with an azide-functionalised polymer surface; however, it was not possible to prove that crystal violet analogue **35** was covalently attached to azide-functionalised PVC. To overcome this issue in the future,

one might consider synthesising a suitable polymer precursor containing a crystal violet analogue. The subsequent polymerisation of this monomeric unit would give a material that contained covalently attached crystal violet moieties. The added advantage of such an approach would be that the amount of crystal violet could be controlled by performing co-polymerisation reactions with varying amounts of the crystal violet-containing monomer unit (Scheme 62).



Scheme 62. A hypothetical co-polymerisation reaction between a monomer (MON) containing crystal violet (CV), and another with no crystal violet moiety.

Despite setbacks with regards to covalently attaching crystal violet analogues **35-37** to a polymer surface, microbiological studies were conducted to assess their efficacy as light-activated antibacterial agents when they were incorporated into polyurethane, which was achieved by a swell-encapsulate-shrink process. The polyurethane film that was incorporated with crystal violet analogue **35** effected the lethal photosensitisation of *S. aureus* after three hours of white light illumination (Figure 43).

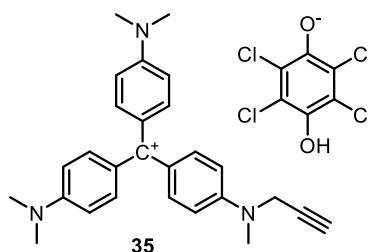


Figure 43. Crystal violet analogue **35**.

A mini-project was devised to investigate whether ethyl violet was more effective as a light-activated antibacterial agent than crystal violet. The superiority of crystal violet was demonstrated; however, should the toxicity of ethyl violet towards mammalian cells be shown to be significantly less than that of crystal violet in the future, it might prove to be a better alternative.

A separate project was devised to investigate the effect of subtle structural changes on the light-activated antibacterial activity of a range of synthetic porphyrins. The porphyrins were synthesised according to literature procedures, and were incorporated into medical grade silicone *via* a swell-

encapsulate-shrink process. The antibacterial activity of the resultant polymer films has not yet been assessed. Eventually, the physical properties of the porphyrin-incorporated films should be studied, if any of the films prove to be effective at killing bacteria. The relative photostability of the biologically active porphyrins when physically incorporated into silicone would be of particular interest.

Finally, attempts were made to synthesise an amine-functionalised crystal violet analogue that could, in theory, be added to a polymerisation reaction to generate polyurethane with covalently attached crystal violet moieties. Problems were encountered with the synthesis of a suitably functionalised crystal violet analogue, and with the generation of the polyurethane film.

4 Experimental

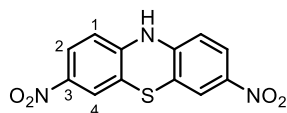
4.1 Techniques, materials, and instrumentation

Commercially available chemicals were used without any further purification, unless stated otherwise. When dry solvents were used, they were either obtained from commercial vendors, or from the anhydrous solvent system set up in UCL. Thin-layer chromatography (TLC) was conducted using pre-coated aluminium backed plates (Merck, Silica Gel 60 F₂₅₄). TLC plates were visualised under UV light and/or by dipping the TLC plate into a solution of vanillin, or alkaline KMnO₄, solution followed by heating. Flash column chromatography was performed using silica gel (Merck Kieselgel 60). All yields quoted refer to isolated yields.

¹H and ¹³C NMR spectra were measured on the following Bruker instruments: Avance 300, Avance III 400, DRX500, and Avance III 600 Cryo (as specified). Chemical shift values are recorded in parts per million (ppm); coupling constants are recorded in Hz. Mass spectra were measured on a Finnigan MAT 900 XP or a Waters Autosampler Manager 2777C connected to Waters LCT Premier XE. IR spectra were measured on a Bruker ALPHA FT-IR spectrometer operating in ATR mode. Melting points were measured using a Reichert-Jung Thermovar hot-stage microscope apparatus and are uncorrected. UV-Vis spectra were measured on a Perkin Elmer Lambda 25 spectrometer. X-ray photoelectron spectroscopy (XPS) was performed using a Thermo Scientific K-alpha spectrometer. Photographs were taken using a Sony Xperia E4 5-megapixel camera. Water droplet contact angles were measured using a First Ten angstroms 1000 device with a side mounted rapid fire camera casting 3 µL water droplet on the surface of each sample and 5 replicates on fresh samples were performed.

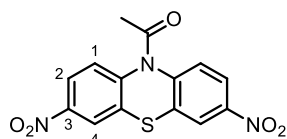
4.2 Procedures for the synthesis of organic compounds and associated data

3,7-Dinitrophenothiazine (1)²⁸⁵



The procedure from a Wista Laboratories Ltd. patent was used.²⁸⁵ To a mixture consisting of phenothiazine (5.00 g, 25.1 mmol, 1.00 eq.), DCM (25 mL) and acetic acid (10 mL) was added NaNO₂ (5.19 g, 75.3 mmol, 3.00 eq.). The reaction was stirred at r.t. for 10 minutes prior to the addition of DCM (25 mL), acetic acid (10 mL) and NaNO₂ (5.19 g, 75.3 mmol, 3.00 eq.). To ensure that efficient stirring could continue, acetic acid (30 mL) was added. The reaction mixture was stirred at r.t. for 3 hours. The resultant solid precipitate was filtered and washed with ethanol (250 mL), water (250 mL) and ethanol (250 mL). The solid was recrystallised from DMF to give 3,7-dinitrophenothiazine **1** as a purple solid (3.79 g, 13.1 mmol, 52%). mp > 240 °C; $\nu_{\max}/\text{cm}^{-1}$ 3328 (NH), 1604, 1564, 1539, 1480, 1298, 1265, 1235, 1140, 1125; δ_{H} (500 MHz, DMSO-*d*₆) 10.13 (1H, s, NH), 7.88 (2H, dd, J = 8.8 and 2.5 Hz, H2), 7.80 (2H, d, J = 2.5 Hz, H4), 6.75 (2H, d, J = 8.8 Hz, H1); δ_{C} (125 MHz, DMSO-*d*₆) 145.1 (C3), 142.5 (CS), 124.8 (C2), 121.8 (C4), 116.7 (CN), 114.7 (C1). Data is consistent with the literature values.²⁸⁵

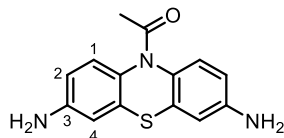
10-Acetyl-3,7-dinitrophenothiazine (2)²⁸⁵



The procedure from a Wista Laboratories Ltd. patent was used.²⁸⁶ To a mixture consisting of 3,7-dinitrophenothiazine **1** (2.00 g, 6.91 mmol, 1.00 eq.), DMF (5 mL) and acetic anhydride (6.5 mL, 69 mmol, 10 eq.) was added triethylamine (3.9 mL, 28 mmol, 4.0 eq.). The reaction mixture was heated to 105 °C and allowed to stir for 3 hours, before being cooled to r.t. and stirred for a further 1 hour. The resultant product was isolated by filtration and washed with methanol (3 × 40 mL). The desired product **2** was obtained as a light yellow solid (1.72 g, 5.19 mmol, 75%). mp 228-229 °C (lit.³³² 221-223 °C); $\nu_{\max}/\text{cm}^{-1}$ 3100 (CH), 1685 (C=O), 1517, 1461, 1340, 1312, 1288, 1252, 1209, 1122; δ_{H} (600 MHz, CDCl₃) 8.35 (2H, d, J = 2.5 Hz, H4), 8.26 (2H, dd, J = 8.8 and 2.5 Hz, H2), 7.69 (2H, d, J = 8.8 Hz, H1), 2.30 (3H, s, CH₃); δ_{C} (150 MHz,

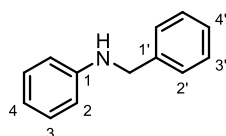
CDCl₃) 168.3 (C=O), 146.4, 143.3 and 136.7 (CN, CS and C3), 127.8 (C1), 123.5 (C4), 123.1 (C2), 23.1 (CH₃). Data is consistent with literature values.²⁸⁵

10-Acetyl-3,7-diaminophenothiazine (**3**)²⁸⁵



The procedure from a Wista Laboratories Ltd. patent was used.²⁸⁵ To a solution of 10-acetyl-3,7-dinitrophenothiazine **2** (1.00 g, 3.02 mmol, 1.00 eq.) in ethanol (25 mL) was added SnCl₂·2H₂O (6.81 g, 30.2 mmol, 10.0 eq.). The resultant solution was heated under reflux for 5 hours. The reaction mixture was cooled to r.t. before being poured into ice water (~100 mL). The pH of the resultant solution was adjusted to 7 using 5% aq. NaHCO₃ (100 mL), before being extracted with ethyl acetate (3 × 100 mL). The combined organic extracts were washed with brine (3 × 200 mL), dried over MgSO₄, and concentrated *in vacuo* to give the title compound **3** as a blue-purple solid (517 mg, 1.91 mmol, 63%). mp 189-191 °C (lit. value not given); $\nu_{\max}/\text{cm}^{-1}$ 3323 and 3200 (NH), 1727 (C=O), 1651, 1615, 1592, 1481, 1368, 1334, 1278, 1224, 1136, 1058, 1013; δ_{H} (500 MHz, DMSO-*d*₆) 7.16-7.10 (2H, m, H1), 6.61 (2H, s, H4), 6.49-6.47 (2H, m, H2), 5.31-5.23 (2H, m, NH₂), 2.01 (3H, s, CH₃); δ_{C} (100 MHz, DMSO-*d*₆, 100 °C) 168.5 (C=O), 146.4 (C3), 132.1, 128.4 and 126.7 (CN, CS and C1), 112.0 and 111.1 (C2 and C4), 21.7 (CH₃). Data is consistent with the literature values.²⁸⁵

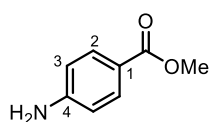
N-Benzylaniline (**6**)³³³



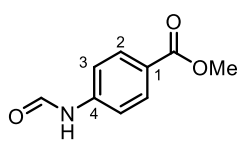
Method A: The procedure of Gray *et al.*²⁸⁷ was used. To a solution of aniline (0.11 mL, 1.2 mmol, 1.0 eq.) and K₂CO₃ (162 mg, 1.17 mmol, 1.00 eq.) in acetonitrile (4 mL, degassed by bubbling argon through the solution for 10 minutes before use) was added benzyl bromide (0.14 mL, 1.2 mmol, 1.0 eq.) dropwise under argon. The reaction mixture was heated at 80 °C for 20 hours under argon, before being cooled to r.t., filtered to remove any solid impurities, and concentrated *in vacuo*. The crude product was purified by flash column chromatography (SiO₂, petroleum ether:diethyl ether 99:1) to give the desired product **6** as a white solid (28 mg, 0.15 mmol, 13%). **Method B:** The procedure of Srivastava *et al.*²⁸⁸ was used. To a solution of aniline (0.11 mL, 1.2 mmol, 1.0 eq.) and

K_2CO_3 (162 mg, 1.17 mmol, 1.00 eq.) in DMSO (0.50 mL, degassed by bubbling argon through the solution for 10 minutes before use) was added benzyl bromide (0.14 mL, 1.2 mmol, 1.0 eq.) dropwise under argon. The reaction mixture was stirred at 80 °C for 18 hours under argon, before being cooled to r.t. and diluted with chloroform (10 mL). The mixture was filtered to remove any solid impurities. The filtrate was poured into water (10 mL) and the organic layer was separated. The aqueous layer was extracted with chloroform (3 × 10 mL). The combined organic extracts were washed with brine (30 mL), dried over Na_2SO_4 , and concentrated *in vacuo*. The crude product was purified by flash column chromatography (SiO_2 , petroleum ether:diethyl ether 99:1) to give the desired product **6** as a white solid (52 mg, 0.28 mmol, 24%). R_f 0.15 (petroleum ether:diethyl ether 99:1); mp 37-39 °C (lit.³³³ 37-40 °C); ν_{max}/cm^{-1} 3417 (NH), 3052, 3023 and 2926 (CH), 1600, 1511, 1492, 1449, 1328, 1302, 1277, 1180, 1151, 1118, 1105, 1079, 1065, 1027; δ_H (500 MHz, $CDCl_3$) 7.39-7.33 (4H, m, H2'-3'), 7.30-7.26 (1H, m, H4'), 7.20-7.16 (2H, m, H3), 6.74-6.71 (1H, m, H4), 6.66-6.64 (2H, m, H2), 4.34 (2H, s, CH_2), 4.04 (1H, br s, NH); δ_C (125 MHz, $CDCl_3$) 148.1 (C1), 139.4 (C1'), 129.3 (C3), 128.0 and 127.5 (C2' and C3'), 127.2 (C4'), 117.6 (C4), 112.8 (C2), 48.3 (CH_2). Data is consistent with the literature values.³³³

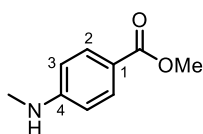
Methyl 4-aminobenzoate (**13**)³³⁴



The procedure of Takamatsu *et al.*²⁹¹ was used. To a solution of 4-aminobenzoic acid (1.00 g, 7.29 mmol, 1.00 eq.) in methanol (20 mL) was added concentrated H_2SO_4 (5 mL) dropwise. The reaction mixture was heated under reflux for 38 hours before being cooled to r.t. and concentrated *in vacuo*. This was followed by dilution with water (15 mL) and adjustment of the pH to 3 using 2M aq. NaOH (20 mL). The resultant solid was separated by filtration and washed with water (50 mL) to give the desired product **13** as an off-white solid (775 mg, 5.13 mmol, 70%). mp 110-112 °C (lit.³³⁴ 111-113 °C); ν_{max}/cm^{-1} 3464 and 3369 (NH), 3247 (CH), 1678 (C=O), 1593, 1568, 1520, 1435, 1313, 1284, 1180, 1167, 1121; δ_H (500 MHz, $CDCl_3$) 7.87-7.85 (2H, m, H2), 6.66-6.63 (2H, m, H3), 3.86 (3H, s, CH_3); δ_C (125 MHz, $CDCl_3$) 167.1 (C=O), 150.8 (C4), 131.6 (C2), 119.8 (C1), 113.8 (C3), 51.6 (CH_3). Data is consistent with the literature values.³³⁴

Methyl 4-(formamido)benzoate (15)³³⁵

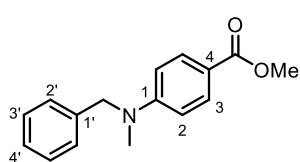
A mixture of acetic anhydride (1.3 mL, 27 mmol, 4.0 eq.) and formic acid (0.5 mL, 27 mmol, 4.0 eq.) was heated to 60 °C for 2 hours in a round-bottomed flask equipped with a drying tube. The mixture was cooled to r.t. before the addition of methyl 4-aminobenzoate **13** (500 mg, 3.31 mmol, 1.00 eq.) in DCM (5 mL) dropwise. The reaction mixture was stirred for 20 hours at r.t. before being concentrated *in vacuo*. An excess of diethyl ether (ca. 70 mL) was added and any solid precipitate was removed by filtration. The filtrate was concentrated *in vacuo*. Water (50 mL) was added, which resulted in the precipitation of a solid, which was isolated by filtration. The solid was washed with water (3 × 50 mL) to afford the desired product **15** as an off-white solid, which was a mixture of rotamers in a 3:1 ratio (380 mg, 2.12 mmol, 64%). mp 120-122 °C (lit.³³⁵ 119-122 °C); $\nu_{\text{max}}/\text{cm}^{-1}$ 1692 (ester C=O), 1602 (formamide C=O), 1437, 1275, 1179, 1113; δ_{H} (500 MHz, DMSO-*d*₆) 10.54 (0.75H, br s, O=CH), 10.47 (0.25H, d, J = 11.4 Hz, O=CH), 8.97 (0.25H, d, J = 11.0 Hz, NH), 8.36 (0.75H, s, NH), 7.93 (1.5H, d, J = 8.7 Hz, H₂), 7.90 (0.5H, d, J = 8.6 Hz, H₂), 7.71 (1.5H, d, J = 8.7 Hz, H₃), 7.32 (0.5H, d, J = 8.6 Hz, H₃), 3.82 (3H, s, CH₃); δ_{C} (125 MHz, DMSO-*d*₆) 165.7 (OC=O), 162.6 (HNC=O, minor), 160.2 (HNC=O, major), 143.0 (C₄, minor), 142.5 (C₄, major), 130.8 (C₂, minor), 130.4 (C₂, major), 124.4 (C₁), 118.2 (C₃, major), 116.4 (C₃, minor), 51.9 (CH₃). Data is consistent with the literature values.³³⁵

Methyl 4-(methylamino)benzoate (14)²⁸⁷

To a solution of methyl 4-(formamido)benzoate **15** (500 mg, 2.79 mmol, 1.00 eq.) in dry THF (25 mL, degassed by bubbling argon through the solution for 10 minutes before use) was added BH₃.THF (1M in THF, 14 mL, 14 mmol, 5.0 eq.) dropwise at 50 °C under argon. The reaction mixture was stirred at 50 °C under argon for 1 hour. The reaction mixture was cooled to r.t. and quenched by the dropwise addition of methanol (20 mL). Once quenched, the resultant solution was concentrated *in vacuo*. The crude product was purified by flash column chromatography (SiO₂, petroleum ether:ethyl acetate 9:1) to give the desired product **14** as a white

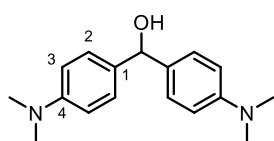
solid (385 mg, 2.33 mmol, 84%). R_f 0.15 (petroleum ether:ethyl acetate 9:1); mp 96-98 °C (lit.²⁸⁷ 96-97 °C); $\nu_{\max}/\text{cm}^{-1}$ 3389 (NH), 1684 (C=O), 1598, 1563, 1532, 1436, 1343, 1311, 1274, 1193, 1170, 1106; δ_{H} (500 MHz, CDCl_3) 7.90-7.87 (2H, m, H2), 6.57-6.54 (2H, m, H3), 4.20 (1H, br s, NH), 3.86 (3H, s, OCH_3), 2.89 (3H, s, HNCH_3); δ_{C} (125 MHz, CDCl_3) 167.4 (C=O), 152.9 (C4), 131.5 (C2), 118.2 (C1), 111.1 (C3), 51.5 (OCH_3), 30.1 (HNCH_3). Data is consistent with the literature values.²⁸⁷

***N*-Methyl-*N*-benzyl-4-(carbomethoxy)aniline (16)**³³⁶



The procedure of Srivastava *et al.*²⁸⁸ was used. To a solution of methyl 4-(methylamino)benzoate **14** (200 mg, 1.21 mmol, 1.00 eq.) in DMSO (3 mL) was added K_2CO_3 (167 mg, 1.21 mmol, 1.00 eq.). This was followed by the dropwise addition of benzyl bromide (0.14 mL, 1.2 mmol, 1.0 eq.). The reaction mixture was stirred at 80 °C for 24 hours and cooled to r.t., before being poured into water (30 mL). The mixture was extracted with chloroform (3 × 10 mL). The combined organic extracts were washed with brine (30 mL), dried over MgSO_4 , and concentrated *in vacuo*. The crude product was purified by flash column chromatography (SiO_2 , petroleum ether:diethyl ether 9:1) to give the desired product **16** as a white solid (177 mg, 0.693 mmol, 57%). R_f 0.10 (petroleum ether:diethyl ether 9:1); mp 82-84 °C (lit.³³⁶ 67-68 °C); $\nu_{\max}/\text{cm}^{-1}$ 1687 (C=O), 1598, 1523, 1453, 1431, 1381, 1351, 1321, 1276, 1182, 1123, 1005; δ_{H} (500 MHz, CDCl_3) 7.90-7.88 (2H, m, H3), 7.35-7.32 (2H, m, H3'), 7.28-7.25 (1H, m, H4'), 7.20-7.18 (2H, m, H2'), 6.72-6.69 (2H, m, H2), 4.63 (2H, s, CH_2), 3.86 (3H, s, OCH_3), 3.13 (3H, s, NCH_3); δ_{C} (125 MHz, CDCl_3) 167.4 (C=O), 152.7 (C1), 137.8 (C1'), 131.4 (C2), 128.7 (C3'), 127.2 (C4'), 126.4 (C2'), 117.4 (C4), 110.9 (C3), 55.9 (CH_2), 51.5 (OCH_3), 38.7 (NCH_3). Data is consistent with the literature values.³³⁶

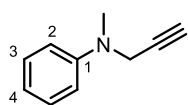
Bis(4-(dimethylamino)phenyl)methanol (20)²⁹⁵



To a slurry of LiAlH_4 (3.54 g, 93.2 mmol, 5.00 eq.) in THF (50 mL) was added bis(4-(dimethylamino)phenyl)methanone (5.00 g, 18.6 mmol, 1.00 eq.) in THF (50 mL) at 0 °C dropwise. The resultant reaction mixture was

stirred at r.t. for 1 hour before diluting with THF (100 mL). The mixture was cooled to 0 °C and water (3.5 mL) was added very cautiously, followed by the addition of 15% aq. NaOH (3.5 mL) and water (10.5 mL). The resultant slurry was stirred for a further 30 minutes at r.t. before addition of Na₂SO₄, filtration, and concentration *in vacuo*. The crude product was recrystallised from benzene to afford the desired product **20** as a pink solid (3.97 g, 14.7 mmol, 79%). mp 106-108 °C (lit.³³⁷ 103-104 °C); $\nu_{\max}/\text{cm}^{-1}$ 3404 (OH), 2837 (CH), 1613, 1517, 1345, 1225, 1165, 1043; δ_{H} (500 MHz, DMSO-*d*₆) 7.10 (4H, d, J = 8.7 Hz, H₂), 6.63 (4H, d, J = 8.8 Hz, H₃), 5.46 (1H, d, J = 3.9 Hz, HOCH), 5.40 (1H, d, J = 4.1 Hz, OH), 2.81 (12H, s, CH₃); δ_{C} (125 MHz, DMSO-*d*₆) 149.5 (C₄), 134.4 (C₁), 127.2 (C₂), 112.3 (C₃), 74.0 (HOCH), 40.6 (CH₃); m/z (CI) found 270 ([M]⁺, ~85%), 253 ([M – OH]⁺, 100%); Accurate mass calc. for C₁₇H₂₂N₂O [M]⁺ 270.1732, found 270.1730, Δ 0.7ppm. Data is consistent with the literature values.²⁹⁵

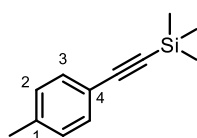
***N*-Methyl-*N*-phenylpropargylamine (**21**)³³⁸**



The procedure of Srivastava *et al.*²⁸⁸ was used. To a solution of *N*-methylaniline (5.00 g, 46.7 mmol, 1.00 eq.) in DMSO (75 mL) was added K₂CO₃ (6.45 g, 46.7 mmol, 1.00 eq.). This was followed by the dropwise addition of propargyl bromide solution (80 wt.% in toluene, 5.2 mL, 47 mmol, 1.0 eq.). The reaction mixture was heated to 80 °C and allowed to stir for 20 hours before being cooled to r.t. and poured into water (750 mL). The mixture was then extracted with chloroform (3 × 250 mL). The combined organic extracts were washed with brine (3 × 250 mL), dried over MgSO₄, and concentrated *in vacuo*. The crude product was purified by flash column chromatography (SiO₂, petroleum ether:diethyl ether 19:1) to give the desired product **21** as a pale yellow oil (5.09 g, 35.1 mmol, 75%). R_f 0.30 (petroleum ether:diethyl ether 19:1); $\nu_{\max}/\text{cm}^{-1}$ 3289 (CH), 1600, 1504, 1357, 1242, 1199, 1114, 1034; δ_{H} (500 MHz, CDCl₃) 7.29-7.26 (2H, m, H₃), 6.88-6.86 (2H, m, H₂), 6.83-6.80 (1H, m, H₄), 4.06 (2H, m, CH₂), 2.98 (3H, s, CH₃), 2.18-2.17 (1H, m, C≡CH); δ_{C} (125 MHz, CDCl₃) 149.0 (C₁), 129.1 (C₃), 118.3 (C₄), 114.3 (C₂), 79.3 (C≡CH), 72.0 (C≡CH), 42.5 (CH₃), 38.6 (CH₂); m/z (EI) found 144 ([M – H]⁺, 100%); Accurate mass calc. for C₁₀H₁₁N [M]⁺

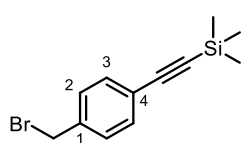
145.0886, found 145.0880, Δ 4.2ppm. Data is consistent with the literature values.³³⁸

4-(Trimethylsilylethynyl)toluene (**23**)³³⁹



A mixture of CuI (44 mg, 0.23 mmol, 0.025 eq.), Pd(PPh₃)₂Cl₂ (322 mg, 0.459 mmol, 0.0500 eq.), triethylamine (40 mL, degassed for 10 min by bubbling argon through the solution before use) and 4-iodotoluene (2.00 g, 9.17 mmol, 1.00 eq.) was stirred for 5 minutes before the dropwise addition of trimethylsilylacetylene (1.5 mL, 11 mmol, 1.2 eq.) at r.t. under argon. The reaction mixture was heated under reflux for 18 hours under argon, before quenching with 1 M aq. HCl (300 mL). The aqueous solution was filtered to remove any solid impurities, before being extracted with petroleum ether (3 × 100 mL). The combined organic extracts were washed with water (100 mL) and brine (100 mL), dried over MgSO₄, and concentrated *in vacuo*. The crude product was purified by flash column chromatography (SiO₂, petroleum ether) to give the desired product **23** as an off-white solid (1.53 g, 8.13 mmol, 89%). R_f 0.25 (petroleum ether); mp 30-32 °C (lit. value not given); $\nu_{\text{max}}/\text{cm}^{-1}$ 2959 (CH), 2157 (C≡C), 1507, 1250; δ_{H} (500 MHz, CDCl₃) 7.37 (2H, d, J = 8.1 Hz, H3), 7.11 (2H, d, J = 8.1 Hz, H2), 2.35 (3H, s, ArCH₃), 0.26 (9H, s, SiCH₃); δ_{C} (125 MHz, CDCl₃) 138.6 (C1), 131.9 (C3), 128.9 (C2), 120.1 (C4), 105.4 (C≡CSi), 93.2 (C≡CSi), 21.5 (ArCH₃), 0.0 (SiCH₃). Data is consistent with the literature values.³³⁹

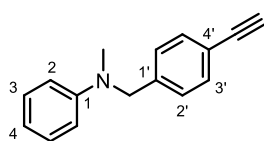
1-Bromomethyl-4-(trimethylsilylethynyl)benzene (**24**)



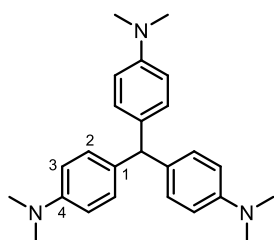
To a solution of 4-(trimethylsilylethynyl)toluene **23** (500 mg, 2.66 mmol, 1.00 eq.) and *N*-bromosuccinimide (473 mg, 2.66 mmol, 1.00 eq.) in benzotrifluoride (10 mL, degassed by bubbling argon through the solution for 10 minutes before use) was added dibenzoyl peroxide (64 mg, 0.27 mmol, 0.10 eq.) under argon. The reaction mixture was heated under reflux for 24 hours under argon, under irradiation by an W6-IQ Group White 150 W Security Pir Transmitter Flood Light. The reaction mixture was cooled to r.t. and concentrated *in vacuo*. The crude product was purified by flash column chromatography (SiO₂, petroleum ether) to give the desired product **24** as a colourless oil (425 mg, 1.59 mmol, 60%).

R_f 0.15 (petroleum ether); ν_{max}/cm^{-1} 2959 (CH), 2158 (C≡C), 1506, 1249, 1221, 863-842, 760, 732, 634, 606, 557; δ_H (500 MHz, CDCl₃) 7.44 (2H, d, J = 8.3 Hz, H3), 7.33 (2H, d, J = 8.2 Hz, H2), 4.47 (2H, s, CH₂), 0.26 (9H, s, SiCH₃); δ_C (125 MHz, CDCl₃) 138.0 (C1), 132.3 (C2), 128.9 (C3), 123.3 (C4), 104.5 (C≡CSi), 95.3 (C≡CSi), 32.9 (CH₂), -0.1 (SiCH₃). m/z (CI) found 187 ([M – Br]⁺, 100%).

***N*-(4-Ethynylbenzyl)-*N*-methylaniline (22)**

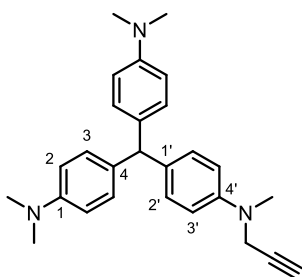


For the first step, the procedure of Srivastava *et al.*²⁸⁸ was used. To a solution of *N*-methylaniline (500 mg, 4.67 mmol, 1.00 eq.) in DMSO (7.5 mL) was added K₂CO₃ (645 mg, 4.67 mmol, 1.00 eq.), followed by 1-bromomethyl-4-(trimethylsilylethynyl)benzene **24** (1.25 g, 4.67 mmol, 1.00 eq.). The reaction mixture was heated to 80 °C and stirred for 20 hours before being cooled to r.t. and poured into water (75 mL). The mixture was then extracted with chloroform (5 × 25 mL). The combined organic extracts were washed with brine (3 × 25 mL), dried over MgSO₄, and concentrated *in vacuo* to afford the trimethylsilyl-protected product, which was not isolated. The crude product was mixed with K₂CO₃ (215 mg, 1.56 mmol, 0.333 eq.) in methanol (10 mL) and DCM (10 mL) at r.t. for 22 hours. The mixture was then diluted with water (100 mL) before being extracted with chloroform (3 × 25 mL). The combined organic extracts were washed with brine (3 × 25 mL), dried over MgSO₄, and concentrated *in vacuo*. The crude product was purified by flash column chromatography (SiO₂, petroleum ether:diethyl ether 49:1) to afford the desired product **22** as a white solid (847 mg, 3.83 mmol, 82%). R_f 0.30 (petroleum ether:diethyl ether 49:1); mp 57-59 °C; ν_{max}/cm^{-1} 3254 (CH), 1595, 1504, 1373, 1344, 1296, 1253, 1210, 1118, 1035; δ_H (500 MHz, CDCl₃) 7.46 (2H, d, J = 8.2 Hz, H3'), 7.25-7.20 (4H, m, H3 and H2'), 6.75-6.73 (3H, m, H2 and H4), 4.54 (2H, s, CH₂), 3.06 (1H, s, C≡CH), 3.03 (3H, s, CH₃); δ_C (125 MHz, CDCl₃) 149.5 (C1), 140.1 (C1'), 132.3 (C3'), 129.2 and 126.7 (C3 and C2'), 120.6 (C4'), 116.8 (C4), 112.4 (C2), 83.6 (C≡CH), 76.9 (C≡CH), 56.6 (CH₂), 38.6 (CH₃); m/z (EI) found 221 ([M]⁺, ~80%), 115 ([M – C₇H₈N]⁺, 100%); Accurate mass calc. for C₁₆H₁₅N [M]⁺ 221.1204, found 221.1200, Δ 2.3ppm.

Tris(4-dimethylaminophenyl)methane (27)³⁴⁰

To a solution of *N,N*-dimethylaniline (500 mg, 4.13 mmol, 1.00 eq.) in methanol (5 mL) was added bis(4-(dimethylamino)phenyl)methanol **20** (1.12 g, 4.13 mmol, 1.00 eq.), followed by *p*-toluenesulfonic acid (78 mg, 0.41 mmol, 0.10 eq.). The reaction mixture was stirred at r.t.

for 24 hours. The resultant product was isolated by filtration and washed with methanol to afford the desired product **27** as a pale purple solid (1.25 g, 3.35 mmol, 81%). mp 184-186 °C (lit.³⁴⁰ 177-179 °C); $\nu_{\text{max}}/\text{cm}^{-1}$ 1611, 1514, 1346, 1163, 1060; δ_{H} (500 MHz, CDCl_3) 7.00 (6H, d, $J = 8.7$ Hz, H2), 6.68 (6H, d, $J = 8.5$ Hz, H3), 5.31 (1H, s, Ar_3CH), 2.92 (18H, s, CH_3); δ_{C} (125 MHz, CDCl_3) 148.9 (C4), 133.8 (C1), 130.0 (C2), 112.7 (C3), 54.1 (Ar_3CH), 40.9 (CH_3); m/z (CI) found 373 ($[\text{M}]^+$, ~95%), 253 ($[\text{M} - \text{C}_8\text{H}_{10}\text{N}]^+$, 100%); Accurate mass calc. for $\text{C}_{25}\text{H}_{31}\text{N}_3$ $[\text{M}]^+$ 373.2518, found 373.2512, Δ 1.7 ppm. Data is consistent with the literature values.³⁴⁰

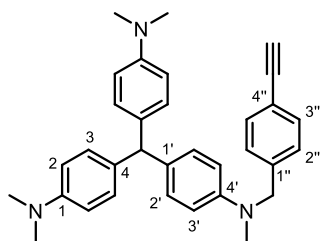
4,4'-((4-(Methyl(prop-2-yn-1-yl)amino)phenyl)methylene)bis(*N,N*-dimethylaniline) (28)

To a solution of *N*-methyl-*N*-phenyl-propargylamine **21** (2.85 g, 19.6 mmol, 1.00 eq.) in methanol (30 mL) was added bis(4-(dimethylamino)phenyl)methanol **20** (5.30 g, 19.6 mmol, 1.00 eq.), followed by *p*-toluenesulfonic acid (373 mg, 1.96 mmol, 0.100 eq.). The reaction mixture was stirred at r.t. for 24 hours. The resultant

product was isolated by filtration and washed with methanol to afford the desired product **28** as a pale purple solid (2.06 g, 5.18 mmol, 26%). mp 136-138 °C; $\nu_{\text{max}}/\text{cm}^{-1}$ 1610, 1514, 1443, 1346, 1188, 1060; δ_{H} (500 MHz, CDCl_3) 7.03-6.99 (6H, m, H3 and H2'), 6.76 (2H, d, $J = 8.7$ Hz, H3'), 6.68 (4H, d, $J = 8.2$ Hz, H2), 5.31 (1H, s, Ar_2CH), 4.02 (2H, d, $J = 2.4$ Hz, CH_2), 2.95 (3H, s, H_2CNCH_3), 2.92 (12H, s, $\text{N}(\text{CH}_3)_2$), 2.17 (1H, t, $J = 2.4$ Hz, $\text{C}\equiv\text{CH}$); δ_{C} (125 MHz, CDCl_3) 148.8 (C1), 147.1 (C4'), 135.3 (C1'), 133.6 (C4), 129.9 (C3 and C2'), 114.1 (C3'), 112.6 (C2), 79.5 ($\text{C}\equiv\text{CH}$), 72.0 ($\text{C}\equiv\text{CH}$), 54.1 (Ar_2CH), 42.6

(CH₂), 40.8 (N(CH₃)₂), 38.7 (H₂CNCH₃); *m/z* (CI) found 397 ([M]⁺, 100%); Accurate mass calc. for C₂₇H₃₁N₃ [M]⁺ 397.2518, found 397.2520, Δ 0.5ppm.

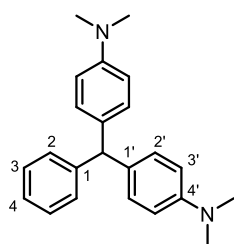
4,4'-((4-((4-Ethynylbenzyl)(methyl)amino)phenyl)methylene)bis(*N,N*-dimethylaniline) (29)



To a solution of *N*-(4-Ethynylbenzyl)-*N*-methylaniline **22** (500 mg, 2.26 mmol, 1.00 eq.) in methanol (5 mL) was added bis(4-(dimethylamino)phenyl)methanol **20** (611 mg, 2.26 mmol, 1.00 eq.), followed by *p*-toluenesulfonic acid (43 mg, 0.23 mmol, 0.10 eq.).

The reaction mixture was stirred at r.t. for 24 hours. The resultant product was isolated by filtration and washed with methanol to afford the desired product **29** as a pale purple solid (412 mg, 0.870 mmol, 38%). mp 156-158 °C; $\nu_{\text{max}}/\text{cm}^{-1}$ 3283 (CH), 1611, 1515, 1330, 1207, 1117; δ_{H} (500 MHz, CDCl₃) 7.43 (2H, d, *J* = 8.2 Hz, H3''), 7.19 (2H, d, *J* = 8.4 Hz, H2''), 6.99-6.95 (6H, m, H3 and H2'), 6.67-6.62 (6H, m, H2 and H3'), 5.28 (1H, s, Ar₂CH), 4.46 (2H, s, CH₂), 3.04 (1H, s, C≡CH), 2.95 (3H, s, H₂CNCH₃), 2.90 (12H, s, N(CH₃)₂); δ_{C} (125 MHz, CDCl₃) 148.8 (C1), 147.8 (C4'), 140.4 (C1''), 133.9 and 133.6 (C4 and C1'), 132.3 (C3''), 130.0 and 129.9 (C3 and C2'), 126.8 (C2''), 120.5 (C4''), 112.6 and 112.3 (C2 and C3'), 83.6 (C≡CH), 76.8 (C≡CH), 56.9 (CH₂), 54.0 (Ar₂CH), 40.8 (N(CH₃)₂), 38.6 (H₂CNCH₃); *m/z* (EI) found 473 ([M]⁺, 100%); Accurate mass calc. for C₃₃H₃₅N₃ [M]⁺ 473.2831, found 473.2830, Δ 0.2ppm.

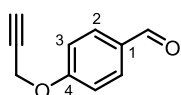
Bis(4-dimethylaminophenyl)phenylmethane (30)³⁴¹



The procedure of Szent-Gyorgyi *et al.*²⁹⁷ was used. To a solution of benzaldehyde (200 mg, 1.88 mmol, 1.00 eq.) and ZnCl₂ (514 mg, 3.77 mmol, 2.00 eq.) in ethanol (5 mL, degassed by bubbling argon through the solution for 10 minutes before use) was added *N,N*-dimethylaniline (0.46 mL, 3.8 mmol, 2.0 eq.). The reaction mixture was heated under reflux for 20 hours under argon, before being cooled to r.t. and concentrated *in vacuo*. The residue was dissolved in water (50 mL) and ethyl acetate (20 mL). The layers were separated and the aqueous layer was extracted with ethyl acetate (2 × 20 mL). The combined organic extracts were washed with water (3 × 20 mL),

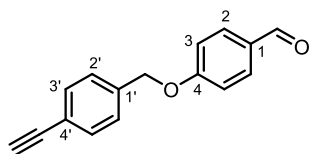
dried over MgSO_4 , and concentrated *in vacuo*. The crude product was purified by flash column chromatography (SiO_2 , petroleum ether:diethyl ether 9:1) to afford the desired product **30** as a pale green solid (254 mg, 0.769 mmol, 41%). R_f 0.05 (petroleum ether:diethyl ether 9:1); mp 92-94 °C (lit.³⁴¹ 92-93 °C); $\nu_{\text{max}}/\text{cm}^{-1}$ 2878 and 2801 (CH), 1610, 1516, 1442, 1349, 1189, 1059; δ_{H} (500 MHz, $\text{DMSO}-d_6$) 7.26-7.23 (2H, m, H3), 7.16-7.13 (1H, m, H4), 7.08 (2H, d, $J = 7.6$ Hz, H2), 6.90-6.87 (4H, m, H2'), 6.45-6.41 (4H, m, H3'), 5.31 (1H, s, Ar_2CH), 2.84 (12H, s, CH_3); δ_{C} (125 MHz, $\text{DMSO}-d_6$) 148.8 (C_4'), 145.4 (C_1), 132.3 (C_1'), 129.4 (C_2'), 128.9 (C_2), 128.0 (C_3), 125.7 (C_4), 112.4 (C_3'), 54.2 (Ar_2CH), 40.3 (CH_3); m/z (EI) found 330 ($[\text{M}]^+$, 100%), 253 ($[\text{M} - \text{C}_6\text{H}_5]^+$, ~70%); Accurate mass calc. for $\text{C}_{23}\text{H}_{26}\text{N}_2$ $[\text{M}]^+$ 330.2096, found 330.2085, Δ 3.3ppm. Data is consistent with the literature values.³⁴¹

4-(Prop-2-yn-1-yloxy)benzaldehyde (**31**)²⁹⁸



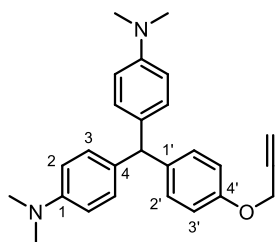
The procedure of Hoogendoorn *et al.*²⁹⁸ was used. To a solution of 4-hydroxybenzaldehyde (1.00 g, 8.19 mmol, 1.00 eq.) in acetone (30 mL) was added K_2CO_3 (1.58 g, 11.5 mmol, 1.40 eq.). The resultant slurry was stirred for 30 minutes at r.t. prior to the addition of propargyl bromide (80 wt.% in toluene, 1.8 mL, 16 mmol, 2.0 eq.). The reaction mixture was heated under reflux for 2 hours before being cooled to r.t. and concentrated *in vacuo*. The residue was dissolved in water (100 mL) and the resultant solution was extracted with ethyl acetate (3 × 100 mL). The combined organic extracts were washed with brine (100 mL), dried over MgSO_4 , and concentrated *in vacuo* to afford the title compound **31** as a white solid (1.24 g, 7.74 mmol, 95%). R_f 0.25 (petroleum ether:ethyl acetate 4:1); mp 76-78 °C (lit.³⁴² 76-78 °C); $\nu_{\text{max}}/\text{cm}^{-1}$ 3205, 2832, 2808 and 2749 (CH), 2122 ($\text{C}\equiv\text{C}$), 1677 ($\text{C}=\text{O}$), 1601, 1574, 1504, 1426, 1395, 1379, 1301, 1248, 1168, 1006; δ_{H} (500 MHz, CDCl_3) 9.90 (1H, s, $\text{HC}=\text{O}$), 7.87-7.84 (2H, m, H2), 7.11-7.08 (2H, m, H3), 4.78 (2H, d, $J = 2.4$ Hz, CH_2), 2.57 (1H, t, $J = 2.4$ Hz, $\text{C}\equiv\text{CH}$); δ_{C} (125 MHz, CDCl_3) 190.8 ($\text{HC}=\text{O}$), 162.4 (C_4), 132.0 (C_2), 130.7 (C_1), 115.3 (C_3), 77.6 ($\text{C}\equiv\text{CH}$), 76.4 ($\text{C}\equiv\text{CH}$), 56.0 (CH_2). Data is consistent with the literature values.²⁹⁸

4-((4-Ethynylbenzyl)oxy)benzaldehyde (**32**)



For the first step, the procedure of Hoogendoorn *et al.*²⁹⁸ was used. To a solution of 4-hydroxybenzaldehyde (594 mg, 4.87 mmol, 1.00 eq.) in acetone (15 mL) was added K_2CO_3 (942 mg, 6.81 mmol, 1.40 eq.). The resultant slurry was stirred at r.t. for 30 minutes prior to the addition of 1-bromomethyl-4-(trimethylsilylethynyl)benzene **24** (1.15 g, 4.87 mmol, 1.00 eq.) in acetone (5 mL). The reaction mixture was heated under reflux for 22 hours before being cooled to r.t. and concentrated *in vacuo*. The residue was dissolved in water (50 mL) and the solution was extracted with ethyl acetate (3 × 50 mL). The combined organic extracts were washed with brine (50 mL), dried over $MgSO_4$, and concentrated *in vacuo* to afford the trimethylsilyl-protected product, which was not isolated. The crude product was mixed with K_2CO_3 (222 mg, 1.61 mmol, 0.333 eq.) in methanol (10 mL) and DCM (10 mL) at r.t. for 24 hours, before concentration *in vacuo*. The residue was dissolved in water (150 mL) and the solution was extracted with ethyl acetate (3 × 50 mL). The combined organic extracts were washed with brine (50 mL), dried over $MgSO_4$, and concentrated *in vacuo*. The crude product was purified by flash column chromatography (SiO_2 , petroleum ether:ethyl acetate 4:1) to afford the desired product **32** as a white solid (530 mg, 2.24 mmol, 46%). R_f 0.25 (petroleum ether:ethyl acetate 4:1); mp 127-129 °C; ν_{max}/cm^{-1} 3224 (CH), 1676 (C=O), 1594, 1505, 1461, 1377, 1313, 1261, 1207, 1156, 1016; δ_H (600 MHz, $CDCl_3$) 9.90 (1H, s, HC=O), 7.86-7.84 (2H, m, H2), 7.54-7.53 (2H, m, H3'), 7.40 (2H, d, $J = 7.9$ Hz, H2'), 7.08-7.06 (2H, m, H3), 5.16 (2H, s, CH_2), 3.11 (1H, s, $C\equiv CH$); δ_C (150 MHz, $CDCl_3$) 190.9 (HC=O), 163.4 (C4), 136.9 (C1'), 132.6 and 132.2 (C2 and C3'), 130.4 (C1), 127.4 (C2'), 122.2 (C4'), 115.2 (C3), 83.3 ($C\equiv CH$), 77.8 ($C\equiv CH$), 69.8 (CH_2); m/z (CI) found 237 ($[M]^+$, 100%); Accurate mass calc. for $C_{16}H_{13}O_2$ $[M + H]^+$ 237.0910, found 237.0911, Δ 0.1ppm.

4,4'-((4-(Prop-2-yn-1-yloxy)phenyl)methylene)bis(*N,N*-dimethylaniline)
(33)

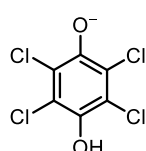
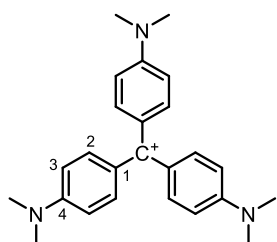


To a solution of 4-(prop-2-yn-1-yloxy)benzaldehyde **31** (200 mg, 1.25 mmol, 1.00 eq.) in ethanol (5 mL, degassed by bubbling argon through the solution for 10 minutes before use) was added acetyl chloride (0.18 mL, 2.5 mmol, 2.0 eq.) followed by *N,N*-dimethylaniline (0.33 mL, 2.6 mmol, 2.1 eq.) at r.t. under argon. The reaction mixture was heated under reflux under argon for 24 hours before being cooled to r.t. and diluted with water (50 mL). The resultant solution was extracted with DCM (3 × 10 mL). The combined organic extracts were washed with water (2 × 10 mL) and brine (10 mL), dried over MgSO₄, and concentrated *in vacuo*. The crude product was purified by flash column chromatography (SiO₂, petroleum ether:ethyl acetate 4:1) to afford the desired product **33** as a white solid (300 mg, 0.780 mmol, 62%). R_f 0.25 (petroleum ether:ethyl acetate 4:1); mp 122-124 °C; $\nu_{\text{max}}/\text{cm}^{-1}$ 3248, 2896, 2855 and 2793 (CH), 1607, 1515, 1451, 1334, 1225, 1162, 1123, 1062, 1027; δ_{H} (500 MHz, CDCl₃) 7.07-7.04 (2H, m, H2'), 6.99-6.96 (4H, m, H3), 6.89-6.87 (2H, m, H3'), 6.67 (4H, d, $J = 8.5$ Hz, H2), 5.33 (1H, s, Ar₂CH), 4.65 (2H, d, $J = 2.4$ Hz, CH₂), 2.91 (12H, s, CH₃), 2.50 (1H, t, $J = 2.4$ Hz, C≡CH); δ_{C} (150 MHz, CDCl₃) 155.8 (C4'), 149.0 (C1), 138.7 (C1'), 133.1 (C4), 130.4 (C2'), 130.0 (C3), 114.5 (C3'), 112.7 (C2), 78.9 (C≡CH), 75.5 (C≡CH), 56.0 (CH₂), 54.3 (Ar₂CH), 40.9 (CH₃); m/z (ES+) found 385 ([M]⁺, 100%); Accurate mass calc. for C₂₆H₂₉N₂O [M + H]⁺ 385.2280, found 385.2266, Δ 3.6ppm.

Tris(4-(dimethylamino)phenyl)methylium

2,3,5,6-tetrachloro-4-

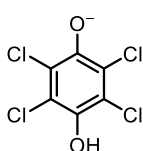
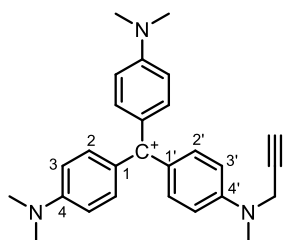
hydroxyphenolate (34)



A modified procedure of Szent-Gyorgyi *et al.*²⁹⁷ was used. To a solution of leucocrystal violet **27** (200 mg, 0.535 mmol, 1.00 eq.) in ethyl acetate (10 mL) was added chloranil (263 mg, 1.07 mmol, 2.00 eq.). The reaction mixture was heated under reflux for 1 hour before being cooled to r.t. and

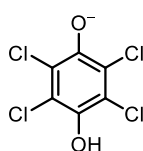
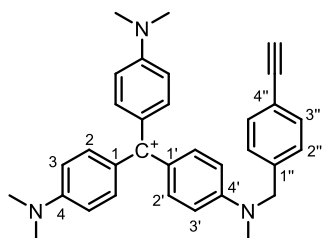
filtered. The solid was washed with cold (0 °C) ethyl acetate and diethyl ether to afford the title compound **34** as a green solid (321 mg, 0.518 mmol, 97%). $\nu_{\max}/\text{cm}^{-1}$ 1585, 1359, 1176; δ_{H} (600 MHz, CDCl_3) 7.33 (6H, d, $J = 9.1$ Hz, H2), 6.87 (6H, d, $J = 9.1$ Hz, H3), 3.28 (18H, s, CH_3); δ_{C} (150 MHz, CDCl_3) 178.4 (Ar_3C^+), 155.7 (C4), 139.9 (C2), 126.8 (C1), 112.5 (C3), 40.8 (CH_3); m/z (ES^+) found 372 ($[\text{M}]^+$, 100%); Accurate mass calc. for $\text{C}_{25}\text{H}_{30}\text{N}_3$ $[\text{M}]^+$ 372.2440, found 372.2438, Δ 0.5ppm; $\lambda_{\max} = 589$ nm ($\epsilon = 76,860$).

Bis(4-(dimethylamino)phenyl)(4-(methyl(prop-2-ynyl)amino)phenyl)methylium 2,3,5,6-tetrachloro-4-hydroxyphenolate (35)



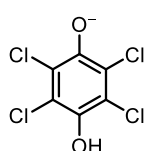
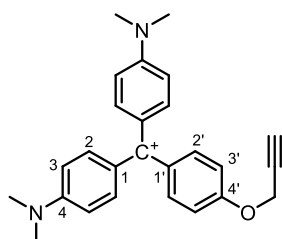
A modified procedure of Szent-Gyorgyi *et al.*²⁹⁷ was used. To a solution of leucocrystal violet analogue **28** (200 mg, 0.503 mmol, 1.00 eq.) in ethyl acetate (10 mL) was added chloranil (248 mg, 1.01 mmol, 2.00 eq.). The reaction mixture was heated under reflux for 1 hour before being cooled to r.t. and filtered. The solid was washed with cold (0 °C) ethyl acetate and diethyl ether to afford the title compound **35** as a purple solid (290 mg, 0.451 mmol, 90%). $\nu_{\max}/\text{cm}^{-1}$ 1683, 1579, 1471, 1360, 1169; δ_{H} (600 MHz, CDCl_3) 7.36-7.33 (6H, m, H2 and H2'), 6.96 (2H, d, $J = 8.8$ Hz, H3'), 6.90 (4H, d, $J = 8.8$ Hz, H3), 4.29 (2H, d, $J = 2.2$ Hz, CH_2), 3.32 (12H, s, $\text{N}(\text{CH}_3)_2$), 3.28 (3H, s, H_2CNCH_3), 2.35 (1H, t, $J = 2.2$ Hz, $\text{C}\equiv\text{CH}$); δ_{C} (150 MHz, CDCl_3) 178.6 (Ar_2C^+), 156.1 (C4), 154.2 (C4'), 140.3 and 139.3 (C2 and C2'), 127.9 (C1'), 127.0 (C1), 113.0 and 112.9 (C3 and C3'), 77.7 ($\text{C}\equiv\text{CH}$), 73.4 ($\text{C}\equiv\text{CH}$), 42.2 (CH_2), 40.9 ($\text{N}(\text{CH}_3)_2$), 39.0 (H_2CNCH_3); m/z (ES^+) found 396 ($[\text{M}]^+$, 100%); m/z (ES^-) found 248 ($[\text{M}]^-$, ~10%), 247 ($[\text{M}]^-$, ~50%), 245 ($[\text{M}]^-$, 100%), 243 ($[\text{M}]^-$, ~80%); Accurate mass calc. for $\text{C}_{27}\text{H}_{30}\text{N}_3$ $[\text{M}]^+$ 396.2440, found 396.2445, Δ 1.3ppm; $\lambda_{\max} = 590$ nm ($\epsilon = 88,230$).

Bis(4-(dimethylamino)phenyl)(4-((4-ethynylbenzyl)(methyl)amino)phenyl)methylium 2,3,5,6-tetrachloro-4-hydroxyphenolate (36)



A modified procedure of Szent-Gyorgyi *et al.*²⁹⁷ was used. To a solution of leucocrystal violet analogue **29** (200 mg, 0.422 mmol, 1.00 eq.) in ethyl acetate (10 mL) was added chloranil (208 mg, 0.845 mmol, 2.00 eq.). The reaction mixture was heated under reflux for 1 hour before being cooled to r.t. and filtered. The solid was washed with cold (0 °C) ethyl acetate and diethyl ether to afford the title compound **36** as a dull green solid (299 mg, 0.416 mmol, 98%*). $\nu_{\max}/\text{cm}^{-1}$ 1574, 1475, 1353, 1161; δ_{H} (600 MHz, CDCl_3) 7.49 (2H, d, $J = 7.4$ Hz, H3''), 7.33-7.28 (6H, m, H2 and H2'), 7.19 (2H, d, $J = 8.0$ Hz, H2''), 6.87 (6H, br s, H3 and H3'), 4.81 (2H, s, CH₂), 3.34 (3H, s, H₂CNCH₃), 3.30 (12H, s, N(CH₃)₂), 3.09 (1H, s, C≡CH); δ_{C} (150 MHz, CDCl_3) 178.4 (Ar₂C⁺), 155.9 (C4), 155.1 (C4'), 143.6 (CO anion), 140.1 and 139.8 (C2 and C2'), 137.4 (C1''), 132.9 (C3''), 127.4 and 126.8 (C1 and C1'), 126.5 (C2''), 121.6 (C4''), 119.5 (CCl anion), 112.7 and 110.6 (C3 and C3'), 83.2 (C≡CH), 77.8 (C≡CH), 56.3 (CH₂), 40.8 (N(CH₃)₂), 39.8 (H₂CNCH₃); m/z (ES⁺) found 472 ([M]⁺, 100%); m/z (ES⁻) found 248 ([M]⁻, ~10%), 247 ([M]⁻, ~50%), 245 ([M]⁻, 100%), 243 ([M]⁻, ~80%); Accurate mass calc. for C₃₃H₃₄N₃ [M]⁺ 472.2753, found 472.2729, Δ 5.1 ppm; $\lambda_{\max} = 590$ nm ($\epsilon = 97,590$). *This compound contained ethyl acetate as an impurity (<3% by mass).

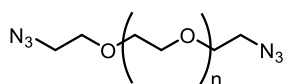
Bis(4-(dimethylamino)phenyl)(4-(prop-2-ynyloxy)phenyl)methylium 2,3,5,6-tetrachloro-4-hydroxyphenolate (37)



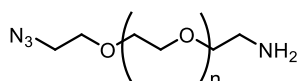
A modified procedure of Szent-Gyorgyi *et al.*²⁹⁷ was used. To a solution of leucocrystal violet analogue **33** (200 mg, 0.520 mmol, 1.00 eq.) in ethyl acetate (10 mL) was added chloranil (256 mg, 1.04 mmol, 2.00 eq.). The reaction mixture was heated under reflux for 1 hour

before being cooled to r.t. and filtered. The solid was washed with cold (0 °C) ethyl acetate and diethyl ether to afford the title compound **37** as a dull green solid (251 mg, 0.398 mmol, 77%). $\nu_{\max}/\text{cm}^{-1}$ 1682, 1578, 1355, 1161, 1009; δ_{H} (600 MHz, CDCl_3) 7.37 (4H, d, $J = 8.6$ Hz, H2), 7.33 (2H, d, $J = 8.7$ Hz, H2'), 7.16 (2H, d, $J = 8.7$ Hz, H3'), 6.97 (4H, d, $J = 8.6$ Hz, H3), 4.86 (2H, d, $J = 2.4$ Hz, CH_2), 3.37 (12H, s, CH_3), 2.64 (1H, t, $J = 2.4$ Hz, $\text{C}\equiv\text{CH}$); δ_{C} (150 MHz, CDCl_3) 177.6 (Ar_2C^+), 162.5 ($\text{C4}'$), 156.9 (C4), 140.9 (C2), 137.5 ($\text{C2}'$), 132.6 (C1), 127.3 (C1), 115.3 ($\text{C3}'$), 113.7 (C3), 77.5 ($\text{C}\equiv\text{CH}$), 76.9 ($\text{C}\equiv\text{CH}$), 56.4 (CH_2), 41.2 (CH_3); m/z (ES^+) found 383 ($[\text{M}]^+$, 100%); m/z (ES^-) found 248 ($[\text{M}]^-$, ~10%), 247 ($[\text{M}]^-$, ~50%), 245 ($[\text{M}]^-$, 100%), 243 ($[\text{M}]^-$, ~50%); Accurate mass calc. for $\text{C}_{26}\text{H}_{27}\text{N}_2\text{O}$ $[\text{M}]^+$ 383.2123, found 383.2120, Δ 0.8ppm; $\lambda_{\max} = 611$ nm ($\epsilon = 66,840$), and 459 nm ($\epsilon = 21,020$).

Diazide-PEG-400 (**38**)³⁰¹

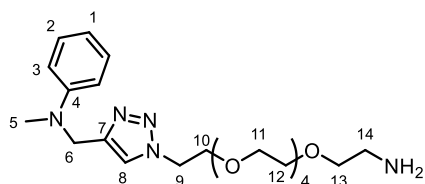


The procedure of Susumu *et al.* was used.³⁰¹ To a solution of PEG-400 (5.00 g, 12.5 mmol, 1.00 eq.) in dry THF (15 mL, degassed by bubbling argon through the solution for 10 minutes before use) was added mesyl chloride (2.2 mL, 29 mmol, 2.3 eq.). The mixture was cooled to 0 °C prior to the dropwise addition of triethylamine (4.4 mL, 31 mmol, 2.5 eq.) under argon. The reaction mixture was then allowed to warm to r.t. and stirred overnight. After 18 hours, the reaction mixture was diluted with water (15 mL) and sodium bicarbonate (893 mg, 10.6 mmol, 0.850 eq.) was added. This was succeeded by addition of sodium azide (2.23 g, 34.4 mmol, 2.75 eq.) and removal of THF by distillation under argon. The reaction was heated to reflux under argon for 24 hours before being cooled to r.t. and extracted with chloroform (5 × 10 mL). The combined organic extracts were dried over MgSO_4 before being concentrated *in vacuo*. The crude product was purified by flash column chromatography (SiO_2 , chloroform:methanol 20:1) to give the desired product **38** as a pale yellow oil (4.89 g, 10.9 mmol, 87%). R_f 0.75 (chloroform:methanol 10:1); $\nu_{\max}/\text{cm}^{-1}$ 2866 (CH), 2097 ($\text{N}\equiv\text{N}$), 1452, 1286, 1101; δ_{H} (500MHz, CDCl_3) 3.69-3.65 (33.5H, m, OCH_2), 3.39 (4H, t, $J = 5$ Hz, N_3CH_2); δ_{C} (125MHz, CDCl_3) 70.7-70.0 (OCH_2), 50.7 (N_3CH_2). Data is consistent with the literature values.³⁰¹

Mono-azide, mono-amine-PEG-400 (39)³⁰¹

The procedure of Susumu *et al.*³⁰¹ was used. To a round-bottomed flask was added diazide-PEG-400 **38** (5.00 g, 11.1 mmol, 1.00 eq.), ethyl acetate (75 mL) and hydrochloric acid (1M in water, 30 mL). The mixture was degassed by bubbling argon through the solution for 10 minutes prior to the addition of triphenylphosphine (3.21 g, 12.2 mmol, 1.10 eq.) in ethyl acetate (50 mL) *via* addition funnel at 0 °C under argon. Once the addition was complete, the reaction mixture was warmed to r.t. and stirred for 20 hours under argon. The organic and aqueous layers were separated, and the aqueous layer was washed with ethyl acetate (2 × 50 mL). The aqueous layer was then transferred to a round-bottomed flask and KOH (12.5 g, 222 mmol, 20.0 eq.) was added slowly. The mixture was stirred until all the KOH had dissolved. The aqueous mixture was then extracted with ethyl acetate (5 × 50 mL). The combined organic extracts were washed with brine (50 mL), before being dried over MgSO₄ and concentrated *in vacuo* to afford the desired product **39** as a pale yellow oil (2.43 g, 5.73 mmol, 52%). R_f 0.10 (chloroform:methanol 5:1); $\nu_{\max}/\text{cm}^{-1}$ 2865 (CH), 2100 (N≡N), 1454, 1298, 1094; δ_{H} (500MHz, CDCl₃) 3.69-3.63 (34H, m, OCH₂), 3.56 (2H, t, *J* = 5.3 Hz, H₂NCH₂), 3.39 (2H, t, *J* = 5.2 Hz, N₃CH₂), 2.91-2.87 (2H, m, NH₂); δ_{C} (125MHz, CDCl₃) 70.8-70.1 (OCH₂), 50.8 (N₃CH₂), 41.7 (H₂NCH₂). Data is consistent with the literature values.³⁰¹

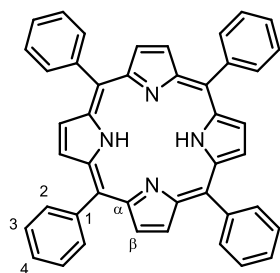
1-(ω-amino-PEG)-4-(*N*-methyl-*N*-phenyl)methylene-1,2,3-triazole OR 1-(ω-amino-PEG)-5-(*N*-methyl-*N*-phenyl)methylene-1,2,3-triazole OR 2-(ω-amino-PEG)-4-(*N*-methyl-*N*-phenyl)methylene-1,2,3-triazole (40**)**



A solution of *N*-methyl-*N*-phenyl-propargylamine **21** (50 mg, 0.34 mmol, 1.0 eq.) and mono-azide, mono-amine-PEG-400 **39** (147 mg, 0.344 mmol, 1.00 eq.) in DCM (1 mL) was degassed by bubbling argon through the solution for 10 minutes. To this solution was added CuBr(PPh₃)₃ (16 mg, 17 μmol, 0.050 eq.), and the reaction mixture was stirred at r.t. for 24 hours under argon. The mixture was then concentrated *in vacuo*, and the crude product was purified by flash

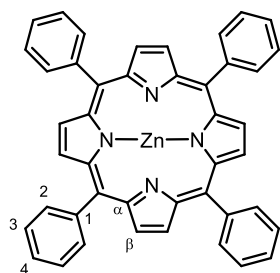
column chromatography to afford the desired product **40** as a mixture of two unidentifiable structural isomers in a 2:1 ratio as a yellow oil (175 mg, 0.306 mmol, 89%*). δ_{H} (600 MHz, CDCl_3) 7.57 (0.67H, s, H8), 7.47 (0.33H, m, H8), 7.24-7.21 (2H, m, H2), 6.81-6.79 (2H, m, H3), 6.74-6.71 (1H, m, H1), 4.64 (2H, s, H6), 4.55 (1.33H, t, $J = 5.2$ Hz, H9), 4.47 (0.67H, t, $J = 5.0$ Hz, H9), 3.89 (1.33H, t, $J = 5.2$ Hz, H10), 3.83-3.81 (0.67H, m, H10), 3.70-3.51 (20H, m, H11-14), 3.03 (2H, s, H5), 3.01 (1H, s, H5); δ_{C} (150 MHz, CDCl_3) 149.2 (C4), 145.3 (C7), 129.3 (C2), 123.1 and 122.9 (C8), 117.2 (C1), 113.1 (C3), 70.7-70.3 (C11, C12 and C13), 69.6 (C10), 50.3 (C9), 48.7 (C6), 38.8 and 38.7 (C5 and C14); m/z (EI) found 451 ($[\text{M}]^+$, ~25%), 422 ($[\text{M} - \text{CH}_3\text{N}]^+$, ~85%), 159 ($[\text{M} - \text{C}_{12}\text{H}_{26}\text{N}_3\text{O}_5]^+$, 100%), 144 ($[\text{M} - \text{C}_{12}\text{H}_{27}\text{N}_4\text{O}_5]^+$, ~70%), 120 ($[\text{M} - \text{C}_{14}\text{H}_{27}\text{N}_4\text{O}_5]^+$, ~70%), 107 ($[\text{M} - \text{C}_{15}\text{H}_{28}\text{N}_4\text{O}_5]^+$, ~60%); Accurate mass calc. for $\text{C}_{22}\text{H}_{37}\text{N}_5\text{O}_5$ $[\text{M}]^+$ 451.27947, found 451.27939, Δ 0.2ppm. *This compound contained minor, unidentifiable impurities.

Meso-tetraphenylporphyrin (**42**)^{343,344}

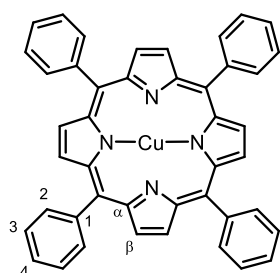


The procedure of Adler *et al.*³¹⁸ was used. To propionic acid (400 mL) under reflux were added freshly distilled pyrrole (6.9 mL, 100 mmol, 1.0 eq.) and benzaldehyde (10 mL, 100 mmol, 1.0 eq.) simultaneously. The reaction mixture was heated under reflux in the dark for 30 minutes before being cooled to r.t. and filtered. The filter

cake was washed copiously with methanol to afford the title compound **42** as a purple solid (2.88 g, 4.68 mmol, 19%). R_f 0.75 (chloroform); mp > 240 °C; $\nu_{\text{max}}/\text{cm}^{-1}$ 3314 (NH), 3054 and 3019 (CH), 1593, 1573, 1555, 1471, 1440, 1400, 1347, 1249, 1219, 1177, 1071; δ_{H} (600 MHz, CDCl_3) 8.86 (8H, s, β -H), 8.23-8.22 (8H, m, H3), 7.80-7.75 (12H, m, H2 and H4), -2.77 (2H, s, NH); δ_{C} (150 MHz, CDCl_3) 142.3 (C1), 134.7 (C3), 127.8 (C4), 126.8 (C2), 120.3 (*meso*-C); m/z (EI) found 614 ($[\text{M}]^+$, 100%); Accurate mass calc. for $\text{C}_{44}\text{H}_{30}\text{N}_4$ $[\text{M}]^+$ 614.2465, found 614.2465, Δ 0.1ppm; $\lambda_{\text{max}} = 412$ nm ($\epsilon = 235,210$), 506 nm ($\epsilon = 21,800$), 583 nm ($\epsilon = 7,190$), and 657 nm ($\epsilon = 2,410$). Data is consistent with the literature values.^{343,344}

Zinc *meso*-tetraphenylporphyrin (43)³⁴⁵

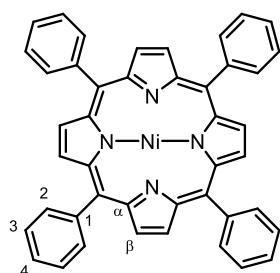
The procedure of He *et al.*³⁴⁵ was used. To a solution of *meso*-tetraphenylporphyrin **42** (200 mg, 0.325 mmol, 1.00 eq.) in chloroform (30 mL) was added zinc acetate (90 mg, 0.49 mmol, 1.5 eq.) in methanol. The reaction mixture was stirred at r.t. in the dark for 1 hour, before being added to water (100 mL). The layers were separated and the aqueous layer was extracted with chloroform (2 × 20 mL). The combined organic extracts were washed with water (20 mL) and brine (20 mL), dried over Na₂SO₄, and concentrated *in vacuo*. The resultant solid was washed thoroughly with methanol to afford the title compound **43** as a dark pink solid (153 mg, 0.226 mmol, 69%). R_f 0.70 (chloroform); mp >240 °C; $\nu_{\max}/\text{cm}^{-1}$ 1593, 1523, 1484, 1439, 1337, 1203, 1174, 1157, 1066; δ_{H} (600 MHz, CDCl₃) 8.96 (8H, s, β -H), 8.24-8.23 (8H, m, H3), 7.80-7.74 (12H, m, H2 and H4); δ_{C} (150 MHz, CDCl₃) 150.3 (α -C), 142.9 (C1), 134.6 (C3), 132.1 (β -C), 127.6 (C4), 126.7 (C2), 121.3 (*meso*-C); m/z (ES⁺) found 709 ([M + CH₃OH]⁺, ~90%), 677 ([M + H]⁺, 100%); Accurate mass calc. for C₄₄H₂₉N₄Zn [M + H]⁺ 677.1684, found 677.1684, Δ 0.1ppm; λ_{\max} = 421 nm (ϵ = 252,820), 550 nm (ϵ = 19,570), and 593 nm (ϵ = 4,060). Data is consistent with the literature values.³⁴⁵

Copper *meso*-tetraphenylporphyrin (44)³⁴⁵

The procedure of He *et al.*³⁴⁵ was used. To a solution of *meso*-tetraphenylporphyrin **42** (200 mg, 0.325 mmol, 1.00 eq.) in chloroform (30 mL) was added copper acetate (89 mg, 0.49 mmol, 1.5 eq.) in methanol. The reaction mixture was heated under reflux for 3 hours in the dark before being cooled to r.t. and added to water (100 mL). The layers were separated and the aqueous layer was extracted with chloroform (2 × 20 mL). The combined organic extracts were washed with water (20 mL) and brine (20 mL), dried over Na₂SO₄, and concentrated *in vacuo*. The resultant solid was washed thoroughly with methanol to afford the title compound **44** as a light purple solid (160 mg, 0.237 mmol, 73%). R_f 0.80

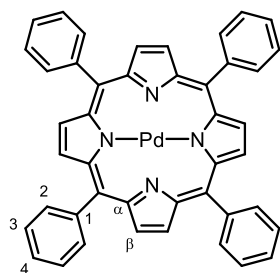
(chloroform); mp >240 °C; $\nu_{\max}/\text{cm}^{-1}$ 1596, 1538, 1520, 1488, 1439, 1345, 1204, 1176, 1156, 1070, 1002; δ_{H} (600 MHz, CDCl_3) 7.65-7.50 (br m); δ_{C} (150 MHz, CDCl_3) 136.1 (C3), 127.2 (C4), 126.5 (C2); m/z (EI) found 675 ($[\text{M}]^+$, 100%); Accurate mass calc. for $\text{C}_{44}\text{H}_{28}\text{N}_4\text{Cu}$ $[\text{M}]^+$ 675.1604, found 675.1606, Δ 0.3ppm; λ_{\max} = 414 nm (ϵ = 239,290), and 539 nm (ϵ = 21,500). Data is consistent with the literature values.³⁴⁵

Nickel *meso*-tetraphenylporphyrin (**45**)³⁴⁵



The procedure of He *et al.*³⁴⁵ was used. To a solution of *meso*-tetraphenylporphyrin **42** (200 mg, 0.325 mmol, 1.00 eq.) in toluene (30 mL) was added nickel acetylacetonate (125 mg, 0.488 mmol, 1.50 eq.). The reaction mixture was heated under reflux for 72 hours in the dark before being cooled to r.t. and added to water (100 mL). The layers were separated and the aqueous layer was extracted with toluene (20 mL). The combined organic extracts were washed with water (20 mL) and brine (20 mL), and concentrated *in vacuo*. The resultant solid was washed thoroughly with methanol to afford the title compound **45** as a purple solid (150 mg, 0.223 mmol, 69%). R_f 0.80 (chloroform); mp >240 °C; $\nu_{\max}/\text{cm}^{-1}$ 3053 and 3021 (C-H), 1598, 1576, 1439, 1350, 1177, 1070, 1005; δ_{H} (600 MHz, CDCl_3) 8.75 (8H, s, β -H), 8.02-8.01 (8H, m, H3), 7.71-7.68 (12H, m, H2 and H4); δ_{C} (150 MHz, CDCl_3) 142.7 (α -C), 141.0 (C1), 133.8 (C3), 132.3 (β -C), 127.9 (C4), 127.0 (C2), 119.1 (*meso*-C); m/z (EI) found 670 ($[\text{M}]^+$, 100%); Accurate mass calc. for $\text{C}_{44}\text{H}_{28}\text{N}_4\text{Ni}$ $[\text{M}]^+$ 670.1662, found 670.1663, Δ 0.2ppm; λ_{\max} = 415 nm (ϵ = 238,590), and 528 nm (ϵ = 22,030). Data is consistent with the literature values.³⁴⁵

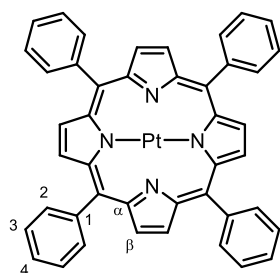
Palladium *meso*-tetraphenylporphyrin (**46**)³⁴⁶



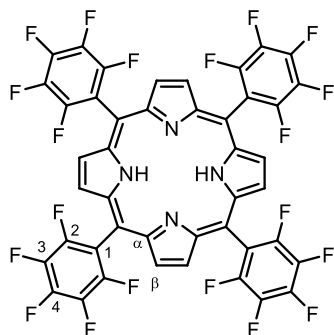
The procedure of Nishibayashi *et al.*³⁴⁶ was used. A solution of *meso*-tetraphenylporphyrin **42** (200 mg, 0.325 mmol, 1.00 eq.) and palladium acetate (292 mg, 1.30 mmol, 4.00 eq.) in chloroform (30 mL, degassed by bubbling argon through the solution for 10 minutes prior to use) was heated under reflux in the dark and under

argon for 96 hours. The reaction mixture was then cooled to r.t. before being added to water (100 mL). The layers were separated and the aqueous layer was extracted with chloroform (3 × 20 mL). The combined organic extracts were washed with brine (60 mL), dried over Na₂SO₄, and concentrated *in vacuo*. The resultant solid was washed thoroughly with methanol to afford the title compound **46** as a dark red solid (173 mg, 0.241 mmol, 74%). R_f 0.75 (chloroform); mp >240 °C; $\nu_{\max}/\text{cm}^{-1}$ 1595, 1439, 1351, 1311, 1174, 1073, 1010; δ_{H} (600 MHz, CDCl₃) 8.82 (8H, s, β -H), 8.19 (8H, m, H3), 7.79-7.73 (12H, m, H2 and H4); δ_{C} (150 MHz, CDCl₃) 141.9 and 141.7 (α -C and C1), 134.2 (C3), 131.1 (β -C), 127.9 (C4), 126.9 (C2), 121.9 (*meso*-C); *m/z* (CI) found 722, 721, 720, 719, 718, 717 and 715 ([M + H]⁺, ~50%, ~95%, ~50%, 100%, ~80%, ~40% and ~5%); Accurate mass calc. for C₄₄H₂₉N₄¹⁰²Pd [M + H]⁺ 715.1443, found 715.1440, Δ 0.5ppm; λ_{\max} = 417 nm (ϵ = 210,710), and 524 nm (ϵ = 19,170). Data is consistent with the literature values.³⁴⁶

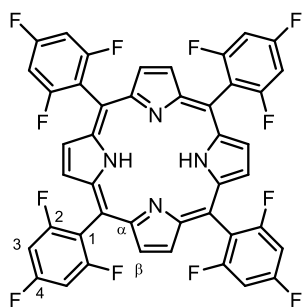
Platinum *meso*-tetraphenylporphyrin (**47**)³⁴⁵



A solution of *meso*-tetraphenylporphyrin **42** (200 mg, 0.325 mmol, 1.00 eq.) and platinum chloride (130 mg, 0.488 mmol, 1.50 eq.) in benzonitrile (40 mL, degassed by bubbling argon through the solution for 10 minutes prior to use) was heated under reflux in the dark and under argon for 18 hours. The reaction mixture was then cooled to r.t. before being added dropwise to methanol (600 mL). The resultant precipitate was separated and the filter cake was washed thoroughly with methanol to afford the title compound **47** as a red solid (200 mg, 0.248 mmol, 76%). R_f 0.80 (chloroform); mp >240 °C; $\nu_{\max}/\text{cm}^{-1}$ 1595, 1440, 1357, 1315, 1174, 1074, 1015; δ_{H} (600 MHz, CDCl₃) 8.76 (8H, s, β -H), 8.16-8.15 (8H, m, H3), 7.81-7.72 (12H, m, H2 and H4); δ_{C} (150 MHz, CDCl₃) 141.5 (C1), 141.0 (α -C), 134.0 (C3), 130.8 (β -C), 128.0 (C4), 126.9 (C2), 122.4 (*meso*-C); *m/z* (EI) found 807, 806, 805, 804, 803 and 802 ([M]⁺, ~95%, 100%, ~70%, ~15% and ~10%); Accurate mass calc. for C₄₄H₂₉N₄¹⁹⁰Pt [M]⁺ 802.1908, found 802.1907, Δ 0.1ppm; λ_{\max} = 402 nm (ϵ = 218,760), 510 nm (ϵ = 24,590), and 539 nm (ϵ = 5,410). Data is consistent with the literature values.³⁴⁵

Meso-tetra(pentafluorophenyl)porphyrin (48)³⁴⁷

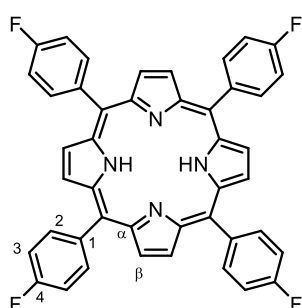
The procedure of Dommaschk *et al.*³²⁰ was used. To a solution of pentafluorobenzaldehyde (1.2 mL, 10 mmol, 1.0 eq.) and freshly distilled pyrrole (0.69 mL, 10 mmol, 1.0 eq.) in dry DCM (400 mL, degassed by bubbling argon through the solution for 10 minutes prior to use) was added $\text{BF}_3 \cdot \text{Et}_2\text{O}$ (0.41 mL, 3.3 mmol, 0.33 eq., 1 M solution in THF). The reaction mixture was heated under reflux in the dark and under argon for 48 hours before the addition of chloranil (615 mg, 2.50 mmol, 0.250 eq.). The reaction mixture was then heated under reflux for a further 3 hours in the dark in air, before being cooled to r.t. and concentrated *in vacuo*. The crude product was purified by flash column chromatography (SiO_2 , petroleum ether:chloroform 3:2) to afford the title compound **48** as a purple solid (419 mg, 0.430 mmol, 17%). R_f 0.55 (petroleum ether:chloroform 3:2); mp >240 °C; $\nu_{\text{max}}/\text{cm}^{-1}$ 3319 (NH), 1650, 1497, 1435, 1343, 1147, 1078, 1046; δ_{H} (600 MHz, CDCl_3) 8.93 (8H, s, β -H), -2.92 (2H, s, NH); δ_{C} (150 MHz, CDCl_3) 146.6 (dm, $J = 248$ Hz, C2 or C3 or C4), 142.5 (dm, $J = 258$ Hz, C2 or C3 or C4), 137.7 (dm, $J = 254$ Hz, C2 or C3 or C4), 131.3 (br s, α -C or β -C), 115.6 (tm, $J = 19.7$ Hz, C1), 103.8 (s, meso-C); δ_{F} (282 MHz, CDCl_3) -136.4-136.6 (m, F2), -151.2 (t, $J = 20.9$ Hz, F4), -161.2-161.4 (m, F3); m/z (ES^+) found 975 ($[\text{M} + \text{H}]^+$, 100%), 976 ($[\text{M} + 2\text{H}]^+$, ~50%); Accurate mass calc. for $\text{C}_{44}\text{H}_{10}\text{F}_{20}\text{N}_4$ $[\text{M} + \text{H}]^+$ 975.0664, found 975.0668, Δ 0.4ppm; $\lambda_{\text{max}} = 412$ nm ($\epsilon = 235,210$), 506 nm ($\epsilon = 21,800$), 583 nm ($\epsilon = 7,190$), and 657 nm ($\epsilon = 2,410$). Data is consistent with the literature values.³⁴⁷

Meso-tetra(2,4,6-trifluorophenyl)porphyrin (49)

The procedure of Dommaschk *et al.*³²⁰ was used. To a solution of 2,4,6-trifluorobenzaldehyde (1.00 g, 6.25 mmol, 1.00 eq.) and freshly distilled pyrrole (0.43 mL, 6.3 mmol, 1.0 eq.) in dry DCM (250 mL, degassed by bubbling argon through the solution for 10 minutes before use) was added $\text{BF}_3 \cdot \text{Et}_2\text{O}$ (0.25 mL, 2.1 mmol,

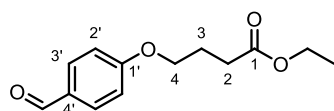
0.33 eq., 1 M solution in THF). The reaction mixture was heated under reflux in the dark and under argon for 48 hours before the addition of chloranil (384 mg, 1.56 mmol, 0.250 eq.). The reaction mixture was then heated under reflux for a further 3 hours in the dark in air, before being cooled to r.t. and concentrated *in vacuo*. The crude product was purified by flash column chromatography (SiO₂, petroleum ether:chloroform 3:2) to afford the title compound **49** as a purple solid (256 mg, 0.308 mmol, 20%). R_f 0.30 (petroleum ether:chloroform 3:2); mp >240 °C; $\nu_{\max}/\text{cm}^{-1}$ 1677, 1635, 1594, 1563, 1481, 1439, 1352, 1257, 1232, 1172, 1115, 1037; δ_{H} (600 MHz, CDCl₃) 8.90 (8H, s, β -H), 7.20-7.17 (8H, m, H3), -2.84 (2H, s, NH); δ_{C} (150 MHz, CDCl₃) 169.7 (s, α -C or β -C), 163.8 (dt, $J = 251.5$ Hz and 14.8 Hz, C4), 162.6 (ddd, $J = 249.7$ Hz, 15.1 Hz and 14.7 Hz, C2), 140.9 (s, *meso*-C), 115.1 (td, $J = 21.6$ Hz and 4.7 Hz, C1), 105.5 (s, α -C or β -C), 100.5 (td, $J = 24.1$ Hz and 5.0 Hz, C2); δ_{F} (282 MHz, CDCl₃) -105.0 (d, $J = 6.5$ Hz, F2), -105.9 (t, $J = 8.5$ Hz, F4); m/z (EI) found 828 ([M - 2H]⁺, 100%); $\lambda_{\max} = 413$ nm ($\epsilon = 207,270$), 508 nm ($\epsilon = 14,830$), 584 nm ($\epsilon = 4,580$), and 655 nm ($\epsilon = 2,300$).

Meso-tetra(4-fluorophenyl)porphyrin (**50**)



The procedure of Adler *et al.*³¹⁸ was used. To propionic acid (40 mL), being heated under reflux, was added freshly distilled pyrrole (0.69 mL, 10 mmol, 1.0 eq.) and 4-fluorobenzaldehyde (1.1 mL, 10 mmol, 1.0 eq.) simultaneously. The reaction mixture was heated under reflux in the dark for 30 minutes before being cooled to r.t. and filtered. The filter cake was washed copiously with methanol to afford the title compound **50** as a purple solid (429 mg, 0.624 mmol, 24%). $\lambda_{\max} = 419$ nm ($\epsilon = 241,670$), 514 nm ($\epsilon = 17,250$), 549 nm ($\epsilon = 7,290$), 589 nm ($\epsilon = 5,660$), and 646 nm (4,030). Only UV-Vis data were obtained for this compound due to its low solubility in all solvents tried.

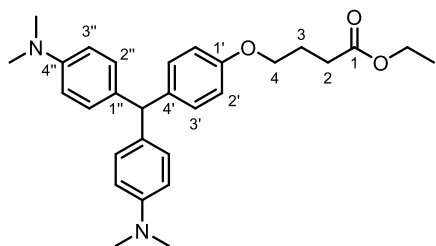
Ethyl 4-(4-formylphenyl)butyrate (**51**)³⁴⁸



The procedure of Fraga-Dubreuil *et al.*³³⁰ was used. To a suspension of 4-hydroxybenzaldehyde (1.00 g, 8.19 mmol, 1.00 eq.) and K₂CO₃ (1.70 g, 12.3 mmol,

1.50 eq.) in acetonitrile (25 mL) was added ethyl 4-bromobutyrate (1.2 mL, 8.2 mmol, 1.0 eq.). The reaction mixture was heated under reflux for 18 hours before being cooled to r.t., filtered and concentrated *in vacuo*. To the residue was added diethyl ether (250 mL), and the resultant suspension was filtered through Celite®. The filtrate was concentrated *in vacuo* to afford the desired product **51** as a pale yellow oil (1.82 g, 7.70 mmol, 94%). R_f 0.30 (petroleum ether:ethyl acetate 7:3); $\nu_{\max}/\text{cm}^{-1}$ 2980 and 2741 (CH), 1728 (aldehyde C=O), 1687 (ester C=O), 1598, 1577, 1509, 1472, 1375, 1312, 1251, 1156, 1110, 1029; δ_{H} (600 MHz, CDCl_3) 9.88 (1H, s, HC=O), 7.84-7.82 (2H, m, H3'), 7.00-6.98 (2H, m, H2'), 4.15 (2H, q, $J = 7.1$ Hz, H_2CCH_3), 4.10 (2H, t, $J = 6.1$ Hz, H4), 2.53 (2H, t, $J = 7.2$ Hz, H2), 2.15 (2H, tt, $J = 7.2$ Hz and 6.1 Hz, H3), 1.26 (3H, t, $J = 7.1$ Hz, CH_3); δ_{C} (150 MHz, CDCl_3) 191.0 (HC=O), 173.1 (C1), 164.0 (C1'), 132.1 (C3'), 130.1 (C4'), 114.9 (C2'), 67.2 (C4), 60.7 (H_2CCH_3), 30.7 (C2), 24.5 (C3), 14.4 (CH_3). Data is consistent with the literature values.³⁴⁸

Ethyl 4-(4-(bis(4-dimethylamino)phenyl)methyl)phenoxy)butyrate (**52**)



A modified procedure of Szent-Gyorgyi *et al.*²⁹⁷ was used. To a solution of ethyl 4-(4-formylphenyl)butyrate **51** (3.00 g, 12.7 mmol, 1.00 eq.) and ZnCl_2 (5.19 g, 38.1 mmol, 3.00 eq.) in ethanol (30 mL, degassed by bubbling

argon through the solution for 10 minutes before use) was added *N,N*-dimethylaniline (4.8 mL, 38 mmol, 3.0 eq.) at r.t. under argon. The reaction mixture was heated under reflux for 24 hours prior to the addition of a second portion of *N,N*-dimethylaniline (1.6 mL, 13 mmol, 1.0 eq.). The reaction mixture was heated under reflux for a further 24 hours, before being cooled to r.t. and concentrated *in vacuo*. The residue was dissolved in a mixture of water (300 mL) and DCM (100 mL) and the layers were separated. The aqueous layer was extracted with DCM (2 × 100 mL). The combined organic extracts were washed with water (100 mL) and brine (100 mL), dried over Na_2SO_4 , and concentrated *in vacuo*. The crude product was purified by flash column chromatography (SiO_2 , petroleum ether:ethyl acetate 7:3), followed by recrystallization from ethanol to afford the title compound **52** as a white solid (1.85 g, 4.02 mmol, 32%). R_f 0.30 (petroleum ether:ethyl acetate 7:3); mp 72-

74 °C; $\nu_{\max}/\text{cm}^{-1}$ 2897 and 2804 (C-H), 1731 (C=O), 1608, 1508, 1470, 1444, 1357, 1317, 1241, 1157, 1123, 1105, 1056, 1019; δ_{H} (600 MHz, CDCl_3) 7.04-7.02 (2H, m, H3'), 6.99-6.97 (4H, m, H2''), 6.80-6.78 (2H, m, H2'), 6.68-6.67 (4H, m, H3''), 5.33 (1H, s, Ar_2CH), 4.15 (2H, q, $J = 7.2$ Hz, H_2CCH_3), 3.97 (2H, t, $J = 6.1$ Hz, H4), 2.92 (12H, s, NCH_3), 2.51 (2H, t, $J = 7.3$ Hz, H2), 2.10 (2H, tt, $J = 7.3$ Hz and 6.1 Hz, H3), 1.26 (3H, t, $J = 7.2$ Hz, H_2CCH_3); δ_{C} (150 MHz, CDCl_3) 173.5 (C1), 157.1 (C1'), 149.0 (C4''), 137.8 (C4'), 133.3 (C1''), 130.4 and 130.0 (C3' and C2''), 114.1 (C2'), 112.7 (C3''), 66.7 (C4), 60.6 (H_2CCH_3), 54.3 (Ar_2CH), 40.9 (NCH_3), 31.0 (C2), 24.8 (C3), 14.4 (H_2CCH_3); m/z (ES^+) found 461 ($[\text{M} + \text{H}]^+$, 100%); Accurate mass calc. for $\text{C}_{29}\text{H}_{37}\text{N}_2\text{O}_3$ $[\text{M} + \text{H}]^+$ 461.2804, found 461.2801, Δ 0.7ppm.

4.3 Procedures for surface modifications, incorporations, leaching experiments, and other miscellaneous experiments

4.3.1 Incorporation of crystal violet analogues into polyurethane

A dip-coating technique, previously described by Noimark *et al.*,²⁷⁰ was used. A sheet of polyurethane was cut into 1 cm × 1 cm squares, which were immersed in aqueous solutions containing the crystal violet analogues (1×10^{-3} M) for 96 hours in the dark. After this time, the samples were removed from solution, rinsed with distilled water, and dried with paper towels.

4.3.2 Preparation of a PVC film

To vigorously stirring THF (150 mL) was added PVC powder (5.00 g, from BDH, $M_w \sim 100,000$) slowly, and with gentle heating to prevent aggregation. Once all the solid had dissolved, the solution was poured into a suitably sized glass container and the THF was allowed to evaporate slowly in air, which took roughly one week. The resultant film was cut into discs using a standard sized hole punch and used without any further purification. The consistency of the preparation process was confirmed by FT-IR spectroscopy.

4.3.3 Modification of PVC with sodium azide

A modified procedure of Sacristán *et al.*³¹⁵ was used. To a solution of sodium azide (0.1 M) in a mixture of DMF:water (6:1, 7 mL for every 2 discs) was added PVC film (cut into discs using a hole punch) and the resultant mixture

was stirred vigorously and heated to 60 °C for 2 days. The PVC discs were then immersed in a solution of acetone:water (6:4, 5 mL for every 2 discs) for 1 day, and this process was repeated 3 times with fresh acetone:water solutions. The discs were then dried with paper towels, before finally being dried under vacuum for 1 day. Analysis of the FT-IR spectrum was used to confirm the presence of the covalently attached azide (observed between 2100-2115 cm^{-1}).

4.3.4 Incorporation of crystal/ethyl violet into medical grade silicone

The “swell-encapsulate-shrink” technique, previously described by Ozkan *et al.*,²⁷¹ was used. A sheet of medical grade silicone (MED82-5010-40, Polymer Systems Technology Ltd.) was cut into 1 cm × 1 cm squares, which were immersed in toluene for 24 hours in the dark. They were then rinsed with distilled water and dried with paper towels, before being allowed to air dry in the dark for 24 hours. The squares were then immersed in solutions of crystal/ethyl violet in chloroform (1×10^{-3} M) for 72 hours in the dark, before being rinsed with distilled water, dried with paper towels, and air dried in the dark for 24 hours.

4.3.5 The extent of dye leaching from medical grade silicone incorporated with crystal/ethyl violet

A 1 cm × 1 cm sample containing crystal/ethyl violet was immersed in PBS solution (2.5 mL) for 168 hours in the dark. The UV-Vis absorbance of the PBS solution was obtained after 30 minutes, 1 hour, 2 hours, 4 hours, 6 hours, 24 hours, 48 hours, 72 hours, 96 hours and 168 hours.

4.3.6 Incorporation of porphyrins into medical grade silicone

A “swell-encapsulate-shrink” technique was used.²⁷¹ A sheet of medical grade silicone (MED82-5010-40, Polymer Systems Technology Ltd.) was cut into 1 cm × 1 cm squares, which were immersed in a solution of a porphyrin (1×10^{-3} M) in chloroform for 72 hours in the dark. The resultant films were rinsed with distilled water, dried with paper towels, and air dried in the dark for 24 hours.

5 References

- (1) Yu, Q.; Wu, Z.; Chen, H. *Acta Biomater.* **2015**, *16*, 1.
- (2) Hume, E. B. H.; Baveja, J.; Muir, B.; Schubert, T. L.; Kumar, N.; Kjelleberg, S.; Griesser, H. J.; Thissen, H.; Read, R.; Poole-Warren, L. A.; Schindhelm, K.; Willcox, M. D. P. *Biomaterials* **2004**, *25*, 5023.
- (3) Lianhua, Y.; Yunchao, H.; Geng, X.; Youquang, Z.; Guangqiang, Z.; Yujie, L. *Cell Biochem. Biophys.* **2013**, *67*, 893.
- (4) Banat, I. M.; Diaz De Rienzo, M. A.; Quinn, G. A. *Appl. Microbiol. Biotechnol.* **2014**, *98*, 9915.
- (5) Anselme, K.; Davidson, P.; Popa, A. M.; Giazzon, M.; Liley, M.; Ploux, L. *Acta Biomater.* **2010**, *6*, 3824.
- (6) Schlenoff, J. B. *Langmuir* **2014**, *30*, 9625.
- (7) Mi, L.; Jiang, S. *Angew. Chem. Int. Ed.* **2014**, *53*, 1746.
- (8) Wang, R.; Neoh, K. G.; Shi, Z.; Kang, E.-T.; Tambyah, P. A.; Chiong, E. *Biotechnol. Bioeng.* **2012**, *109*, 336.
- (9) Lafarge, J.; Kébir, N.; Schapman, D.; Gadenne, V.; Burel, F. *Cellulose* **2013**, *20*, 2779.
- (10) Francolini, I.; Donelli, G.; Vuotto, C.; Baroncini, F. A.; Stoodley, P.; Taresco, V.; Martinelli, A.; D'Ilario, L.; Piozzi, A. *Pathogens and Disease* **2014**, *70*, 401.
- (11) Trentin, D. S.; Silva, D. B.; Frasson, A. P.; Rzhapishevskaya, O.; da Silva, M. V.; Pulcini, E. L.; James, G.; Soares, G. V.; Tasca, T.; Ramstedt, M.; Giordani, R. B.; Lopes, N. P.; Macedo, A. J. *Sci. Rep.* **2015**, *5*, 8287.
- (12) Campoccia, D.; Montanaro, L.; Arciola, C. R. *Biomaterials* **2013**, *34*, 8533.
- (13) Kingshott, P.; Griesser, H. J. *Curr. Opin. Solid State Mater. Sci.* **1999**, *4*, 403.
- (14) Lejars, M.; Margailan, A.; Bressy, C. *Chem. Rev.* **2012**, *112*, 4347.
- (15) Desrousseaux, C.; Sautou, V.; Descamps, S.; Traoré, O. *J. Hosp. Infect.* **2013**, *85*, 87.
- (16) Harding, J. L.; Reynolds, M. M. *Trends Biotechnol.* **2014**, *32*, 140.

- (17) Costerton, J. W.; Cheng, K. J.; Geesey, G. G.; Ladd, T. I.; Nickel, J. C.; Dasgupta, M.; Marrie, T. J. *Annu. Rev. Microbiol.* **1987**, *41*, 435.
- (18) Costerton, J. W.; Stewart, P. S.; Greenberg, E. P. *Science* **1999**, *284*, 1318.
- (19) An, y.; Friedman, R. *Handbook of Bacterial Adhesion Principles, Methods, and Applications*; Humana: New York City, USA, 2000.
- (20) Jass, J.; Surman, S.; Walker, J. *Medical Biofilms Detection Prevention and Control*; Wiley: West Sussex, England, 2003.
- (21) Messing, B.; Peitra-Cohen, S.; Debure, A.; Beliah, M.; Bernier, J.-J. *JPEN J. Parenter. Enteral Nutr.* **1988**, *12*, 185.
- (22) Krzywda, E. A.; Andris, D. A.; Edmiston, C. E.; Quebbeman, E. J. *Infect. Control Hosp. Epidemiol.* **1995**, *16*, 596.
- (23) Gaillard, J.-L.; Merlino, R.; Pajot, N.; Goulet, O.; Fauchere, J.-L.; Ricour, C.; Veron, M. *JPEN J. Parenter. Enteral Nutr.* **1990**, *14*, 593.
- (24) Saltissi, D.; Macfarlane, D. J. *Postgrad. Med. J.* **1994**, *70*, 47.
- (25) Guggenbichler, J. P.; Berchtold, D.; Allerberger, F.; Bonatti, H.; Hager, J.; Pfaller, W.; Dierich, M. P. *Eur. J. Clin. Microbiol. Infect. Dis.* **1992**, *11*, 408.
- (26) Rao, J. S.; Meara, A. O.; Harvey, T.; Breatnach, F. *J. Hosp. Infect.* **1992**, *22*, 109.
- (27) Benoit, J.-L.; Carandang, G.; Sitrin, M.; Arnow, P. M. *Clin. Infect. Dis.* **1995**, *21*, 1286.
- (28) Messing, B.; Man, F.; Colimon, R.; Thuillier, F.; Beliah, M. *Clin. Nutr.* **1990**, *9*, 220.
- (29) Andris, D. A.; Krzywda, E. A.; Edmiston, C. E.; Krepel, C. J.; Gohr, C. M. *Nutrition* **1998**, *14*, 427.
- (30) Justo, J. A.; Bookstaver, P. B. *Infect. Drug Resist.* **2014**, *7*, 343.
- (31) Kohnen, W.; Jansen, B. *Zbl. Bakt.* **1995**, *283*, 175.
- (32) Trooskin, S. Z.; Harvey, R. A.; Lennard, T. w. J.; Greco, R. S. *Perit. Dial. Int.* **1990**, *10*, 57.
- (33) Raad, I.; Darouiche, R.; Hachem, R.; Sacilowski, M.; Bodey, G. P. *Antimicrob. Agents Chemother.* **1995**, *39*, 2397.
- (34) Jansen, B.; Jansen, S.; Peters, G.; Pulverer, G. *J. Hosp. Infect.* **1992**, *22*, 93.

- (35) Schierholz, J.; Jansen, B.; Jaenicke, L.; Pulverer, G. *Biomaterials* **1994**, *15*, 996.
- (36) Kohnen, W.; Schäper, J.; Klein, O.; Tieke, B.; Jansen, B. *Zbl. Bakt.* **1998**, *287*, 147.
- (37) Schierholz, J. M.; Fleck, C.; Beuth, J.; Pulverer, G. *J. Antimicrob. Chemother.* **2000**, *46*, 45.
- (38) DiTizio, V.; Ferguson, G. W.; Mittelman, M. W.; Khoury, A. E.; Bruce, A. W.; DiCosmo, F. *Biomaterials* **1998**, *19*, 1877.
- (39) Marconi, W.; Francolini, I.; Piozzi, A.; Di Rosa, R. *J. Bioact. Compatible Polym.* **2001**, *16*, 393.
- (40) Cottarel, G.; Wierzbowski, J. *Trends Biotechnol.* **2007**, *25*, 547.
- (41) Monzón, M.; Oteiza, C.; Leiva, J.; Amorena, B. *J. Antimicrob. Chemother.* **2001**, *48*, 793.
- (42) Ramritu, P.; Halton, K.; Collignon, P.; Cook, D.; Fraenkel, D.; Battistutta, D.; Whitby, M.; Graves, N. *Am. J. Infect. Control* **2008**, *36*, 104.
- (43) Gutiérrez-González, R.; Boto, G. R. *J. Infect.* **2010**, *61*, 9.
- (44) Casey, A. L.; Mermel, L. A.; Nightingale, P.; Elliott, T. S. J. *The Lancet infectious diseases* **2008**, *8*, 763.
- (45) Darouiche, R. O.; Raad, I. I.; Heard, S. O.; Thornby, J. I.; Wenker, O. C.; Gabrielli, A.; Berg, J.; Khardori, N.; Hanna, H.; Hachem, R.; Harris, R. L.; Mayhall, G. *New Engl. J. Med.* **1999**, *340*, 1.
- (46) Jamal, M. A.; Rosenblatt, J. S.; Hachem, R. Y.; Ying, J.; Pravinkumar, E.; Nates, J. L.; Chافتari, A.-M. P.; Raad, I. I. *Antimicrob. Agents Chemother.* **2014**, *58*, 1179.
- (47) Fisher, L. E.; Hook, A. L.; Ashraf, W.; Yousef, A.; Barrett, D. A.; Scurr, D. J.; Chen, X.; Smith, E. F.; Fay, M.; Parmenter, C. D. J.; Parkinson, R.; Bayston, R. *J. Controlled Release* **2015**, *202*, 57.
- (48) Aumsuwan, N.; Heinhorst, S.; Urban, M. W. *Biomacromolecules* **2007**, *8*, 713.
- (49) Aumsuwan, N.; Heinhorst, S.; Urban, M. W. *Biomacromolecules* **2007**, *8*, 3525.
- (50) Aumsuwan, N.; Danyus, R. C.; Heinhorst, S.; Urban, M. W. *Biomacromolecules* **2008**, *9*, 1712.

- (51) Aumsuwan, N.; Mcconnell, M. S.; Urban, M. W. *Biomacromolecules* **2009**, *10*, 623.
- (52) Kugel, A.; Chisholm, B.; Ebert, S.; Jepperson, M.; Jarabek, L.; Stafslin, S. *Polym. Chem.* **2010**, *1*, 442.
- (53) Komnatnyy, V. V.; Chiang, W.-C.; Tolker-Nielsen, T.; Givskov, M.; Nielsen, T. E. *Angew. Chem.* **2014**, *126*, 449.
- (54) Hawkey, P. M. *J. Antimicrob. Chemother.* **2008**, *62*, i1.
- (55) Taylor, P. K.; Yeung, A. T. Y.; Hancock, R. E. W. *J. Biotechnol.* **2014**, *191*, 121.
- (56) Rodriguez, R. A.; Steed, D. B.; Kawamata, Y.; Su, S.; Smith, P. A.; Steed, T. C.; Romesberg, F. E.; Baran, P. S. *J. Am. Chem. Soc.* **2014**, *136*, 15403.
- (57) Ling, L. L.; Schneider, T.; Peoples, A. J.; Spoering, A. L.; Engels, I.; Conlon, B. P.; Mueller, A.; Schäberle, T. F.; Hughes, D. E.; Epstein, S.; Jones, M.; Lazarides, L.; Steadman, V. A.; Cohen, D. R.; Felix, C. R.; Fetterman, K. A.; Millett, W. P.; Nitti, A. G.; Zullo, A. M.; Chen, C.; Lewis, K. *Nature* **2015**, *517*, 455.
- (58) Hui, F.; Debiemme-Chouvy, C. *Biomacromolecules* **2013**, *14*, 585.
- (59) Barnes, K.; Liang, J.; Worley, S. D.; Lee, J.; Broughton, R. M.; Huang, T. S. *J. Appl. Polym. Sci.* **2007**, *105*, 2306.
- (60) Badrossamay, M. R.; Sun, G. *Macromolecules* **2009**, *42*, 1948.
- (61) Sun, X.; Cao, Z.; Porteous, N.; Sun, Y. *Acta Biomater.* **2012**, *8*, 1498.
- (62) Tan, K. T.; Obendorf, S. K. *J. Membr. Sci.* **2007**, *289*, 199.
- (63) Badrossamay, M.; Sun, G. *React. Funct. Polym.* **2008**, *68*, 1636.
- (64) Ren, X. H.; Kou, L.; Kocer, H. B.; Zhu, C. Y.; Worley, S. D.; Broughton, R. M.; Huang, T. S. *Colloids Surf., A* **2008**, *317*, 711.
- (65) Ren, X. H.; Kocer, H. B.; Worley, S. D.; Broughton, R. M.; Huang, T. S. *Carbohydr. Polym.* **2009**, *75*, 683.
- (66) Hong, K. H.; Liu, N.; Sun, G. *Eur. Polym. J.* **2009**, *45*, 2443.
- (67) Kou, L.; Liang, J.; Ren, X.; Kocer, H. B.; Worley, S. D.; Broughton, R. M.; Huang, T. S. *Colloids Surf., A* **2009**, *345*, 88.

- (68) Wei, X. Y.; Wang, Z.; Zhang, Z.; Wang, J. X.; Wang, S. C. *J. Membr. Sci.* **2010**, *351*, 222.
- (69) Wei, X. Y.; Wang, Z.; Chen, J.; Wang, J. X.; Wang, S. C. *J. Membr. Sci.* **2010**, *346*, 152.
- (70) Chen, Y.; Han, Q. X. *Appl. Surf. Sci.* **2011**, *257*, 6034.
- (71) Zhao, N.; Liu, S. *Eur. Polym. J.* **2011**, *47*, 1654.
- (72) Zhao, N.; Zhanel, G. G.; Liu, S. *J. Appl. Polym. Sci.* **2011**, *120*, 611.
- (73) Liu, S.; Zhao, N.; Rudenja, S. *Macromol. Chem. Phys.* **2010**, *211*, 286.
- (74) Ahmed, A.; Hay, J. N.; Bushell, M. E.; Wardell, J. N.; Cavalli, G. *React. Funct. Polym.* **2008**, *68*, 1448.
- (75) Kocer, H. B.; Worley, S. D.; Broughton, R. M.; Huang, T. S. *React. Funct. Polym.* **2011**, *71*, 561.
- (76) Ahmed, A.; Hay, J. N.; Bushell, M. E.; Wardell, J. N.; Cavalli, G. *React. Funct. Polym.* **2008**, *68*, 248.
- (77) Wessels, S.; Ingmer, H. *Regul. Toxicol. Pharmacol.* **2013**, *67*, 456.
- (78) Carmona-Ribeiro, A. M.; de Melo Carrasco, L. D. *Int. J. Mol. Sci.* **2013**, *14*, 9906.
- (79) Domagk, G. *Dtsch. Med. Wocheschr.* **1935**, *61*, 829.
- (80) Mermel, L. A.; Stolz, S. M.; Maki, D. G. *J. Infect. Dis.* **1993**, *167*, 920.
- (81) Tebbs, S. E.; Elliott, T. S. J. *J. Antimicrob. Chemother.* **1993**, *31*, 261.
- (82) Tebbs, S. E.; Elliott, T. S. J. *Eur. J. Clin. Microbiol. Infect. Dis.* **1994**, *13*, 111.
- (83) Sampath, L. A.; Chowdhury, N.; Caraos, L.; Modak, S. M. *J. Hosp. Infect.* **1995**, *30*, 201.
- (84) Jaeger, K.; Osthaus, A.; Heine, J.; Ruschulte, H.; Kuhlmann, C.; Weissbrodt, H.; Ganser, A.; Karthaus, M. *Chemotherapy* **2001**, *47*, 50.
- (85) Shih, C.-K.; Huang, S.-H.; Tsai, C.-J.; Chu, K.-S.; Wu, S.-H. *J. Clin. Anesth.* **2010**, *22*, 632.

- (86) Dutta, P. K.; Tripathi, S.; Mehrotra, G. K.; Dutta, J. *Food Chem.* **2009**, *114*, 1173.
- (87) Majeti, N. V.; Kumar, R. *React. Funct. Polym.* **2000**, *46*, 1.
- (88) Dash, M.; Chiellini, F.; Ottenbrite, R. M.; Chiellini, E. *Prog. Polym. Sci.* **2011**, *36*, 981.
- (89) Rembaum, A.; Senyei, A. E.; Rajaraman, R. *J. Biomed. Mater. Res.* **1977**, *11*, 101.
- (90) Mondrzyk, A.; Fischer, J.; Ritter, H. *Polym. Int.* **2014**, *63*, 1192.
- (91) Wynne, J. H.; Fulmer, P. A.; McCluskey, D. M.; Mackey, N. M.; Buchanan, J. P. *ACS Appl. Mater. Interfaces* **2011**, *3*, 2005.
- (92) Yagci, M. B.; Bolca, S.; Heuts, J. P. A.; Ming, W.; de With, G. *Prog. Org. Coat.* **2011**, *72*, 305.
- (93) Dizman, B.; Elasri, M. O.; Mathias, L. J. *J. Appl. Polym. Sci.* **2004**, *94*, 635.
- (94) Kenawy, E.-R.; Abdel-Hay, F. I.; El-Magd, A. A.; Mahmoud, Y. *React. Funct. Polym.* **2006**, *66*, 419.
- (95) Sellenet, P. H.; Allison, B.; Applegate, B. M.; Youngblood, J. P. *Biomacromolecules* **2007**, *8*, 19.
- (96) Cakmak, I.; Ulukanli, Z.; Tuzcu, M.; Karabuga, S.; Genctav, K. *Eur. Polym. J.* **2004**, *40*, 2373.
- (97) Zheng, A.; Xu, X.; Xiao, H.; Guan, Y.; Li, S.; Wei, D. *Journal of Materials Science* **2012**, *47*, 7201.
- (98) Xu, X.; Xiao, H.; Ziaee, Z.; Wang, H.; Guan, Y.; Zheng, A. *Journal of Materials Science* **2013**, *48*, 1162.
- (99) Beyth, N.; Yudovin-Farber, I.; Bahir, R.; Domb, A. J.; Weiss, E. I. *Biomaterials* **2006**, *27*, 3995.
- (100) Xue, Y.; Xiao, H.; Zhang, Y. *Int. J. Mol. Sci.* **2015**, *16*, 3626.
- (101) Klibanov, A. M. *J. Mater. Chem.* **2007**, *17*, 2479.
- (102) Fadida, T.; Kroupitski, Y.; Peiper, U. M.; Bendikov, T.; Sela (Saldinger), S.; Poverenov, E. *Colloids Surf. B. Biointerfaces* **2014**, *122*, 294.
- (103) Lafarge, J.; Kébir, N.; Schapman, D.; Burel, F. *React. Funct. Polym.* **2013**, *73*, 1464.
- (104) Ding, X.; Yang, C.; Lim, T. P.; Hsu, L. Y.; Engler, A. C.; Hedrick, J. L.; Yang, Y.-Y. *Biomaterials* **2012**, *33*, 6593.

- (105) Lin, Y.; Liu, Q.; Cheng, L.; Lei, Y.; Zhang, A. *React. Funct. Polym.* **2014**, *85*, 36.
- (106) Mizerska, U.; Fortuniak, W.; Chojnowski, J.; Hałasa, R.; Konopacka, A.; Werel, W. *Eur. Polym. J.* **2009**, *45*, 779.
- (107) Riva, R.; Lussis, P.; Lenoir, S.; Jérôme, C.; Jérôme, R.; Lecomte, P. *Polymer* **2008**, *49*, 2023.
- (108) Sharma, S. K.; Chauhan, G. S.; Gupta, R.; Ahn, J. H. *J. Mater. Sci. - Mater. Med.* **2010**, *21*, 717.
- (109) Garg, G.; Chauhan, G. S.; Gupta, R.; Ahn, J. H. *J. Colloid Interface Sci.* **2010**, *344*, 90.
- (110) Kenawy, E.-R.; Abdel-Hay, F. I.; El-Shanshoury, A. E. R. R.; El-Newehy, M. H. *J. Controlled Release* **1998**, *50*, 145.
- (111) Kenawy, E.-R.; Abdel-Hay, F. I.; El-Shanshoury, A. E. R. R.; El-Newehy, M. H. *J. Polym. Sci., Part A: Polym. Chem.* **2002**, *40*, 2384.
- (112) Kanazawa, A.; Ikeda, T.; Endo, T. *J. Appl. Polym. Sci.* **1994**, *53*, 1245.
- (113) El-Newehy, M. H.; Kenawy, E.-R.; Al-Deyab, S. S. *Int. J. Polymer. Mater.* **2014**, *63*, 758.
- (114) Gao, B.; Liu, Q.; Li, Y. *J. Polym. Environ.* **2010**, *18*, 474.
- (115) Garcia-Arguelles, S.; Serrano, M. C.; Gutiérrez, M. C.; Ferrer, M. L.; Yuste, L.; Rojo, F.; del Monte, F. *Langmuir* **2013**, *29*, 9525.
- (116) Qiu, T.; Zeng, Q.; Ao, N. *Mater. Lett.* **2014**, *122*, 13.
- (117) Onaizi, S. A.; Leong, S. S. J. *Biotechnol. Adv.* **2011**, *29*, 67.
- (118) Jen, M. C.; Serrano, M. C.; van Lith, R.; Ameer, G. A. *Adv. Funct. Mater.* **2012**, *22*, 239.
- (119) Nablo, B. J.; Schoenfisch, M. H. *J. Biomed. Mater. Res. A* **2003**, *67A*, 1276.
- (120) Nablo, B. J.; Schoenfisch, M. H. *Biomacromolecules* **2004**, *5*, 2034.
- (121) Nablo, B. J.; Prichard, H. L.; Butler, R. D.; Klitzman, B.; Schoenfisch, M. H. *Biomaterials* **2005**, *26*, 6984.
- (122) Nablo, B. J.; Rothrock, A. R.; Schoenfisch, M. H. *Biomaterials* **2005**, *26*, 917.
- (123) Nablo, B. J.; Schoenfisch, M. H. *Biomaterials* **2005**, *26*, 4405.

- (124) Hetrick, E. M.; Schoenfisch, M. H. *Biomaterials* **2007**, *28*, 1948.
- (125) Engelsman, A. F.; Krom, B. P.; Busscher, H. J.; van Dam, G. M.; Ploeg, R. J.; van der Mei, H. C. *Acta Biomater.* **2009**, *5*, 1905.
- (126) Caro, H.; Kern, A. Manufacture of dye stuff. US290856, 25 December 1883.
- (127) Gessner, T.; Mayer, U. In *Ullman's Encyclopedia of Industrial Chemistry 6th Edition*; Wiley: Weinheim, Germany, 2002; Vol. 37.
- (128) Churchman, J. W.; Michael, W. H. *J. Exp. Med.* **1912**, *16*, 822.
- (129) Adams, E. *J. Pharm. Pharmacol.* **1967**, *19*, 821.
- (130) Maley, A. M.; Arbiser, J. L. *Exp. Dermatol.* **2013**, *22*, 775.
- (131) Bakker, P.; Van Doorne, H.; Gooskens, V.; Wieringa, N. F. *Int. J. Dermatol.* **1992**, *31*, 210.
- (132) Hachem, R.; Reitzel, R.; Borne, A.; Jiang, Y.; Tinkey, P.; Uthamanthil, R.; Chandra, J.; Ghannoum, M.; Raad, I. *Antimicrob. Agents Chemother.* **2009**, *53*, 5145.
- (133) Reitzel, R.; Rosenblatt, J.; Jiang, Y.; Hachem, R.; Raad, I. *Am. J. Infect. Control* **2014**, *42*, 55.
- (134) Jamal, M. A.; Hachem, R. Y.; Rosenblatt, J.; McArthur, M. J.; Felix, E.; Jiang, Y.; Taylor, R. C.; Raad, I. *Antimicrob. Agents Chemother.* **2015**, *59*, 5611.
- (135) Mani, S.; Bharagava, R. N. *Rev. Environ. Contam. Toxicol.* **2016**, *237*, 71.
- (136) Schweizer, H. P. *FEMS Microbiol. Lett.* **2001**, *202*, 1.
- (137) Wang, Z. X.; Jiang, C. P.; Cao, Y.; Ding, Y. T. *Br. J. Surg.* **2013**, *100*, 465.
- (138) Petersen, R. C. *AIMS Mol. Sci.* **2016**, *3*, 88.
- (139) Junker, L. M.; Hay, A. G. *J. Antimicrob. Chemother.* **2004**, *53*, 989.
- (140) Kalyon, B. D.; Olgun, U. *Am. J. Infect. Control* **2001**, *29*, 124.
- (141) Luo, J.; Deng, Y.; Sun, Y. *J. Bioact. Compatible Polym.* **2010**, *25*, 185.
- (142) Piotto, S.; Concilio, S.; Sessa, L.; Iannelli, P.; Porta, A.; Calabrese, E. C.; Galdi, M. R.; Incarnato, L. *Polym. Compos.* **2013**, *34*, 1489.
- (143) Tran, P. A.; Webster, T. J. *Nanotechnology* **2013**, *24*, 155101.

- (144) Knetsch, M. L. W.; Koole, L. H. *Polymers* **2011**, *3*, 340.
- (145) Eckhardt, S.; Brunetto, P. S.; Gagnon, J.; Priebe, M.; Giese, B.; Fromm, K. M. *Chem. Rev.* **2013**, *113*, 4708.
- (146) Guo, L.; Yuan, W.; Lu, Z.; Li, C. M. *Colloids Surf. Physicochem. Eng. Aspects* **2013**, *439*, 69.
- (147) Palza, H. *Int. J. Mol. Sci.* **2015**, *16*, 2099.
- (148) Feng, Q. L.; Wu, J.; Chen, G. Q.; Cui, F. Z.; Kim, T. N.; Kim, J. O. *J. Biomed. Mater. Res.* **2000**, *52*, 662.
- (149) Lemire, J. A.; Harrison, J. J.; Turner, R. J. *Nat. Rev. Microbiol.* **2013**, *11*, 371.
- (150) Park, H.-J.; Kim, J. Y.; Kim, J.; Lee, J.-H.; Hahn, J.-S.; Gu, M. B.; Yoon, J. *Water Res.* **2009**, *43*, 1027.
- (151) Inoue, Y.; Hoshino, M.; Takahashi, H.; Noguchi, T.; Murata, T.; Kanzaki, Y.; Hamashima, H.; Sasatsu, M. *J. Inorg. Biochem.* **2002**, *92*, 37.
- (152) Sintubin, L.; De Gussemme, B.; Van der Meeren, P.; Pycke, B. F. G.; Verstraete, W.; Boon, N. *Appl. Microbiol. Biotechnol.* **2011**, *91*, 153.
- (153) Xiu, Z.-M.; Ma, J.; Alvarez, P. J. J. *Environ. Sci. Technol.* **2011**, *45*, 9003.
- (154) Gordon, O.; Vig Slenters, T.; Brunetto, P. S.; Villaruz, A. E.; Sturdevant, D. E.; Otto, M.; Landmann, R.; Fromm, K. M. *Antimicrob. Agents Chemother.* **2010**, *54*, 4208.
- (155) Baker, C.; Pradhan, A.; Pakstis, L.; Pochan, D. J.; Shah, S. I. J. *J. Nanosci. Nanotechnol.* **2005**, *5*, 244.
- (156) Panáček, A.; Kvítek, L.; Pucek, R.; Kolář, M.; Večeřová, R.; Pizúrová, N.; Sharma, V. K.; Nevěčná, T.; Zbořil, R. *J. Phys. Chem. B* **2006**, *110*, 16248.
- (157) Choi, O.; Hu, Z. *Environ. Sci. Technol.* **2008**, *42*, 4583.
- (158) Pal, S.; Tak, Y. K.; Song, J. M. *Appl. Environ. Microbiol.* **2007**, *73*, 1712.
- (159) Liu, J.; Sonshine, D. A.; Shervani, S.; Hurt, R. H. *ACS Nano* **2010**, *4*, 6903.
- (160) El Badawy, A. M.; Silva, R. G.; Morris, B.; Scheckel, K. G.; Suidan, M. T.; Tolaymat, T. M. *Environ. Sci. Technol.* **2011**, *45*, 283.

- (161) Furno, F.; Morley, K. S.; Wong, B.; Sharp, B. L.; Arnold, P. L.; Howdle, S. M.; Bayston, R.; Brown, P. D.; Winship, P. D.; Reid, H. J. *J. Antimicrob. Chemother.* **2004**, *54*, 1019.
- (162) Rai, M. K.; Deshmukh, S. D.; Ingle, A. P.; Gade, A. K. *J. Appl. Microbiol.* **2012**, *112*, 841.
- (163) Lok, C.-N.; Ho, C.-M.; Chen, R.; He, Q.-Y.; Yu, W.-Y.; Sun, H.; Tam, P. K.-H.; Chiu, J.-F.; Che, C.-M. *J. Biol. Inorg. Chem.* **2007**, *12*, 527.
- (164) Xiu, Z.-M.; Zhang, Q.-B.; Puppala, H. L.; Colvin, V. L.; Alvarez, P. J. J. *Nano Lett.* **2012**, *12*, 4271.
- (165) Choi, O.; Deng, K. K.; Kim, N.-J.; Ross Jr., L.; Surampalli, R. Y.; Hu, Z. *Water Res.* **2008**, *42*, 3066.
- (166) Liu, J.; Hurt, R. H. *Environ. Sci. Technol.* **2010**, *44*, 2169.
- (167) Bae, E.; Park, H.-J.; Lee, J.; Kim, Y.; Yoon, J.; Park, K.; Choi, K.; Yi, J. *Environ. Toxicol. Chem.* **2010**, *29*, 2154.
- (168) Leaper, D. J. *Int. Wound J.* **2006**, *3*, 282.
- (169) Ip, M.; Lui, S. L.; Poon, V. K. M.; Lung, I.; Burd, A. *J. Med. Microbiol.* **2006**, *55*, 59.
- (170) Imber, D.; Bittner, E. A.; Pinciroli, R.; Berra, L. *Curr. Respir. Med. Rev.* **2012**, *8*, 475.
- (171) Tokmaji, G.; Vermeulen, H.; Muller, M. C. A.; Kwakman, P. H. S.; Schultz, M. J.; Zaat, S. A. J. *Cochrane Database Syst. Rev.* **2015**, *12*, CD009201.
- (172) Darouiche, R. O. *Clin. Infect. Dis.* **1999**, *29*, 1371.
- (173) Rupp, M. E.; Fitzgerald, T.; Marion, N.; Helget, V.; Puumala, S.; Anderson, J. R.; Fey, P. D. *Am. J. Infect. Control* **2004**, *32*, 445.
- (174) Schierholz, J. M.; Lucas, L. J.; Rump, A.; Pulverer, G. *J. Hosp. Infect.* **1998**, *40*, 257.
- (175) Lajcak, M.; Heidecke, V.; Haude, K. H.; Rainov, N. G. *Acta Neurochir. (Wien.)* **2013**, *155*, 875.
- (176) Bach, A.; Böhrer, H.; Motsch, J.; Martin, E.; Geiss, H. K.; Sonntag, H. G. *J. Antimicrob. Chemother.* **1994**, *33*, 969.
- (177) Hernández-Richter, T.; Schardey, H. M.; Wittmann, F.; Mayr, S.; Schmitt-Sody, M.; Blasenbrey, S.; Heiss, M. M.; Gabka, C.; Angele, M. K. *Eur. J. Vasc. Endovasc. Surg.* **2003**, *26*, 550.

- (178) Ricco, J.-B.; Assadian, O. *Semin. Vasc. Surg.* **2011**, *24*, 234.
- (179) Corrêa, J. M.; Mori, M.; Sanches, H. L.; Dibo, A.; Poiate Jr., E.; Poiate, I. A. V. P. *Int. J. Biomater.* **2015**, *2015*, 1.
- (180) Li, C.; Zhang, X.; Whitbourne, R. *J. Biomater. Appl.* **1999**, *13*, 206.
- (181) Boswald, M.; Girisch, M.; Greil, J.; Spies, T.; Stehr, K.; Krall, T.; Guggenbichler, J.-P. *Zbl. Bakt.* **1995**, *283*, 187.
- (182) Guggenbichler, J. P. *Materialwiss. Werkstofftech.* **2003**, *34*, 1145.
- (183) Roohpour, N.; Moshaverinia, A.; Wasikiewicz, J. M.; Paul, D.; Wilks, M.; Millar, M.; Vadgama, P. *Biomedical materials* **2012**, *7*, 015007.
- (184) Mtimet, I.; Lecamp, L.; Kebir, N.; Burel, F.; Jouenne, T. *Polym. J.* **2012**, *44*, 1230.
- (185) Varghese, S.; Elfakhri, S.; Sheel, D. W.; Sheel, P.; Bolton, F. J.; Foster, H. A. *J. Appl. Microbiol.* **2013**, *115*, 1107.
- (186) Silver, S. *FEMS Microbiol. Rev.* **2003**, *27*, 341.
- (187) Asharani, P. V.; Lianwu, Y.; Gong, Z.; Valiyaveetil, S. *Nanotoxicology* **2011**, *5*, 43.
- (188) Park, E.-J.; Yi, J.; Kim, Y.; Choi, K.; Park, K. *Toxicol. In Vitro* **2010**, *24*, 872.
- (189) Liu, W.; Wu, Y.; Wang, C.; Li, H. C.; Wang, T.; Liao, C. Y.; Cui, L.; Zhou, Q. F.; Yan, B.; Jiang, G. B. *Nanotoxicology* **2010**, *4*, 319.
- (190) Kim, S.; Choi, J. E.; Choi, J.; Chung, K.-H.; Park, K.; Yi, J.; Ryu, D.-Y. *Toxicol. In Vitro* **2009**, *23*, 1076.
- (191) Kim, J.; Kim, S.; Lee, S. *Nanotoxicology* **2011**, *5*, 208.
- (192) Kawata, K.; Osawa, M.; Okabe, S. *Environ. Sci. Technol.* **2009**, *43*, 6046.
- (193) Ivask, A.; Kurvet, I.; Kasemets, K.; Blinova, I.; Aruoja, V.; Suppi, S.; Vija, H.; Käkinen, A.; Titma, T.; Heinlaan, M.; Visnapuu, M.; Koller, D.; Kisand, V.; Kahru, A. *PLoS One* **2014**, *9*, e102108.
- (194) Greulich, C.; Braun, D.; Peetsch, A.; Diendorf, J.; Siebers, B.; Epple, M.; Koller, M. *RSC Advances* **2012**, *2*, 6981.
- (195) Scheiber, I.; Dringen, R.; Mercer, J. F. B. *Copper: Effects of Deficiency and Overload*; Springer: New York City, USA, 2013.

- (196) Grass, G.; Rensing, C.; Solioz, M. *Appl. Environ. Microbiol.* **2011**, *77*, 1541.
- (197) Sehmi, S. K.; Noimark, S.; Weiner, J.; Allan, E.; MacRobert, A. J.; Parkin, I. P. *ACS Appl. Mater. Interfaces* **2015**, *7*, 22807.
- (198) Raab, O. *Z. Biol.* **1900**, *39*, 524.
- (199) Carp, O.; Huisman, C. L.; Reller, A. *Prog. Solid State Chem.* **2004**, *32*, 33.
- (200) Hashimoto, K.; Irie, H.; Fujishima, A. *Jpn. J. Appl. Phys.* **2005**, *44*, 8269.
- (201) Mills, A.; le Hunte, S. *J. Photochem. Photobiol. A: Chem.* **1997**, *108*, 1.
- (202) Foster, H. A.; Ditta, I. B.; Varghese, S.; Steele, A. *Appl. Microbiol. Biotechnol.* **2011**, *90*, 1847.
- (203) Draper, R. B.; Fox, M. A. *Langmuir* **1990**, *6*, 1396.
- (204) Draper, R. B.; Fox, M. A. *J. Phys. Chem.* **1990**, *94*, 4628.
- (205) Tachikawa, T.; Tojo, S.; Fujitsuka, M.; Majima, T. *Langmuir* **2004**, *20*, 2753.
- (206) Tachikawa, T.; Tojo, S.; Fujitsuka, M.; Majima, T. *J. Phys. Chem. B* **2004**, *108*, 5859.
- (207) de Nardo, L.; Raffaini, G.; Ganazzoli, F.; Chiesa, R. *Metal surface oxidation and surface interactions*; Woodhead Publishing: Cambridge, UK, 2011.
- (208) Chun, M. J.; Shim, E.; Kho, E. H. *Angle Orthod.* **2007**, *77*, 483.
- (209) Heidenau, F.; Mittelmeier, W.; Detsch, R. *J. Mater. Sci. Mater. Med.* **2005**, *16*, 883.
- (210) Kambala, V. S.; Naidu, R. *J. Biomed. Nanotechnol.* **2009**, *5*, 121.
- (211) Marugán, J.; Christensen, P.; Egerton, T.; Purnama, H. *Appl. Catal., B* **2009**, *89*, 273.
- (212) Santillán, M. J.; Quaranta, N. E.; Boccaccini, A. R. *Surf. Coat. Technol.* **2010**, *205*, 2562.
- (213) Szymanowski, H.; Sobczyk-Guzenda, A.; Rylski, A.; Jakubowski, W.; Gazicki-Lipman, M.; Herberth, U.; Olcaytug, F. *Thin Solid Films* **2007**, *515*, 5275.
- (214) Evans, P.; Sheel, D. W. *Surf. Coat. Technol.* **2007**, *201*, 9319.

- (215) Baba, K.; Hatada, R. *Surf. Coat. Technol.* **2001**, *136*, 241.
- (216) Suketa, N.; Sawase, T.; Kitaura, H.; Naito, M.; Baba, K.; Nakayama, K.; Wennerberg, A.; Atsuta, M. *Clin. Implant Dent. Relat. Res.* **2005**, *7*, 105.
- (217) Shiraishi, K.; Koseki, H.; Tsurumoto, T.; Baba, K.; Naito, M.; Nakayama, K.; Shindo, H. *Surf. Interface Anal.* **2009**, *41*, 17.
- (218) Jing, F. J.; Wang, L.; Fu, R. K. Y.; Leng, Y. X.; Chen, J. Y.; Huang, N.; Chu, P. K. *Surf. Coat. Technol.* **2007**, *201*, 6874.
- (219) Sánchez, E.; Bannier, E.; Cantavella, V.; Salvador, M. D.; Klyatskina, E.; Morgiel, J.; Grzonka, J.; Boccaccini, A. R. *J. Therm. Spray Technol.* **2008**, *17*, 329.
- (220) Visai, L.; De Nardo, L.; Punta, C.; Melone, L.; Cigada, A.; Imbriani, M.; Arciola, C. R. *Int. J. Artif. Organs* **2011**, *34*, 929.
- (221) Sekiguchi, Y.; Yao, Y.; Ohko, Y.; Tanaka, K.; Ishido, T.; Fujishima, A.; Kubota, Y. *Int. J. Urol.* **2007**, *14*, 426.
- (222) Shah, R. R.; Kaewgun, S.; Lee, B. I.; Tzeng, T. R. J. *J. Biomed. Nanotechnol.* **2008**, *4*, 339.
- (223) Miyagi, T.; Kamei, M.; Mitsuhashi, T.; Ishigaki, T.; Yamazaki, A. *Chem. Phys. Lett.* **2004**, *390*, 399.
- (224) Dunnill, C. W.; Parkin, I. P. *Dalton trans.* **2011**, *40*, 1635.
- (225) Zaleska, A. *Recent Patents on Engineering* **2008**, *2*, 157.
- (226) Yu, J. C.; Ho, W.; Yu, J.; Yip, H.; Wong, P. K.; Zhao, J. *Environ. Sci. Technol.* **2005**, *39*, 1175.
- (227) Skorb, E. V.; Antonouskaya, L. I.; Belyasova, N. A.; Shchukin, D. G.; Möhwald, H.; Sviridov, D. V. *Appl. Catal., B* **2008**, *84*, 94.
- (228) Karvinen, S. M. *Ind. Eng. Chem. Res.* **2003**, *42*, 1035.
- (229) Wong, M.-S.; Chu, W.-C.; Sun, D.-S.; Huang, H.-S.; Chen, J.-H.; Tsai, P.-J.; Lin, N.-T.; Yu, M.-S.; Hsu, S.-F.; Wang, S.-L.; Chang, H.-H. *Appl. Environ. Microbiol.* **2006**, *72*, 6111.
- (230) Rengifo-Herrera, J. A.; Mielczarski, E.; Mielczarski, J.; Castillo, N. C.; Kiwi, J.; Pulgarin, C. *Appl. Catal., B* **2008**, *84*, 448.
- (231) Gamage, J.; Zhang, Z. *Int. J. Photoenergy* **2010**, *1*.
- (232) Blossey, E. C.; Neckers, D. C.; Thayer, A. L.; Schaap, A. P. *J. Am. Chem. Soc.* **1973**, *97*, 5820.

- (233) Bezman, S. A.; Burtis, P. A.; Izod, T. P. J.; Thayer, M. A. *Photochem. Photobiol.* **1978**, *28*, 325.
- (234) Noimark, S.; Dunnill, C. W.; Parkin, I. P. *Adv. Drug Del. Rev.* **2012**, *65*, 570.
- (235) Craig, R. A.; McCoy, C. P.; Gorman, S. P.; Jones, D. S. *Expert opin. Drug Deliv.* **2015**, *12*, 85.
- (236) Alves, E.; Faustino, M. A. F.; Neves, M. G. P. M. S.; Cunha, Â.; Nadais, H.; Almeida, A. J. *Photochem. Photobiol. C: Photochem. Rev.* **2015**, *22*, 34.
- (237) Bonnett, R. *Chem. Soc. Rev.* **1995**, *24*, 19.
- (238) Eshghi, H.; Sazgarnia, A.; Rahimizadeh, M.; Attaran, N.; Bakavoli, M.; Soudmand, S. *Photodiagnosis Photodyn. Ther.* **2013**, *10*, 304.
- (239) Bonnett, R.; Buckley, D. G.; Burrow, T.; Galia, A. B. B.; Savilleb, B.; Songca, S. P. *J. Mater. Chem.* **1993**, *3*, 323.
- (240) Sherrill, J.; Michielsen, S.; Stojiljkovic, I. *J. Polym. Sci., Part A: Polym. Chem.* **2003**, *41*, 41.
- (241) Bozja, J.; Sherrill, J.; Michielsen, S.; Stojiljkovic, I. *J. Polym. Sci., Part A: Polym. Chem.* **2003**, *41*, 2297.
- (242) Bonnett, R.; Krysteva, M. A.; Lalov, I. G.; Artarsky, S. V. *Water Res.* **2006**, *40*, 1269.
- (243) Krouit, M.; Granet, R.; Branland, P.; Verneuil, B.; Krausz, P. *Bioorg. Med. Chem. Lett.* **2006**, *16*, 1651.
- (244) Krouit, M.; Granet, R.; Krausz, P. *Biorg. Med. Chem.* **2008**, *16*, 10091.
- (245) Krouit, M.; Granet, R.; Krausz, P. *Eur. Polym. J.* **2009**, *45*, 1250.
- (246) Ringot, C.; Sol, V.; Granet, R.; Krausz, P. *Mater. Lett.* **2009**, *63*, 1889.
- (247) Ringot, C.; Sol, V.; Barri, M.; Saad, N.; Bressollier, P.; Granet, R.; Couleaud, P.; Krausz, P. *Biomacromolecules* **2011**, *12*, 1716.
- (248) Memmi, A.; Granet, R.; Aouni, M.; Bakhrouf, A. *e-Polymers* **2012**, *040*, 1.
- (249) Mbakidi, J.-P.; Herke, K.; Alvès, S.; Chaleix, V.; Granet, R.; Krausz, P.; Leroy-Lhez, S.; Ouk, T.-S.; Sol, V. *Carbohydr. Polym.* **2013**, *91*, 333.

- (250) Funes, M. D.; Caminos, D. A.; Alvarez, M. G.; Fungo, F.; Otero, L. A.; Durantini, E. N. *Environ. Sci. Technol.* **2009**, *43*, 902.
- (251) Alvarez, M. G.; Gómez, M. L.; Mora, S. J.; Milanesio, M. E.; Durantini, E. N. *Biorg. Med. Chem.* **2012**, *20*, 4032.
- (252) Felgenträger, A.; Maisch, T.; Späth, A.; Schröder, J. A.; Bäumlner, W. *PCCP* **2014**, *16*, 20598.
- (253) Merchat, M.; Bertolini, G.; Giacomini, P.; Villanueva, A.; Jori, G. *J. Photochem. Photobiol. B: Biol.* **1996**, *32*, 153.
- (254) Yu, K. G.; Li, D. H.; Zhou, C. H.; Diao, J. L. *Chin. Chem. Lett.* **2009**, *20*, 411.
- (255) Nitzan, Y.; Dror, R.; Ladan, H.; Malik, Z.; Kimel, S.; Gottfried, V. *Photochem. Photobiol.* **1995**, *62*, 342.
- (256) Lyutakov, O.; Hejna, O.; Solovyev, A.; Kalachyova, Y.; Svorcik, V. *RSC Advances* **2014**, *4*, 50624.
- (257) Wainwright, M.; Phoenix, D. A.; Marland, J.; Wareing, D. R. A.; Bolton, F. J. *FEMS Immunol. Med. Microbiol.* **1997**, *19*, 75.
- (258) Wilson, M. *Infect. Control Hosp. Epidemiol.* **2003**, *24*, 782.
- (259) Decraene, V.; Pratten, J.; Wilson, M. *Appl. Environ. Microbiol.* **2006**, *72*, 4436.
- (260) Decraene, V.; Pratten, J.; Wilson, M. *Curr. Microbiol.* **2008**, *57*, 269.
- (261) Decraene, V.; Pratten, J.; Wilson, M. *Infect. Control Hosp. Epidemiol.* **2008**, *29*, 1181.
- (262) Perni, S.; Piccirillo, C.; Pratten, J.; Prokopovich, P.; Chrzanowski, W.; Parkin, I. P.; Wilson, M. *Biomaterials* **2009**, *30*, 89.
- (263) Perni, S.; Prokopovich, P.; Piccirillo, C.; Pratten, J.; Parkin, I. P.; Wilson, M. *J. Mater. Chem.* **2009**, *19*, 2715.
- (264) Noimark, S.; Dunnill, C. W.; Kay, C. W. M.; Perni, S.; Prokopovich, P.; Ismail, S.; Wilson, M.; Parkin, I. P. *J. Mater. Chem.* **2012**, *22*, 15388.
- (265) Perni, S.; Piccirillo, C.; Kafizas, A.; Uppal, M.; Pratten, J.; Wilson, M.; Parkin, I. P. *J. Cluster Sci.* **2010**, *21*, 427.
- (266) Perni, S.; Prokopovich, P.; Parkin, I. P.; Wilson, M.; Pratten, J. *J. Mater. Chem.* **2010**, *20*, 8668.

- (267) Naik, A. J. T.; Ismail, S.; Kay, C.; Wilson, M.; Parkin, I. P. *Mater. Chem. Phys.* **2011**, *129*, 446.
- (268) Ismail, S.; Perni, S.; Pratten, J.; Parkin, I.; Wilson, M. *Infect. Control Hosp. Epidemiol.* **2013**, *32*, 1130.
- (269) Piccirillo, C.; Perni, S.; Gil-Thomas, J.; Prokopovich, P.; Wilson, M.; Pratten, J.; Parkin, I. P. *J. Mater. Chem.* **2009**, *19*, 6167.
- (270) Noimark, S.; Bovis, M.; MacRobert, A. J.; Correia, A.; Allan, E.; Wilson, M.; Parkin, I. P. *RSC Advances* **2013**, *3*, 18383.
- (271) Ozkan, E.; Allan, E.; Parkin, I. P. *RSC Advances* **2014**, *4*, 51711.
- (272) Noimark, S.; Allan, E.; Parkin, I. P. *Chem. Sci.* **2014**, *5*, 2216.
- (273) Page, K.; Correia, A.; Wilson, M.; Allan, E.; Parkin, I. P. *J. Photochem. Photobiol. A: Chem.* **2015**, *296*, 19.
- (274) Ozkan, E.; Ozkan, F. T.; Allan, E.; Parkin, I. P. *RSC Advances* **2014**, *5*, 8806.
- (275) Noimark, S.; Weiner, J.; Noor, N.; Allan, E.; Williams, C. K.; Shaffer, M. S. P.; Parkin, I. P. *Adv. Funct. Mater.* **2015**, *25*, 1367.
- (276) Sehmi, S. K.; Noimark, S.; Bear, J. C.; Peveler, W. J.; Bovis, M.; Allan, E.; MacRobert, A. J.; Parkin, I. P. *J. Mater. Chem. B* **2015**, *3*, 6490.
- (277) Bonnett, R.; Martínez, G. *Tetrahedron* **2001**, *57*, 9513.
- (278) Green, J.-B. D.; Fulghum, T.; Nordhaus, M. A. *Biointerphases* **2011**, *6*, 13.
- (279) Kiskan, B.; Demiray, G.; Yagci, Y. *J. Polym. Sci., Part A: Polym. Chem.* **2008**, *46*, 3512.
- (280) Pawlak, M.; Mistlberger, G.; Bakker, E. *J. Mater. Chem.* **2012**, *22*, 12796.
- (281) Earla, A.; Braslau, R. *Macromol. Rapid Commun.* **2014**, *35*, 666.
- (282) Fournier, D.; De Geest, B. G.; Du Prez, F. E. *Polymer* **2009**, *50*, 5362.
- (283) Fournier, D.; Du Prez, F. *Macromolecules* **2008**, *41*, 4622.
- (284) Rana, S.; Lee, S. Y.; Cho, J. W. *Polym. Bull.* **2010**, *64*, 401.
- (285) Wischik, C. M.; Rickard, J. E.; Harrington, C. R.; Horsley, D.; Storey, J. M. D.; Marshall, C.; Sinclair, J. P.; Baddeley, T. C. Wista Laboratories Ltd. 3,7-Diamino-10H-phenothiazine salts and their use. WO 2007/110627 A2, October 4th 2007.

- (286) Clunas, S.; Storey, J. M. D.; Sinclair, J. P.; Baddeley, T. C.; Ishaq, A.; Simpson, M.; Williamson, C.; Wood, B. A.; Wischik, C. M.; Harrington, C. R.; Rickard, J. E.; Horsley, D.; Loh, Y. S. Wista Laboratories Ltd. Phenothiazine diaminium salts and their use. WO 2012/107706 A1, 16 August 2012.
- (287) Gray, V. J.; Wilden, J. D. *Tetrahedron Lett.* **2012**, *53*, 41.
- (288) Srivastava, S. K.; Chauhan, P. M. S.; Bhaduri, A. P. *Synth. Commun.* **2007**, *29*, 2085.
- (289) Jonnalagadda, S. B.; Dumba, M. *Int. J. Chem. Kinet.* **1993**, *25*, 745.
- (290) Taber, D. F.; Meagley, R. P.; Supplee, D. *J. Chem. Educ.* **1996**, *73*, 259.
- (291) Takamatsu, D.; Fukui, K.-i.; Aroua, S.; Yamakoshi, Y. *Org. Biomol. Chem.* **2010**, *8*, 3655.
- (292) Borrell, J. I.; Teixido, J.; Matallana, J. L.; Martinez-Teipel, B.; Couceiro, E. *Heterocycles* **2000**, *52*, 1207.
- (293) Schneider, H.-J.; Schiestel, T.; Zimmermann, P. *J. Am. Chem. Soc.* **1992**, *114*, 7698.
- (294) Yang, W.; Luo, Y.; Liu, W.; Deng, X.; Du, X.; Li, M. *J. Labelled Compd. Radiopharmaceut.* **2011**, *54*, 211.
- (295) Costero, A. M.; Parra, M.; Gil, S.; Gotor, R.; Martínez-Mañez, R.; Sancenón, F.; Royo, S. *Eur. J. Org. Chem.* **2012**, *2012*, 4937.
- (296) Blangetti, M.; Deagostino, A.; Rosso, H.; Prandi, C.; Zavattaro, C.; Venturello, P. *Eur. J. Org. Chem.* **2007**, *35*, 5867.
- (297) Szent-Gyorgyi, C.; Schmidt, B. F.; Creeger, Y.; Fisher, G. W.; Zakel, K. L.; Adler, S.; Fitzpatrick, J. A. J.; Woolford, C. A.; Yan, Q.; Vasilev, K. V.; Berget, P. B.; Bruchez, M. P.; Jarvik, J. W.; Waggoner, A. *Nat. Biotechnol.* **2008**, *26*, 235.
- (298) Hoogendoorn, S.; Blom, A. E. M.; Willems, L. I.; van der Marel, G. A.; Overkleeft, H. S. *Org. Lett.* **2011**, *13*, 5656.
- (299) Irish, D. E.; McCarroll, B.; Young, T. F. *J. Chem. Phys.* **1963**, *39*, 3436.
- (300) Jozwiakowski, M. J.; Connors, K. A. *J. Pharm. Sci.* **1988**, *77*, 241.

- (301) Susumu, K.; Mei, B. C.; Mattoussi, H. *Nat. Protoc.* **2009**, *4*, 424.
- (302) Lal, S.; Díez-González, S. *J. Org. Chem.* **2011**, *76*, 2367.
- (303) Díez-González, S. *Catal. Sci. Technol.* **2011**, *1*, 166.
- (304) Rostovtsev, V. V.; Green, L. G.; Fokin, V. V.; Sharpless, K. B. *Angew. Chem.* **2002**, *114*, 2708.
- (305) Ratner, B. D.; Hoffman, A. S.; Schoen, F. J.; Lemons, J. E. *Biomaterials Science: An Introduction to materials in medicine*; Elsevier Academic Press: California, USA, 2004.
- (306) Sodhi, R. N. S.; Sahi, V. P.; Mittelman, M. W. *J. Electron. Spectrosc. Relat. Phenom.* **2001**, *121*, 249.
- (307) Ko, Y. G.; Kim, Y. H.; Park, K. D.; Lee, H. J.; Lee, W. K.; Park, H. D.; Kim, S. H.; Lee, G. S.; Ahn, D. J. *Biomaterials* **2001**, *22*, 2115.
- (308) Fujimoto, K.; Takebayashi, Y.; Inoue, H.; Ikada, Y. *J. Polym. Sci., Part A: Polym. Chem.* **1993**, *31*, 1035.
- (309) *PeroxiDetect™ Kit For the Determination of aqueous and lipid hydroperoxides, Sigma Aldrich technical bulletin.*
- (310) Zhou, C.-Y.; Li, J.; Peddibhotla, S.; Romo, D. *Org. Lett.* **2010**, *12*, 2104.
- (311) Alferiev, I. S.; Fishbein, I. *Biomaterials* **2002**, *23*, 4753.
- (312) Ameer, A. A.; Abdallah, M. S.; Ahmed, A. A.; Yousif, E. A. *OJPChem* **2013**, *3*, 11.
- (313) Braun, D. *Pure Appl. Chem.* **1971**, *26*, 173.
- (314) Takeishi, M.; Okawara, M. *J. Polym. Sci. B Polym. Lett.* **1969**, *7*, 201.
- (315) Sacristan, J.; Reinecke, H.; Mijangos, C. *Polymer* **2000**, *41*, 5577.
- (316) Sun, X.-W.; Xu, P.-F.; Zhang, Z.-Y. *Magn. Reson. Chem.* **1998**, *36*, 459.
- (317) Mellish, K. J.; Cox, R. D.; Vernon, D. I.; Griffiths, J.; Brown, S. B. *Photochem. Photobiol.* **2002**, *75*, 392.
- (318) Adler, A. D.; Longo, F. R.; Finarelli, J. D.; Goldmacher, J.; Assour, J.; Korsakoff, L. *J. Org. Chem.* **1967**, *32*, 476.
- (319) Fleischer, E. B.; Foust, R.; Jeter, D.; Near, R. *Inorg. Nucl. Chem. Leters* **1973**, *9*, 1219.

- (320) Dommaschk, M.; Gutzeit, F.; Boretius, S.; Haag, R.; Herges, R. *Chem. Commun.* **2014**, *50*, 12476.
- (321) Lindsey, J. S.; Wagner, R. W. *J. Org. Chem.* **1989**, *54*, 828.
- (322) Giovannetti, R. In *Macro to Nano Spectroscopy*; Uddin, J., Ed.; InTech: 2012.
- (323) Marsh, D. F.; Mink, L. M. *J. Chem. Educ.* **1996**, *73*, 1188.
- (324) Gouterman, M. *J. Mol. Spectrosc.* **1961**, *6*, 138.
- (325) Kasha, M. *Discuss. Faraday Soc.* **1950**, *9*, 14.
- (326) Harriman, A. *J. Chem. Soc., Faraday Trans. 1* **1980**, *77*, 1978.
- (327) Prashanthi, S.; Kumar, P. H.; Wang, L.; Perepogu, A. K.; Bangal, P. R. *J. Fluoresc.* **2010**, *20*, 571.
- (328) Chung, Y. C.; Yang, K.; Choi, J. W.; Chun, B. C. *Color. Technol.* **2014**, *130*, 305.
- (329) Chung, Y.-C.; Choi, J. W.; Lee, S. H.; Chun, B. C. *Bull. Korean Chem. Soc.* **2011**, *32*, 2988.
- (330) Fraga-Dubreuil, J.; Bazureau, J. P. *Tetrahedron* **2003**, *59*, 6121.
- (331) Murray, J.; Nowak, D.; Pukenas, L.; Azhar, R.; Guillorit, M.; Walti, C.; Critchley, K.; Johnson, S.; Bon, R. S. *J. Mater. Chem. B* **2014**, *2*, 3741.
- (332) Khutornenko, G. A.; Panshina, N. S.; Zhuravlev, S. V. *Chem. Heterocycl. Compd.* **1972**, *8*, 294.
- (333) Cano, R.; Ram, D. J.; Yus, M. *J. Org. Chem.* **2011**, *76*, 5547.
- (334) Sharma, S.; Kumar, M.; Kumar, V.; Kumar, N. *J. Org. Chem.* **2014**, *79*, 9433.
- (335) Rasheed, S.; Rao, D. N.; Reddy, A. S.; Shankar, R.; Das, P. *RSC Advances* **2015**, *5*, 10567.
- (336) Wolfe, J. P.; Buchwald, S. L. *J. Org. Chem.* **2000**, *65*, 1144.
- (337) Humphries, B. A.; Rohrbach, M. S.; Brookhart, M. S.; Kenan, W. R. *Bioorg. Chem.* **1974**, *3*, 163.
- (338) Rajagopal, B.; Chou, C.-H.; Chung, C.-C.; Lin, P.-C. *Org. Lett.* **2014**, *16*, 3752.
- (339) Colobert, F.; Castanet, A.-S.; Abillard, O. *Eur. J. Org. Chem.* **2005**, *2005*, 3334.
- (340) Cheng, Y.; Jiao, P.; Williams, D. J.; Cohn, O.-M. *J. Chem. Soc., Perkin Trans. 1* **2001**, *1*, 44.

(341) Bachhav, H. M.; Takale, B. S.; Telvekar, V. N. *Synth. Commun.* **2013**, *43*, 1909.

(342) Chinthala, Y.; Thakur, S.; Tirunagari, S.; Chinde, S.; Domatti, A. K.; Arigari, N. K.; Srinivas, K. V. N. S.; Alam, S.; Jonnala, K. K.; Khan, F.; Tiwari, A.; Grover, P. *Eur. J. Med. Chem.* **2015**, *93*, 564.

(343) Schlabach, M.; Wehrle, B.; Rumpel, H.; Braun, J.; Scherer, G.; Limbach, H.-H. *Ber. Bunsenges. Phys. Chem.* **1992**, *96*, 821.

(344) Sharghi, H.; Nejad, A. H. *Tetrahedron* **2004**, *60*, 1863.

(345) He, C.; He, Q.; Deng, C.; Shi, L.; Zhu, D.; Fu, Y.; Cao, H.; Cheng, J. *Chem. Commun.* **2010**, *46*, 7536.

(346) Nishibayashi, R.; Kurahashi, T.; Matsubara, S. *Synlett* **2014**, *25*, 1287.

(347) Castro, K. A. D. F.; Silva, S.; Pereira, P. M. R.; Simões, M. M. Q.; Neves, M. P. M. S.; Cavaleiro, J. A. S.; Wypych, F.; Tomé, J. P. C.; Nakagaki, S. *Inorg. Chem.* **2015**, *54*, 4382.

(348) Kostas, I. D.; Coutsolelos, A. G.; Charalambidis, G.; Skondra, A. *Tetrahedron Lett.* **2007**, *48*, 6688.